Vol. 71, No. 4, October 1998

MATHEMATICS MAGAZINE

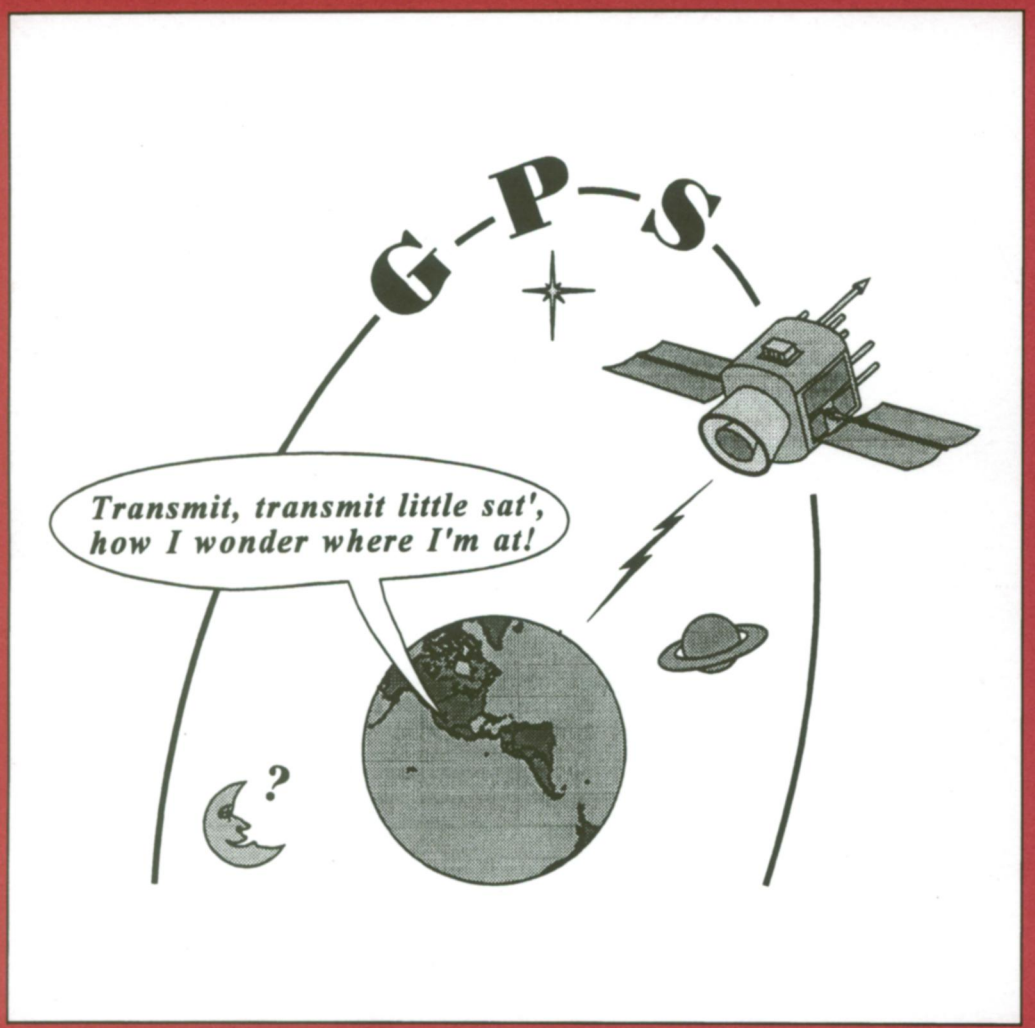

An Official Publication of The MATHEMATICAL ASSOCIATION OF AMERICA

EDITORIAL POLICY

Mathematics Magazine aims to provide lively and appealing mathematical exposition. This is not a research journal and, in general, the terse style appropriate for such a journal (lemma-theorem-proof-corollary) is not appropriate for an article for the *Magazine*. Articles should include examples, applications, historical background, and illustrations, where appropriate. They should be attractive and accessible to undergraduates and would, ideally, be helpful in supplementing undergraduate courses or in stimulating student investigations. Manuscripts on history are especially welcome, as are those showing relationships between various branches of mathematics and between mathematics and other disciplines.

A more detailed statement of author guidelines appears in this *Magazine*, Vol. 71, pp. 76–78, and is available from the Editor. Manuscripts to be submitted should not be concurrently submitted to, accepted for publication by, or published by another journal or publisher.

Send new manuscripts to Paul Zorn, Editor, Department of Mathematics, St. Olaf College, 1520 St. Olaf Avenue, Northfield, MN 55057-1098. Manuscripts should be laser-printed, with wide line-spacing, and prepared in a style consistent with the format of *Mathematics Magazine*. Authors should submit three copies and keep one copy. In addition, authors should supply the full five-symbol Mathematics Subject Classification number, as described in *Mathematical Reviews*, 1980 and later. Copies of figures should be supplied on separate sheets, both with and without lettering added.

AUTHORS

Richard Bagby received his B.A. in 1962 and his Ph.D. in 1968, both from Rice University. He has been teaching at New Mexico State University since then, except for year-long visits to Washington University, the University of South Carolina, and the University of Maryland. His research is in real and harmonic analysis, but he's easily distracted by elementary problems. When he's not involved in mathematical pursuits, he enjoys all sorts of other challenges, including word puzzles, woodworking, and tinkering. Since his retirement from distance running, he has stayed fit by swimming and bicycling.

Richard B. Thompson earned a Ph.D. in algebraic topology from the University of Wisconsin in 1967 and has taught at the University of Arizona since that time. His current interests are in curriculum design and development in mathematics and statistics, with particular emphasis on the introduction of computers into the undergraduate program. His experience with ocean sailing led him to study the mathematics of celestial and then satellite navigational systems.

Don Saari received his bachelor's degree from Michigan Technological University and his Ph.D. in mathematics from Purdue University. After a postdoctoral position in the Yale University astronomy department, he moved to Northwestern University, where he is currently the Arthur and Gladys Pancoe Professor of Mathematics. His research interests emphasize applications of dynamical systems to mathematical physics (in particular, the Newtonian n-body problem) and to issues arising in economics and the other social sciences. The disturbing conclusion of Arrow's theorem sparked by his interest in the areas of decision and voting theory; this led to his recent book *Basic Geometry of Voting*.

Fabrice Valognes is a Ph.D. student in mathematical economics and a teaching assistant at the University of Caen (France-Normandy), where he received all his degrees. In 1995, he received his DEA in Microeconomic Theory (the DEA is the equivalent of the first year in a Ph.D. program). In that year, after he followed Professor Saari's lectures on geometry of voting, he decided to write his thesis on voting theory.

Vol. 71, No. 4, October 1998

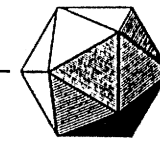

MATHEMATICS MAGAZINE

The *MATHEMATICS MAGAZINE* (ISSN 0025-570X) is published by the Mathematical Association of America at 1529 Eighteenth Street, N.W., Washington, D.C. 20036 and Montpelier, VT, bimonthly except July/August.

The annual subscription price for the MATHEMATICS MAGAZINE to an individual member of the Association is $16 included as part of the annual dues. (Annual dues for regular members, exclusive of annual subscription prices for MAA journals, are $64. Student and unemployed members receive a 66% dues discount; emeritus members receive a 50% discount; and new members receive a 40% dues discount for the first two years of membership.) The nonmember/library subscription price is $68 per year.

Subscription correspondence and notice of change of address should be sent to the Membership/Subscriptions Department, Mathematical Association of America, 1529 Eighteenth Street, N.W., Washington, D.C. 20036. Microfilmed issues may be obtained from University Microfilms International, Serials Bid Coordinator, 300 North Zeeb Road, Ann Arbor, MI 48106.

Advertising correspondence should be addressed to Ms. Elaine Pedreira, Advertising Manager, the Mathematical Association of America, 1529 Eighteenth Street, N.W., Washington, D.C. 20036.

Second class postage paid at Washington, D.C. and additional mailing offices.

Postmaster: Send address changes to Mathematics Magazine, Membership/Subscriptions Department, Mathematical Association of America, 1529 Eighteenth Street, N.W., Washington, D.C. 20036-1385.

PRINTED IN THE UNITED STATES OF AMERICA

ARTICLES

Geometry, Voting, and Paradoxes

DONALD G. SAARI
Northwestern University
Evanston, IL 60208–2730

FABRICE VALOGNES
CREME, Université de Caen
Caen
France

1. Problems

What could be easier than "voting?" After all, to vote we just count how many people favor each candidate. What can go wrong with something so elementary as this?

Actually, a lot. As mathematicians and others have shown over the last two centuries, once there are at least three candidates—not an atypical situation—the winner need not be whom the voters really want. Such bad outcomes may occur not only because some voters continue to vote long after death; bad outcomes can also be caused by hidden mathematical peculiarities.

We illustrate with an example from **[6]**, where fifteen people select a common beverage from among M (Milk), B (Beer), and W (Wine). If " $\succ$ " means "is preferred to" and if the voters' preferences are as follows:

Number	Preference
6	$M \succ W \succ B$
5	$B \succ W \succ M$
4	$W \succ B \succ M$

(1)

then the plurality outcome (where each person votes for his or her favorite beverage) is $M \succ B \succ W$ with the 6:5:4 tally. Apparently, Milk is the beverage of choice.

Before ordering a keg of Milk, let's pause. Is Milk truly the voters' beverage of choice? If so, we would expect voters to prefer Milk to Beer. But as the next table shows, these voters actually prefer Beer to Milk:

Number	Preferences	Milk	Beer
6	$M \succ W \succ B$	6	0
5	$B \succ W \succ M$	0	5
4	$W \succ B \succ M$	0	4
	Total	6	9

Similarly, 9 voters prefer Wine to Milk and 10 prefer Wine to Beer. This creates a contradiction and potential controversy among the party goers, because these pairwise comparisons suggest that the voters really prefer $W \succ B \succ M$, the *ranking opposite to the plurality outcome*. What went wrong?

Mathematicians This type of problem, coupled with the obvious importance of elections, motivated several eighteenth century mathematicians to investigate the mathematical peculiarities of elections. The mathematician J. C. de Borda was probably the first to consider these issues from an academic perspective when, in 1770, he questioned whether the French Academy of Science was electing to membership whom they really wanted. His concern, as illustrated by the beverage example, is that the "winner" of the widely used plurality vote can be the candidate the voters view as "inferior."

Borda [1] devised an alternative procedure, now called the *Borda Count*, which assigns 2, 1, and 0 points, respectively, to a voter's top, middle, and bottom-ranked candidate; candidates are then ranked according to the sum of assigned points. To see that this method can change the outcome, consider the Borda Count tally for the beverage example:

Number	Preferences	Milk	Beer	Wine
6	$M \succ W \succ B$	6×2	0	6×1
5	$B \succ W \succ M$	0	5×2	5×1
4	$W \succ B \succ M$	0	4×1	4×2
	Total	12	14	19

(2)

This produces the $W \succ B \succ M$ outcome, which agrees with the pairwise election rankings.

The Borda Count appears to be the "correct" voting procedure—at least for this example. But what happens in general? Are there examples of sets of voters' preferences, called *profiles*, for which the Borda Count does poorly? Why not use other weights, such as $(6,5,0)$ or $(4,1,0)$, instead of Borda's choice of $(2,1,0)$? Tallying methods that assign a specified number of points to a voter's first, second, and third ranked candidate are called *positional voting methods*. When normalized to assign a single point to a voter's top-ranked candidate, the point assignment defines a *voting vector* $\mathbf{w}_\lambda = (1, \lambda, 0)$, $0 \le \lambda \le 1$. For instance, the normalized forms of $(6,5,0)$ and the Borda Count are, respectively, $\mathbf{w}_{\frac{5}{6}} = (\frac{6}{6}, \frac{5}{6}, 0)$ and $\mathbf{w}_{\frac{1}{2}} = (1, \frac{1}{2}, 0)$. Because $\mathbf{w}_1 = (1,1,0)$ effectively requires a voter to vote against his or her bottom-ranked candidate, it is called the *antiplurality method.*

The $\mathbf{w}_\lambda$ normalization makes it clear that there is a continuum of tallying methods where each is characterized by the weight (the λ-value) placed on a voter's second-ranked candidate. Faced with all these possibilities, it was only natural for Borda's mathematical colleagues, such as Laplace, Condorcet, and others, to question which $\mathbf{w}_\lambda$ method is optimal in the sense that its outcomes best reflect the views of the voters. The debate they started continues today.

Condorcet Marie-Jean-Antoine-Nicolas de Caritat Condorcet, the French mathematician, philosopher, and politician, added to the controversy in the 1780's by arguing that, instead of using a $\mathbf{w}_\lambda$ method, the outcomes should be decided strictly in terms of the pairwise vote. The *Condorcet winner* is the candidate who beats all other candidates in pairwise elections. With the preferences of table (1), Wine, which wins a majority vote over each of the other beverages, is the Condorcet winner. Milk is the *Condorcet loser*.

Until recently the Condorcet winner was almost universally accepted as the ultimate choice. (See [6, 7, 8] for arguments questioning this concept.) But, it has problems. To illustrate just one difficulty, suppose a mathematics department uses pairwise voting to choose a calculus book from among the choices $\{A, B, C\}$. A natural way to select the book is by elimination, where after comparing two choices, say $\{A, B\}$, the winner is compared with the remaining choice, C. Suppose the views of the department members are

Number	Preferences
5	$A \succ B \succ C$
5	$B \succ C \succ A$
5	$C \succ A \succ B$

(3)

As the following table shows, A wins the initial $\{A, B\}$ comparison only to be beaten by C. In both elections the winner wins with a landslide two-thirds of the vote, so it seems safe to declare that the departmental ranking is the decisive $C \succ A \succ B$.

Number	Preference	A	B	A	C
5	$A \succ B \succ C$	5	0	5	0
5	$B \succ C \succ A$	0	5	5	0
5	$C \succ A \succ B$	5	0	0	5
	Totals	10	5	5	10

Although the outcome appears to be unquestionable, let's question it. We already know that C beats A and A beats B, so it remains to determine whether "top-ranked" C beats "bottom-ranked" B. We might expect no surprises, but there is one: B beats C by the same two-thirds landslide vote. In other words, this profile defines the *cyclic* election outcomes

$$A \succ B, \qquad B \succ C, \qquad C \succ A,$$

whereby whichever candidate is voted upon last, wins—decisively. In particular, there is no Condorcet winner or loser.

Condorcet understood that cycles could arise from pairwise voting; he demonstrated this behavior by introducing the example of table (3). Such an example is now known as a *Condorcet profile*.

Cycles, then, make it impossible to select an "optimal" candidate. (For a companion discussion of the problems of cycles, see [9].) But elections are intended to decide, so competing approaches have been devised to avoid stalemates. For instance, A. Copeland, a mathematician from the University of Michigan, developed a method which is similar to how hockey teams are ranked. A competing procedure, which involves counting the number of transpositions needed to convert one ranking into another, was devised by the mathematician J. Kemeny, from Dartmouth. (For a geometric analysis of both approaches, see [10, 11].)

Complexity and geometry Which method is best? Although this issue appears straightforward, progress has been seriously hindered by the complexity of the combinatorics. A traditional way to compare procedures is to construct profiles that show how one method has a failing not suffered by another. But to construct

examples, we need to determine how many voters must be of each type so that the resulting election outcomes capture the desired phenomenon.

To illustrate the complexity of the combinatorics, we offer some challenges. For instance, can the Condorcet and Borda winners differ? If so, find an illustrating profile. The beverage example proves that different positional methods create different election outcomes. Is there a general description explaining how election results change with changes in the $\mathbf{w}_\lambda$ methods? When using different $\mathbf{w}_\lambda$ voting vectors to tally ballots in the profile of table (1), either Wine, Milk, or both always emerges as the top choice (see **[6]**). Are there voters' profiles where *each* candidate is the "winner" for an appropriate $\mathbf{w}_\lambda$? Are the supporting examples isolated or robust? Can we characterize *all* possible examples? What is the minimum number of voters needed to create each election oddity?

In recent years, progress has been made on these concerns by replacing the traditional combinatoric method with a geometric perspective. A summary of this "geometry of voting" approach for three candidates is in the textbook **[6]**, while progress for any number of candidates (obtained by use of symmetry groups, etc.) is reported in **[7, 8]**. In this essay we demonstrate how geometry dramatically reduces these previously complicated issues into forms simple enough to be presented to students who can graph elementary algebraic equations.

2. Voter Types

A voter's "type" is defined by how the voter strictly ranks the candidates $\{A, B, C\}$. For convenience, denote these types by the following numbers:

Type	Preference	Type	Preference
1	$A \succ B \succ C$	4	$C \succ B \succ A$
2	$A \succ C \succ B$	5	$B \succ C \succ A$
3	$C \succ A \succ B$	6	$B \succ A \succ C$

(4)

These types are reflected in the geometry of the equilateral triangle of FIGURE 1, where each candidate is identified with a vertex. Each point in the triangle is assigned an ordinal ranking of the candidates according to how close the point is to each vertex

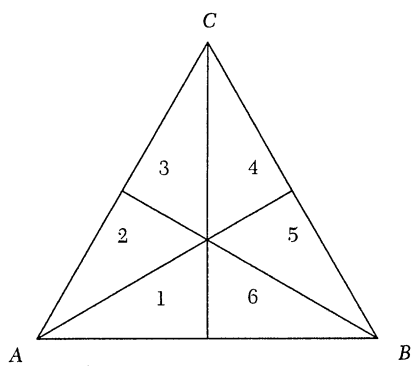

FIGURE 1
The representation triangle and ranking regions.

where, as in love, "closer is better." Points on the vertical line, for instance, are equidistant from A and B, so all of them are *indifferent* between these options; this is denoted by $A \sim B$. Similarly, all points in the triangular sector "1" are closest to A, next closest to B, and farthest from C, and so define the $A \succ B \succ C$ ranking.

Considerable insight and unexpected conclusions already arise when the voters' beliefs are restricted to only three specified preference types. This is what we discuss here. But selecting three of six voter types creates $\binom{6}{3} = 20$ situations to examine. Fortunately, as shown in Section 5, symmetry arguments reduce the number to three.

3. Condorcet Examples

The mystery of the pairwise voting cycles justifies starting with the setting where voters' preferences come from the three types involved in the Condorcet profile of table (3). This setting is captured in FIGURE 2a, where the three preference types define a symmetric "pinwheel" configuration. (This "$\mathbb{Z}_3$ orbit" symmetry causes the cycles.)

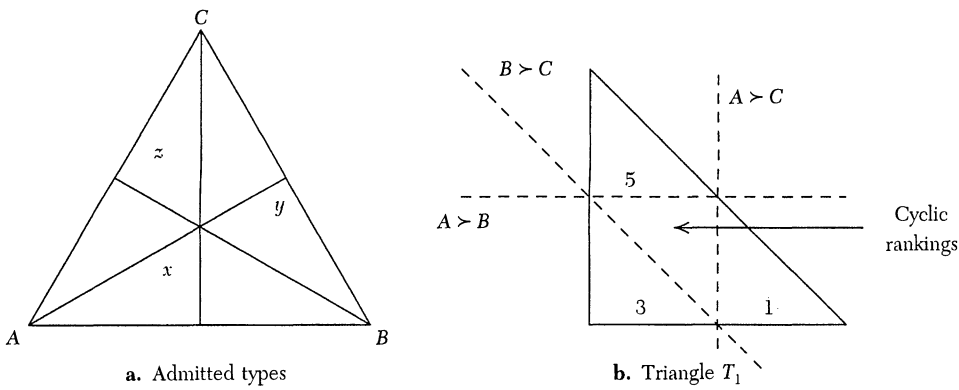

a. Admitted types **b.** Triangle T_1

FIGURE 2
Condorcet example setting.

If n_j is the number of voters of type j, then the total number of voters is $n_1 + n_3 + n_5 = n$. Instead of dealing with integers, we divide by n, so that $x = n_1/n$, $y = n_5/n$, and $z = n_3/n$ represent the fractions of all voters that are of each type. In the textbook example, for instance, $x = y = z = \frac{5}{15}$.

The constraint $x + y + z = 1$, or $z = 1 - (x + y)$, allows us to represent all possible profiles as the (rational) points of the triangle

$$T_1 = \{ (x, y) \mid x, y \geq 0, x + y \leq 1 \}$$

of FIGURE 2b. (The origin is at the lower left corner.) For a point $(x, y) \in T_1$, the fraction of all voters with type 1 and 5 preferences are given, respectively, by the x and y values; the fraction of all voters with a type 3 preference is $1 - x - y$.

Pairwise outcomes One hindrance to our understanding of election behavior is the difficulty of associating profiles with their election outcomes. With geometry, however, this reduces to graphing elementary algebraic equations. In an $\{A, B\}$ election, for instance, it follows from FIGURE 2a that only a type 5 voter votes for B; all other

voters are on the A side of the $A \sim B$ line, so they vote for A. Therefore, B beats A if and only if $y > x + z = x + (1 - x - y)$, or if $y > \frac{1}{2}$. The T_1 boundary for this region is the horizontal dashed line of FIGURE 2b.

The analysis for the remaining two pairs is similar. For an $\{A, C\}$ election, it follows from FIGURE 2a that only type 1 voters prefer $A \succ C$, so A beats C if and only if $x > \frac{1}{2}$; the boundary is the vertical dashed line of FIGURE 2b. Likewise with $\{B, C\}$: candidate C wins if and only if $z = 1 - (x + y) > \frac{1}{2}$, or if $(x + y) < \frac{1}{2}$; the T_1 boundary is the slanted dashed line in FIGURE 2b.

As it is easy to determine which pairwise outcomes occur on each side of each dashed T_1 boundary line, we know which election rankings are associated with each of the four resulting regions of profiles. For instance, the region to the extreme right, with T_1 vertex $(1, 0)$, is on the $A \succ B$, $A \succ C$, $B \succ C$ sides of the boundary lines, so all of these profiles define the type 1 ranking $A \succ B \succ C$. Similarly, two of the other regions identify all profiles resulting in type 3 or type 5 pairwise outcomes. Our real interest is in the remaining small triangle in the center, which identifies all profiles that cause cyclic pairwise outcomes.

To illustrate how to use this geometry, suppose we want to determine the minimum number of voters required to construct examples for any of the admitted outcomes. To do so, notice that n, the total number of voters, is a common denominator for x and y. The answer, then, just involves finding in each region the points (x, y) with the smallest common denominator.

As all points (x, y) with common denominator 2 are either vertices of T_1 or vertices of the small triangle that causes cyclic outcomes, all two-voter examples have either unanimity outcomes, or *non-transitive rankings involving tie votes*. To illustrate, point $(\frac{1}{2}, 0)$ defines the rankings $A \sim C$, $C \sim B$, even though $A \succ B$. (So, peculiar election outcomes already arise with only two voters.) With three voters, $(\frac{1}{3}, \frac{1}{3})$ is in the center of the cyclic region. (Point $(\frac{1}{3}, \frac{1}{3})$ corresponds to modifying table (3) to have only one voter of each type.) Similar arguments show that points on the boundary lines require four voters. Therefore, with no more than four voters, we can create examples of all admitted pairwise rankings.

One of the many oddities of voting theory is how conclusions can depend upon whether the number of voters is odd or even. The geometry shows that this peculiarity is caused by how rational points are distributed within a region, depending on the parity of the smallest common denominator. We illustrate by raising another question: Can cycles occur if only one voter in a large population has type 3 preferences? With n voters, this condition requires $z = 1/n$, so a required (x, y) point must satisfy $x + y = 1 - 1/n$ and be in the cyclic region near $(\frac{1}{2}, \frac{1}{2})$. If n is even, the only choices of $(\frac{n-2}{2n}, \frac{1}{2})$ or $(\frac{1}{2}, \frac{n-2}{2n})$ are not admissible because they are boundary points. Thus, this particular behavior occurs if and only if n is odd and $x = y = \frac{n-1}{2n}$.

Probabilities There is a large literature in which complicated techniques are used to compute the probabilities of various election outcomes. (See, for instance, the excellent bibliography **[4]**.) With geometry, however, it is easy to compute the likelihood of each outcome. For instance, if each point (i.e., each profile) in T_1 is equally likely, then the common areas of the four regions prove that each outcome occurs with probability $\frac{1}{4}$. Similarly, say that a profile probability is *centrally distributed* if the likelihood of profile (p_1, p_2, p_3) is the same as (p_2, p_1, p_3), or of any of the four other ways these p_j values can be permuted. An example is the multinomial distribution. This symmetry over voter types means that with a centrally distributed profile probability, all three transitive outcomes are equally likely. By appealing to the central limit theorem, we identify a wide class of settings where the likelihood of cyclic rankings dominates.

These $\frac{1}{4}$ probability values represent *limits* as the number of voters becomes very large. To explain with n voters, notice that the number of fractions x and y with common denominator n that satisfy $x + y = 0$ (so $z = 1$) is the number of admissible numerators for x; it is 1. Similarly, if $n - j$ of the n voters have type 3 beliefs (so $z = 1 - j/n$), the number of points (x, y) satisfying $x + y = j/n$ is $j + 1$. The standard identity

$$\sum_{j=1}^{k} j = \binom{k+1}{2} = \frac{k(k+1)}{2} \tag{5}$$

ensures that there are $\binom{n+2}{2}$ rational points in T_1 with common denominator n. Therefore, n voters create $\binom{n+2}{2}$ different profiles among these three beliefs.

An important observation (illustrated with $n = 2, 3$) is that these $\binom{n+2}{2}$ points need not be equally distributed among the four regions. So, to compute the number of points (or profiles) in each region, notice that the points in the small triangle defining cyclic outcomes are those (x, y) with $x < 1/2$, $y < 1/2$, and $x + y > \frac{1}{2}$. For odd values of n, j different (x, y) points in the cyclic region satisfy $x + y = 1 - \frac{j}{n} = 1 - z$, $j = 2, \ldots, (n-1)/2$. Using equation (5), this total of $\frac{(n-1)(n+1)}{8}$ points means that the fraction of the T_1 points in the cyclic region is

$$\frac{(n-1)(n+1)}{4(n+1)(n+2)} = \frac{1}{4}\left(1 - \frac{3}{n+2}\right);$$

this tends to $\frac{1}{4}$ as $n \to \infty$. Similarly, for even values of n we have the smaller

$$\frac{1}{4}\left(1 - \frac{9n-6}{(n+1)(n+2)}\right) \to \frac{1}{4}.$$

The following theorem results from similarly easy computations.

THEOREM 1. *When voters are restricted to types* 1, 3, *and* 5, *the four possible strict pairwise outcomes include these three types and the cyclic rankings* $A \succ B \succ C \succ A$. *If profile points in* T_1 *are assumed to be centrally distributed, then the three transitive rankings are equally likely. In the case of n voters, and we assume that all points in* T_1 *are equally likely, the probability of strict rankings with cyclic outcomes is* $\frac{1}{4}\left(1 - \frac{3}{n+2}\right)$ *if n is odd and* $\frac{1}{4}\left(1 - \frac{9n-6}{(n+1)(n+2)}\right)$ *if n is even. The likelihood of a strict transitive ranking is* $\frac{1}{4}\left(1 + \frac{1}{n+2}\right)$ *if n is odd and* $\frac{1}{4}\left(1 - \frac{1}{n+1}\right)$ *if n is even.*

While the $\frac{1}{4}$ probabilities are rapidly approached as the number of voters increases, notice the strikingly different values that occur for small n-values. For instance, with $n = 3$, instead of approximately $\frac{1}{4}$ of the points in the cyclic region, there are only $\frac{1}{10}$ of them. For $n = 4$, this probability drops to zero, then rebounds to $\frac{1}{7}$ for $n = 5$ only to drop to $\frac{1}{28}$ for $n = 6$. Again, this oddity involving the parity of n reflects the distribution of rational points in T_1.

Positional outcomes The geometry also identifies all possible conflicts between the pairwise and the $\mathbf{w}_\lambda$ outcomes. Using FIGURE 1 to compute candidate B's $\mathbf{w}_\lambda = (1, \lambda, 0)$ tally of an election, notice that she receives one point from each voter who has her top-ranked; these voters are of types 5 and 6, where B is a vertex of the ranking regions. With our FIGURE 2a restriction, B receives $y \times 1$ points. The second place

votes of λ points per voter come from the adjacent 1 and 4 regions of FIGURE 1. With FIGURE 2a, this adds λx points for B. As the remaining two regions (2 and 3) represent where B is bottom-ranked, they contribute no points, so the total tally is $y + \lambda x$. The $\mathbf{w}_\lambda$ tallies for all candidates are as follows:

Candidate	Tally
A	$(-\lambda)x - \lambda y + \lambda$
B	$y + \lambda x$
C	$1 - x + (\lambda - 1)y$

(6)

The rest of the analysis mimics what we did with the pairwise vote. Namely, to determine which profiles define the relative $A \succ B$ or $B \succ A$ rankings, plot the $A \sim B$ boundary line defined by equating the A and B tallies. This defines the parametrized family of equations $(1 - 2\lambda)x - (1 + \lambda)y + \lambda = 0$. Because $x = \frac{1}{3}$, $y = \frac{1}{3}$ satisfies this equation for all λ-values, all of these lines pass through $(\frac{1}{3}, \frac{1}{3})$, which we call the *rotation point*. The line defined by λ is determined by the rotation point and $\left(\frac{-\lambda}{1-2\lambda}, 0\right)$, its x-intercept. The results for all candidate pairs follow:

Pair	Equation	Rotation Pt	x-axis Pt
$A \sim B$	$(1 - 2\lambda)x - (1 + \lambda)y = -\lambda$	$(\frac{1}{3}, \frac{1}{3})$	$\left(\frac{-\lambda}{1-2\lambda}, 0\right)$
$A \sim C$	$(2 - \lambda x + (1 - 2\lambda)y = 1 - \lambda$	$(\frac{1}{3}, \frac{1}{3})$	$\left(\frac{1-\lambda}{2-\lambda}, 0\right)$
$B \sim C$	$(1 + \lambda)x + (2 - \lambda)y = 1$	$(\frac{1}{3}, \frac{1}{3})$	$\left(\frac{1}{1+\lambda}, 0\right)$

(7)

The effects of these lines are depicted in FIGURE 3 for three special cases: the plurality vote ($\lambda = 0$); the Borda Count ($\lambda = \frac{1}{2}$); and the antiplurality method ($\lambda = 1$). This figure identifies interesting behavior because it displays how election outcomes change with the procedure. To explain, notice that although the three boundary lines for the $\lambda = 0$ and $\lambda = 1$ triangles agree, each line is identified with a different pair of candidates. Connecting them is a fascinating rotation where, as the value of λ increases, each boundary line rotates in a clockwise direction from its $\lambda = 0$ setting to reach the adjacent boundary line position when $\lambda = 1$. For instance, the $A \sim C$

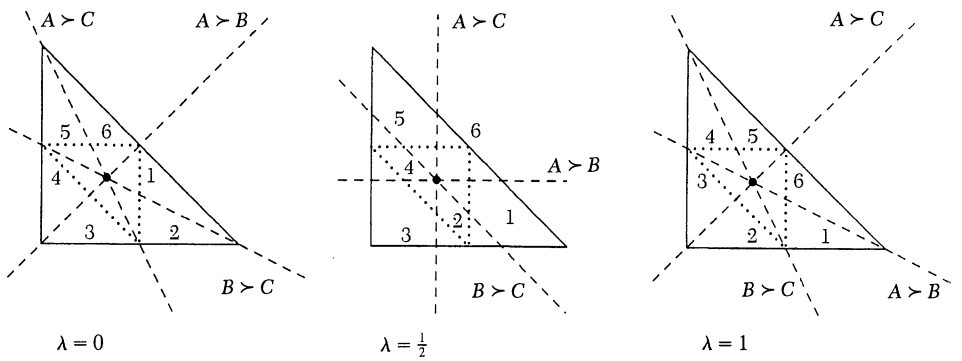

FIGURE 3
Computing $\mathbf{w}_\lambda$ outcomes.

boundary line passes through the $(0, 1)$ vertex of T_1 when $\lambda = 0$ (the plurality vote), becomes vertical when $\lambda = \frac{1}{2}$ (the Borda Count), and stops at what had been the $A \sim B$ original position when $\lambda = 1$.

An immediate consequence of this rotation is that, with the exception of the $(\frac{1}{3}, \frac{1}{3})$ point (the Condorcet profile where all $\mathbf{w}_\lambda$ methods have a completely tied outcome), each profile experiences *three different* $\mathbf{w}_\lambda$ *election rankings as* λ *varies through its admissible values*. If a point is on a boundary line when $\lambda = 0$, then two of the rankings have ties and one is strict. Otherwise, two of the rankings are strict and one involves a pairwise tie. The geometry shows that, rather than being an isolated phenomenon, conflict is unavoidable.

As a second consequence, consider a region with transitive pairwise votes; say, the region labeled "1" in FIGURE 2b. (In FIGURE 3, this set of profiles is the region to the right of the vertical dotted line.) By examining this region in the $\lambda = 0$ and $\lambda = 1$ triangles, we see that these profiles allow two different strict plurality and antiplurality election outcomes. For instance, the pairwise $A \succ B \succ C$ outcome is accompanied by a plurality ranking of either $A \succ B \succ C$ (type 1) or the conflicting $A \succ C \succ B$ (type 2). While the difference in outcomes creates a conflict, at least the plurality and pairwise procedures agree on which candidate is top-ranked. A similar analysis holds for the antiplurality $\lambda = 1$ where the conflicting ranking is $B \succ A \succ C$ (type 6). Here, however, the pairwise and antiplurality methods agree only on who should be bottom-ranked; they can disagree on the rest of the ranking and who should win.

The Borda Count allows not only two but *three* strict rankings for profiles from each of the three strict pairwise ranking regions. In fact, the rotation of the indifference lines and the monotonicity of the x coordinate (of the "x-axis point" in table (7) proves that for each $\lambda \in (0, 1)$, $\mathbf{w}_\lambda$ *admits three different strict election rankings for each of the three sets of profiles*. This, of course, provides plenty of robust examples of conflict between the pairwise and $\mathbf{w}_\lambda$ rankings.

The triangle defining cyclic pairwise outcomes admits even more conflict: here, anything can happen with any $\mathbf{w}_\lambda$ method. Namely, accompanying a pairwise cycle, we can have any strict $\mathbf{w}_\lambda$ ranking, any $\mathbf{w}_\lambda$ ranking with one pair tied, or a completely tied outcome.

Because (from elementary trigonometry) all ranking regions of the $\lambda = 0$ and $\lambda = 1$ triangles have the same area, each has the (limiting) probability of $\frac{1}{6}$. This is also true for the smaller triangle with cyclic pairwise voting. Consequently in either case—whether we consider all profiles in T_1 or restrict attention to profiles causing pairwise cycles—the limiting probability for any strict ranking for the $\lambda = 0, 1$ procedures is $\frac{1}{6}$. The Borda Count ($\lambda = \frac{1}{2}$) favors the three outcomes of types 1, 3, and 5 (the types from the profile) with limiting probability of $\frac{2}{9}$; the remaining three types have limiting probabilities of $\frac{1}{9}$. What connects these different values is that (from the x-axis values of table (7)) the areas of some regions monotonically decrease, while others increase, as $\lambda \to \frac{1}{2}^-$. Then they change to monotonically approach the common value $\frac{1}{6}$ as $\lambda \to 1$. These statements, and others are equally easy to verify, are collected in the following theorem:

THEOREM 2. *If the three voter types* 1, 3, *and* 5 *are allowed, then each profile that is not a Condorcet profile admits three different* $\mathbf{w}_\lambda$ *election outcomes as* λ *varies.*

The set of profiles with pairwise votes that define a particular strict transitive outcome allows only two strict election rankings with the plurality and with the antiplurality vote. In each case, one of these outcomes agrees with the pairwise rankings. All other $\mathbf{w}_\lambda$ *outcomes admit three different strict rankings, one of which agrees with the pairwise ranking. The profile set causing cyclic pairwise outcomes admits all possible* $\mathbf{w}_\lambda$ *rankings.*

If all T_1 points are equally likely, then the limiting probability of any strict election ranking (in either the set of all profiles or the cyclic region) is $\frac{1}{6}$ for $\lambda = 0, 1$. For the Borda Count the limiting probability for either setting is $\frac{2}{9}$ for outcomes of types 1, 3, and 5, and $\frac{1}{9}$ for the remaining three types.

The likelihood of an election outcome being of a particular type either strictly increases or strictly decreases as $\lambda \to \frac{1}{2}$.

These results show that even with only three types of voter preferences, conflict can arise among the pairwise and positional election outcomes. So, which procedure is "best?" Frankly, the answer is not clear from this information. For instance, the fact that the plurality and pairwise outcomes identify the same candidate as being top-ranked can be fashioned into a strong argument in favor of the plurality vote—at least for this setting. On the other hand, the ranking of a unanimity profile should be its election ranking, so we should expect election outcomes to favor the three particular types represented in the profile. This is true for the Borda Count, but only to a lesser degree for the other $\mathbf{w}_\lambda$ methods. This observation can be developed into an argument supporting the Borda Count. With a little imagination, an argument can probably be fashioned to support any other procedure. So which procedure should we use?

4. The Beverage Example Revisited

While the Condorcet setting allows profiles to have different $\mathbf{w}_\lambda$ outcomes, the conflict is nowhere near as spectacular as that displayed in the beverage example, where completely reversed $\mathbf{w}_\lambda$ election rankings occur for different λ values. This example, where two of the preferences share an edge of the FIGURE 1 triangle and the third ranking is from a ranking region with the remaining vertex, captures a familiar election setting where one candidate, A, is favored (top-ranked) by a portion of the voters, but strongly opposed (bottom-ranked) by the rest of them. The voters who dislike A, however, split in their opinions about the other two candidates. (This may have been the situation created by the candidacy of P. Buchanan during the 1996 Republican Presidential primaries.) As in FIGURE 4a, define $x = n_2/n$, $y = n_5/n$, and $z = n_4/n$. To connect the beverage example with FIGURE 4a, identify M, B, W respectively with A, B, C so that beverage profile of equation (1) becomes $x = \frac{6}{15}$, $y = \frac{4}{15}$, and $z = \frac{5}{15}$.

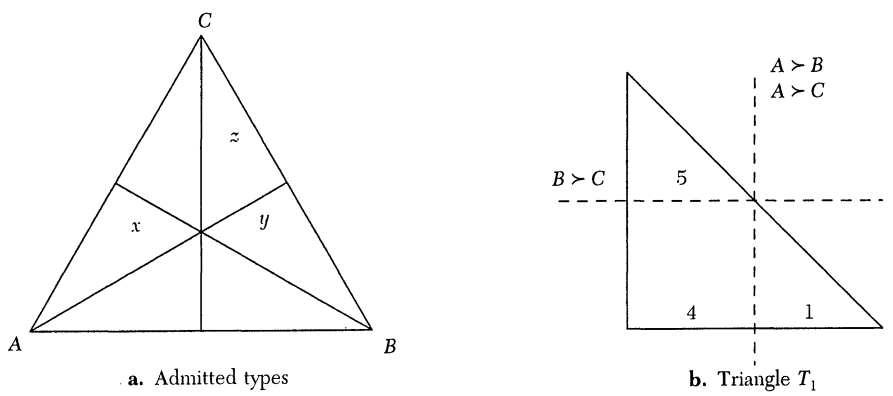

a. Admitted types **b.** Triangle T_1

FIGURE 4
The beverage example setting.

Again, the $z = 1 - (x + y)$ restriction allows all possible profiles to be represented as (rational) points in the FIGURE 4b triangle $T_2 = \{(x, y) \mid x, y \geq 0, x + y \leq 1\}$.

Pairwise outcomes Just as in Section 3, identifying profiles with their accompanying pairwise outcomes involves only elementary algebra. As FIGURE 4a shows, in an $\{A, B\}$ election only type 2 voters vote for A, so A beats B if and only if $x > \frac{1}{2}$. Similarly, in an $\{A, C\}$ election, A beats C if and only if $x > \frac{1}{2}$. The common T_2 boundary for these conditions is the vertical dashed line of FIGURE 4b. For the remaining pair $\{B, C\}$, B wins if and only if $y > \frac{1}{2}$; here the T_2 boundary is the horizontal dashed line in FIGURE 4b.

The pairwise election combinations allow only three (strict) transitive pairwise ranking outcomes; no real surprises occur with the pairwise vote. The election rankings are denoted in FIGURE 4b with the voter type numbers. Again, by assuming that each T_2 point is equally likely, the areas of these regions show that the pairwise outcomes define the type 4 ranking $C \succ B \succ A$ (of the beverage example) with limiting probability $\frac{1}{2}$, and each of the other two types with limiting probability $\frac{1}{4}$. Again, elementary computations using equation (5) show that these limiting values are approached with order $1/n$.

Positional outcomes This setting's particular interest is in the conflict among the pairwise and $\mathbf{w}_\lambda$ outcomes. As in Section 3, the $\mathbf{w}_\lambda$ tally for each candidate is as follows:

Candidate	Tally
A	x
B	$y + \lambda z = (1 - \lambda)y - \lambda x + \lambda$
C	$z + \lambda(x + y) = 1 - (1 - \lambda)(x + y)$

(8)

By setting pairs of tallies equal to each other, the $\mathbf{w}_\lambda$ outcomes change according to the following table of parametrized equations.

Pair	Equation	Rotation Pt	x-axis Pt
$A \sim B$	$(1 + \lambda)x - (1 - \lambda)y = \lambda$	$\left(\frac{1}{2}, \frac{1}{2}\right)$	$\left(\frac{\lambda}{1+\lambda}, 0\right)$
$A \sim C$	$(2 - \lambda)x + (1 - \lambda)y = 1$	$(1, -1)$	$\left(\frac{1-\lambda}{1-2\lambda}, 0\right)$
$B \sim C$	$(1 - 2\lambda)x + 2(1 - \lambda)y = 1 - \lambda$	$\left(0, \frac{1}{2}\right)$	$\left(\frac{1-\lambda}{1-2\lambda}, 0\right)$

(9)

A major difference from Section 3 is that the rotation point of each line differs with each pair. As we will see, this is what causes new kinds of election outcomes to occur. The boundary lines, and the resulting division of profiles identified with the plurality ($\lambda = 0$), Borda ($\lambda = \frac{1}{2}$), and antiplurality ($\lambda = 1$) voting systems, are represented in FIGURE 5. (The three rotation points are indicated by the solid dots.)

These figures immediately disclose all sorts of conflicting election outcomes. For instance, the square defined by the dotted lines are all profiles defining the $C \succ B \succ A$ pairwise ranking. The $\lambda = 0$ portion of FIGURE 5 shows that these pairwise rankings can be accompanied by *any* plurality ranking. In other words, expect conflict; the table (1) example demonstrates only the one possibility of a $A \succ B \succ C$ plurality outcome.

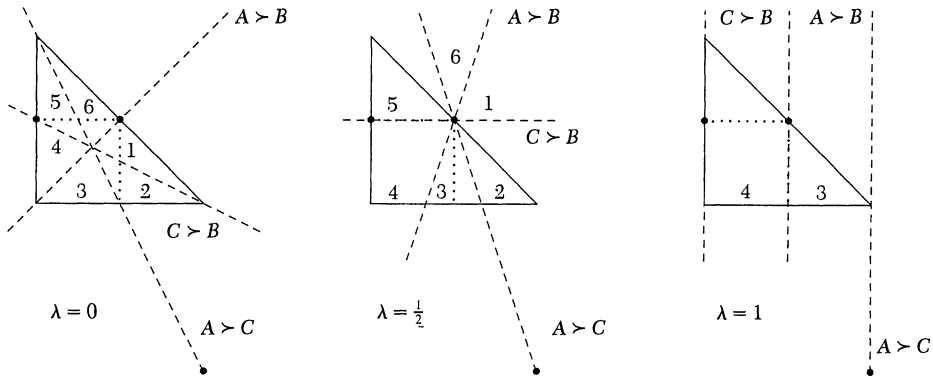

FIGURE 5
Computing $\mathbf{w}_\lambda$ outcomes.

Moreover, it appears from these figures (and we show next why it is true) that the same serious conflict holds for *all* $\mathbf{w}_\lambda$ where $0 \le \lambda < \frac{1}{2}$.

To find even more fascinating changes, notice the importance of the profile which defines a completely tied $\mathbf{w}_\lambda$ election outcome. By being on the boundary for all $\mathbf{w}_\lambda$ ranking regions, this point identifies how election rankings vary with λ. We already know there are significant changes because for $\lambda = 0$ the point is at the safe $(\frac{1}{3}, \frac{1}{3})$ location (with one voter for each of the three preferences); it moves to the T_2 boundary at $(\frac{1}{2}, \frac{1}{2})$ when $\lambda = \frac{1}{2}$; it vanishes at infinity when $\lambda = 1$. These changes in position are direct consequences of the different locations of the rotation points for each pair.

This observation suggests that important information about election behavior is obtained by plotting how this point of a completely tied election varies with λ. This point is the intersection of the $A \sim B$ and $B \sim C$ boundary surfaces, so, by solving these equations for (x, y) in terms of λ, the equation for this point is

$$(x, y) = \left(\frac{1+\lambda}{3}, \frac{1-\lambda+\lambda^2}{3(1-\lambda)} \right), \qquad 0 \le \lambda \le 1, \tag{10}$$

or, because $\lambda = 3x - 1$,

$$y = \frac{1-3x+3x^2}{2-3x} = -x + \frac{1}{3} - \frac{1}{3(3x-2)}.$$

This curve is plotted in FIGURE 6 along with the $\lambda = 0$ boundary lines. The accompanying magnified version shows the translated $\lambda = \frac{1}{4}$ boundary lines.

As FIGURE 6 offers a wealth of information about election behavior, so we describe only what happens to the profiles in the square defined by the dotted lines (with a $C \succ B \succ A$ pairwise ranking); analysis of the other regions is left to the interested reader. First, the fact that the curve approaches infinity as $\lambda \to 1$ is what allows the $\lambda = 1$ figure to have parallel, vertical boundary lines; this is true for no other λ value. Consequently, *for all* $\lambda < 1$, *at least two different* $\mathbf{w}_\lambda$ *strict rankings accompany the* $C \succ B \succ A$ *pairwise outcomes*. Because the point of complete ties leaves T_2 only after the Borda Count, *for* $\lambda < \frac{1}{2}$ *any conflicting* $\mathbf{w}_\lambda$ *ranking can accompany these pairwise rankings*.

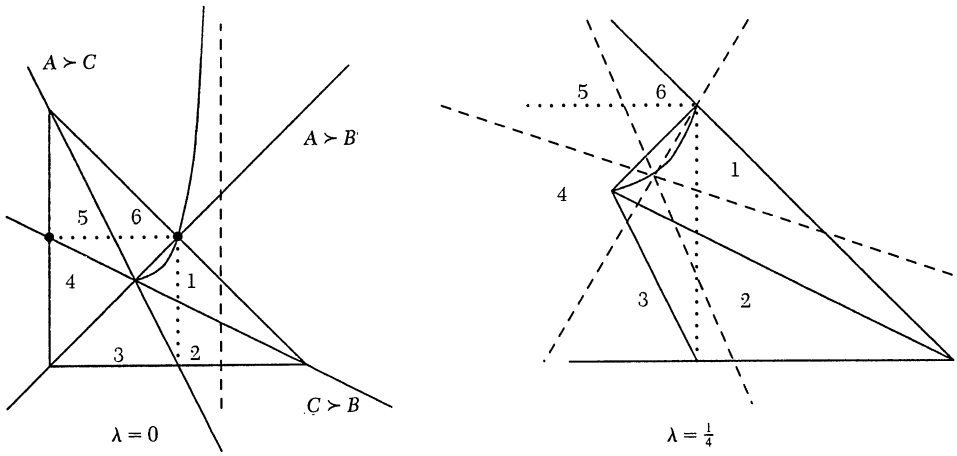

FIGURE 6
Locus of the completely tied points.

This curve also determines how $\mathbf{w}_\lambda$ rankings change with a fixed profile. To indicate the analysis, consider a profile $\mathbf{p}$ located between the curve and the $A \sim B$ plurality line. Although the plurality election ranking for $\mathbf{p}$ is $A \succ B \succ C$, as λ increases in value the $\mathbf{w}_\lambda$ complete tie point moves along the curve forcing different ranking regions to cross $\mathbf{p}$. This can be illustrated with the magnified version of a portion of T_2 in FIGURE 6 which shows the $\lambda = \frac{1}{4}$ regions. If $\mathbf{p}$ has a type 4 election outcome for $\lambda = \frac{1}{4}$, then $\mathbf{p}$ already produced election outcomes of types 1, 6, and 5 for earlier λ values. As table (4) shows, $\mathbf{p}$ has the property that each candidate wins with the appropriate $\mathbf{w}_\lambda$. Furthermore, counting tied outcomes shows that each profile in the region between the curve and the $A \sim B$ plurality boundary line admits *seven different election rankings* for different $\mathbf{w}_\lambda$ procedures. (A similar argument shows that profiles below the curve and with the $A \succ B \succ C$ plurality election outcome have seven rankings where each candidate is bottom-ranked with some $\mathbf{w}_\lambda$.)

The next natural question is to find the smallest number of voters allowing the peculiarity that anyone can be elected. This requires finding a point (x, y) in this region with the smallest possible common denominator. Because (x, y) must satisfy $\frac{1}{3} < x < \frac{1}{2}$ and $y < x$, while being above the curve (so $y > \frac{1}{3}$), we start by seeking a point with least common denominator so that $\frac{1}{3} < y < x < \frac{1}{2}$. This point is $(\frac{5}{11}, \frac{4}{11})$, so examples require at least eleven voters. As the first point above the curve is $(\frac{8}{19}, \frac{7}{19})$, the desired profile involves nineteen voters. It is

Number	Preferences
8	$A \succ C \succ B$
7	$B \succ C \succ A$
4	$C \succ B \succ A$

(11)

where $\lambda \in (\frac{1}{4}, \frac{3}{11})$ ensures the victory of B.

We can find even more. The limiting probability of this peculiar behavior depends on the area between the curve and the $\lambda = 0$ boundary line for $A \sim B$ (that is, the line

$y = x$). This area is

$$\int_{\frac{1}{3}}^{\frac{1}{2}} \left(2x - \frac{1}{3} + \frac{1}{3(3x-2)}\right) dx = \frac{1}{12} - \frac{1}{9}\ln 2.$$

By considering only the profiles in the square (with area $\frac{1}{4}$), the limiting probability is four times this value, or $\frac{1}{3} - \frac{4}{9}\ln 2 \approx 0.0253$.

A small selection of the election behavior attributed to profiles restricted to the "beverage-type" preferences follows.

THEOREM 3. *Suppose the profiles are restricted to preferences from the beverage example. With limiting probability* $\frac{1}{6} - \frac{2}{9}\ln 2$, *it is possible for a profile to elect all three candidates when the ballots are tallied with different* $\mathbf{w}_\lambda$ *methods. The profile must have at least* 19 *voters; the smallest such profile is given in table* (11). *When restricted to where the pairwise votes define the* $C \succ B \succ A$ *ranking, the probability of this behavior is* $\frac{1}{3} - \frac{4}{9}\ln 2$.

The election phenomenon where each candidate is bottom-ranked with some $\mathbf{w}_\lambda$ *procedure has limiting probability* $\frac{1}{6} - [\frac{1}{6} - \frac{2}{9}\ln 2] = \frac{2}{9}\ln 2 \approx 0.1540$. (*When restricted to the profiles with* $C \succ B \succ A$ *pairwise outcomes, the probability is* 0.308.) *All such profiles involve at least nine voters; a nine-voter example results if two voters are removed from each type in table* (1).

For $\lambda = 0$ *the limiting probability of all six possible strict outcomes are equal. For the Borda Count, there are four possible strict outcomes. The limiting probability of a type* 2 *or type* 3 *outcome is* $\frac{1}{6}$, *of a type* 4 *outcome is* $\frac{7}{12}$, *and of a type* 5 *outcome is* $\frac{1}{4}$. *For the antiplurality vote, the limiting probabilities for the type* 3 *and* 4 *outcomes are, respectively,* $\frac{1}{4}$ *and* $\frac{3}{4}$.

5. Symmetry

We have discussed only two of the $\binom{6}{3}$ possible cases. However, by exploiting the symmetry admitted by voting, we have nearly completed the analysis.

Neutrality To introduce the first symmetry, suppose that, for totally unexplained reasons, *everyone* in the beverage example of table (1) confused Beer and Wine. (For instance, a ranking listed as $M \succ W \succ B$ was intended to be $M \succ B \succ W$.) It is easy to correct this mistake: if *all* voters interchanged Wine and Beer on their ballots, then we just interchange Wine and Beer in the election outcomes.

This property, where if every voter permutes the names of the candidates in the same manner, then the election outcome experiences a similar change, is called *neutrality*. More precisely, if σ is a permutation of the names of the candidates, then let $\sigma(\mathbf{p})$ be the profile where these changes occur for each voter in the profile $\mathbf{p}$. Then a voting procedure f satisfies *neutrality* if for any permutation of names σ and for any profile $\mathbf{p}$ we have

$$f(\sigma(\mathbf{p})) = \sigma(f(\mathbf{p})). \tag{12}$$

Neutrality converts our analysis in Section 4 of what happens when voters have types $(2, 4, 5)$ into what happens when voters have types $(1, 4, 5)$. This is because, according to table 1, the second situation is obtained from the first by flipping the triangle about the $B \sim C$ axis. In mathematical terms, by interchanging B and C

names in each ranking of the first setting, we obtain the second one. Thus, the two settings are related by equation (12) and the permutation interchanging B and C.

Other permutations and the resulting settings are listed below. This symmetry and the $(2,4,5)$ prototype account for six of the 20 possibilities.

Setting	Permutation	Setting	Permutation
$(2,4,5)$	Identity	$(1,4,5)$	$B \to C, C \to B$
$(2,3,5)$	$A \to B, B \to A$	$(1,3,6)$	$A \to C, C \to A$
$(2,3,6)$	$A \to B, B \to C, C \to A$	$(1,4,6)$	$A \to C, C \to B, B \to A$

(13)

Similarly, neutrality converts the analysis of Section 3, where voters' preferences come from $\{1,3,5\}$ types, into the setting where voters' preferences come from $\{2,4,6\}$. Here, any transposition, such as $A \to B, B \to A$ suffices. This accounts for eight of the 20 cases.

Reversal To introduce the next voting symmetry, suppose for the beverage example of table (1) that each voter misunderstood the instructions and marked the ballots in a completely reversed order. For instance, voters who marked their ballots as $M \succ W \succ B$ really meant $B \succ W \succ M$. If this reversal holds for all voters, then it is reasonable to assume that the election ranking can be corrected by reversing the original one. Namely, if ρ represents the operation of reversing a ranking, it is natural to assume that

$$f(\rho(\mathbf{p})) = \rho(f(\mathbf{p})).$$

The only difficulty with this assumption is that, in general, it is false. To illustrate with the beverage example, apply the plurality vote to the bottom-ranked candidates to discover that, when preferences are reversed, the plurality election outcome *remains* $M \succ B \succ W$, with a 9:6:0 tally.

To discover what does occur with reversal symmetry, recall that the antiplurality vote requires a voter to vote *against* his or her bottom-ranked candidate. Thus, it is equivalent to voting for our bottom-ranked candidate and then reversing the outcome. So, if we apply the plurality vote to $\rho(\mathbf{p})$ and reverse the resulting ranking, we obtain the antiplurality ranking for $\mathbf{p}$. (Readers may wish to carry out this computation with the beverage example of table (1).) The following theorem asserts that the same reversal effect applies more generally.

THEOREM 4. (*See* [6].) *Let* $f(\mathbf{p}, \mathbf{w}_\lambda)$ *be the* $\mathbf{w}_\lambda$ *election ranking for profile* $\mathbf{p}$. *All profiles* $\mathbf{p}$ *and positional methods satisfy*

$$f(\mathbf{p}, \mathbf{w}_\lambda) = \rho(f(\rho(\mathbf{p}), \mathbf{w}_{1-\lambda})). \tag{14}$$

Equation (14) allows us to handle six more of the $\binom{6}{3}$ cases. To illustrate what happens, some details are given for what we call the "reversed beverage" example, where the preferences are denoted by FIGURE 7a. As A is top-ranked by two types of voters and bottom-ranked by the remaining type, it is reasonable to expect no election surprises. This is not the case; instead, the election behavior is very similar to that described in Section 4. Indeed, the reason for the similarity of outcomes and the "reversed beverage" nomenclature comes from comparing FIGURE 4a and FIGURE 7a. Each letter x, y, and z is reversed relative to the complete indifference point. We emphasize the consequences of this reversal.

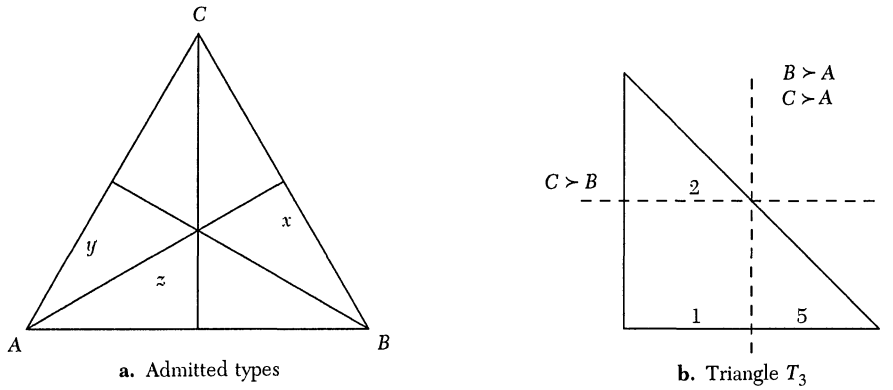

FIGURE 7
The reversed beverage example setting.

One aspect of reversing preference is apparent by comparing FIGURE 4b and 7b: the figures agree, but the rankings are reversed. This reversal continues with the following table, which catalogues information about the $\mathbf{w}_\lambda$ boundary lines:

Pair	Equation	Rotation Pt	x-axis Pt
$A \sim B$	$(2-\lambda)x - \lambda y = 1-\lambda$	$\left(\frac{1}{2}, \frac{1}{2}\right)$	$\left(\frac{1-\lambda}{2-\lambda}, 0\right)$
$A \sim C$	$(1+\lambda)x + \lambda y = 1$	$(1, -1)$	$\left(\frac{1}{1+\lambda}, 0\right)$
$B \sim C$	$(1-2\lambda)x - 2\lambda y = -\lambda$	$\left(0, \frac{1}{2}\right)$	$\left(\frac{-\lambda}{1-2\lambda}, 0\right)$

(15)

To convert table (15) into table (9), let $\mu = 1 - \lambda$. This means that the analysis of table (15) is exactly that of Section 4, except that $\mathbf{w}_{1-\lambda}$ assumes the role of $\mathbf{w}_\lambda$; for example, the antiplurality and plurality methods swap roles, properties, illustrating examples, and peculiarities. This is, of course, a special case of equation (14). For instance, the antiplurality ($\lambda = 1$) outcome is $C \succ B \succ A$ for $(x, y) = \left(\frac{6}{15}, \frac{5}{15}\right)$ from FIGURE 7a. As this profile is the reversal of the beverage example equation (1) with plurality ($\lambda = 0$) outcome $A \succ B \succ C$, the outcome is as Theorem 4 requires.

An easy way to use Theorem 4 to convert results from Section 4 to the current setting is to add or subtract 3 from all of the type numbers of FIGURE 5 and FIGURE 6, and replace statements about λ with statements about $1 - \lambda$. This completes the analysis for the reversed beverage examples. It means, for instance, that only nine voters are needed to create an example where all candidates can be elected with some $\mathbf{w}_\lambda$ and that the likelihood of this occurring is higher than the likelihood of each candidate being bottom-ranked by some procedure. Namely, the reversal of preferences reverses the conclusions obtained from FIGURE 6. Only the Borda Count has essentially identical conclusions for both settings; this is because $\lambda = \frac{1}{2}$ is the only procedure allowing $\mathbf{w}_\lambda = \mathbf{w}_{1-\lambda}$. Incidentally, this symmetry condition turns out to be a technical reason which ensures that the Borda Count has strongly favorable properties.

By applying this analysis along with equation (14) to all of the settings in table (13), we account for six more settings. This leaves only six more to consider.

Final case The final situation is where voters come from types 1, 2, and 3. There are no real surprises in the analysis, so it is left for the interested reader. By use of the symmetry of neutrality, the same analysis extends to the six remaining cases.

6. Summary

Surprisingly subtle, unexpected election behaviors can arise when voters are restricted to only three kinds of preferences. Of particular interest is that the questions raised in Section 1 about potential paradoxical election behavior can be answered by using elementary geometric arguments. As shown, conflict between pairwise and positional methods occurs in abundance and, when it occurs, it is supported by an open set of profiles. (This answers the robustness question.) Problems about the likelihood of strange behavior, or finding supporting profiles with the minimum number of voters, reduce to elementary arguments. Moreover, the geometry allows us to "see" where conflict occurs and to determine whether paradoxical outcomes are, or are not, isolated. For instance, FIGURE 6 identifies the profiles where each candidate wins with an appropriate $\mathbf{w}_\lambda$ method. So, when preferences are restricted as indicated, we must expect such pathological behavior in about 1 in 40 elections (with a sufficient number of voters). As shown by FIGURE 7, other settings increase the likelihood of this behavior to about 3 in 20 elections.

Although we emphasized those election surprises that occur when voters' preferences come from only three possible types, other surprises already occur when preferences are restricted to only two types. Indeed, this is a special case of our analysis because it just requires setting one of x, y, or z equal to zero; it is the behavior on one of the edges of the triangles T_1, T_2, or T_3. For instance, by considering the vertical leg (where $x = 0$) of the triangles in FIGURE 5, we discover how this highly restrictive case allows two strict pairwise rankings to be accompanied with conflicting $\mathbf{w}_\lambda$ outcomes. Without question, elections admit surprising behavior.

Acknowledgment This work was started while Saari was visiting CREME; he thanks his host M. Salles. Saari's research was supported by his Arthur and Gladys Pancoe Professorship; Valognes' research was supported by CREME. We thank P. Zorn for his several helpful suggestions.

REFERENCES

1. J. C. de Borda, *Mémoire sur les élections au scrutin*, Histoire de l'Académie Royale des Sciences, Paris, 1781.
2. M. -J. Condorcet, *Éssai sur l'application de l'analyse à la probabilité des décisions rendues à la pluralité des voix*, Paris, 1785.
3. A. H. Copeland, A reasonable social welfare function. Mimeo, University of Michigan, 1951.
4. J. S. Kelly, Social choice bibliography, *Social Choice & Welfare* 8 (1991), 97–169.
5. J. Kemeny, Mathematics without numbers, *Daedalus* 88 (1959), 571–591.
6. D. G. Saari, *Basic Geometry of Voting*, Springer-Verlag, New York, NY, 1995.
7. D. G. Saari, Voting paradoxes revealed and explained 1: Simple case, Northwestern University Discussion paper #1179 (Jan. 1997).
8. D. G. Saari, Voting paradoxes revealed and explained 2: General case, Northwestern University Discussion paper #1187 (April 1997).
9. D. G. Saari, Are individual rights possible?, this MAGAZINE 70 (April 1997), 83–92.
10. D. G. Saari and V. Merlin, A geometric examination of Kemeny's rule, Northwestern University, preprint (April 1997).
11. D. G. Saari and V. Merlin, The Copeland method 1: Relationships and the dictionary, *Econ. Theory* 8 (1996), 51–76.

Global Positioning System: The Mathematics of GPS Receivers

RICHARD B. THOMPSON
University of Arizona
Tucson, AZ 85721

Introduction

GPS satellite navigation, with small hand-held receivers, is widely used by military units, surveyors, sailors, utility companies, hikers, and pilots. Such units are even available in many rental cars. We will consider the mathematical aspects of three questions concerning satellite navigation.

How does a GPS receiver use satellite information to determine our position?

Why does the determined position change with each new computation, even though we are not moving?

What is done to improve the accuracy of these varying positions?

We will see that receivers use very simple mathematics, but that they use it in highly ingenious ways.

Being able to locate our position on the surface of the earth has always been important for commercial, scientific, and military reasons. The development of navigational methods has provided many mathematical challenges, which have been met and overcome by some of the best mathematicians of all time.

Navigation by means of celestial observation, spherical trigonometry, and hand computation had almost reached its present form by the time of Captain James Cook's 1779 voyage to the Hawaiian Islands. For the next 150 years these methods were used to determine our location on land or sea. In the 1940s electronic navigation began with the use of fixed, land-based, radio transmitters. The present-day *LOng RAnge Navigation* (LORAN-C) system uses sequenced chains of such transmitters.

The use of satellites in navigation became common in the 1970s, with the introduction of the *Navy Navigation Satellite System* (NAVSAT or TRANSIT). This system uses the Doppler shift in radio frequencies to determine lines of position and locations.

The Satellites

Almost all satellite navigation now uses the *Global Positioning System* (GPS). This system, operated by the United States Department of Defense, was developed in the 1980s and became fully operational in 1995. The system uses a constellation of satellites transmitting on radio frequencies, 1227.60 mHz and 1575.42 mHz.

The original design of the system provided for eighteen satellites, with three satellites in each of six orbits. Currently, there are four satellites in each orbit. In the basic plan, the six orbits are evenly spaced every 60° around the Earth, in planes that

FIGURE 1
The System of Satellites.

are inclined at 55° from the Equator. Orbits are circular, at a rather high altitude of 20,200 kilometers above the surface of the Earth, with periods of twelve hours. FIGURE 1 displays one configuration of the basic eighteen satellites. Although not drawn to scale, it gives the correct feeling that we are living inside a cage of orbiting satellites, several of which are "visible" from any point on the surface of the Earth at any given time.

Receivers

Current GPS receivers are electronic marvels. They are hand-held, run on small batteries, weigh as little as nine ounces, and can cost under $150. We can turn on a receiver at any point on or above the surface of the Earth and, within a few minutes, see a display showing our latitude, longitude, and altitude. The indicated surface position is usually accurate to within 100 meters, and the altitude is usually in error by no more than 160 meters.

How does a small radio receiver listen to a group of satellites, and then compute our position, with great accuracy? We start by noting exactly what sort of information is received from the satellites. Each satellite sends signals, on both of its frequencies, giving (i) its position and (ii) the exact times at which the signals were transmitted.

The receiver also picks up time signals from the satellites, and uses them to maintain its own clock. When a signal comes in from a satellite, the receiver records the difference, Δt, in the time at which the signal was transmitted and the time at which it was received. If the Earth had no atmosphere, the receiver could use the speed, c, of radio waves in a vacuum to compute our distance $d = c \cdot \Delta t$ from the known position of the satellite. This information would suffice to show that we are located at some point on a huge sphere of radius d, centered at the point from which the satellite transmitted. However, the layer of gasses surrounding the Earth slows down radio waves and, therefore, distorts the measurement of distance. Receivers can partially correct for this by allowing for the effect of mean atmospheric density and thickness. Information from several satellites is combined to give the coordinates—latitude, longitude, and altitude—of our position in any selected reference system.

Several factors restrict the accuracy of this process, including: (i) errors in the determined positions of the satellites; (ii) poor satellite positioning; (iii) limitations on

the precision with which times and distances can be measured; and (iv) the varying density of Earth's atmosphere and the angles at which the radio signals pass through the atmosphere. Some of these difficulties are overcome by the use of an ingenious plan that provides the key to GPS technology. It is rather complicated to explore this method in the actual setting of positioning on the Earth: The distances are large, the time differences are small, and the geometry is all in three dimensions. Fortunately, we can capture most of the salient features of GPS receiver operation in a simple two-dimensional model.

A Simple Model

Suppose that you are standing somewhere in a circular lot, with a radius of 100 ft. The lot is paved, except for an irregularly-shaped gravel plot that surrounds you. The mean distance from your position to the edge of the gravel is 20 ft. Cars circle the lot on a road. To determine your position, messengers leave from cars on the road and walk straight toward you. When such a messenger arrives, he tells you where and at what time he left the road. You have a watch and know that all messengers walk at a rate of 5 ft/sec on pavement but slow down to 4 ft/sec on gravel. Our model is shown in FIGURE 2.

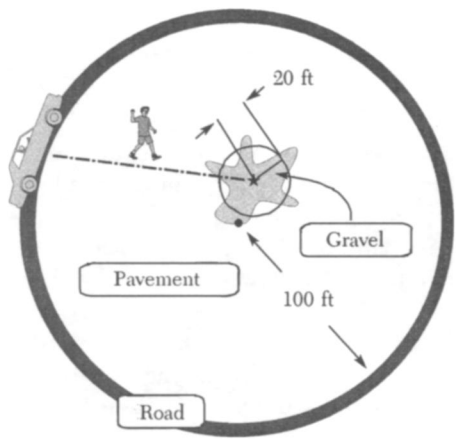

FIGURE 2
The Model.

Consider a rectangular coordinate system with its origin at the center of the lot. Distances will be measured to tenths of a foot, and time will be measured to tenths of a second. The location of a point on the road will be described by its angular distance from due north, measured in a clockwise direction.

At noon a messenger leaves a position 45° from north. When he arrives, your watch shows that it is 20.2 seconds after noon. Since you have no way to know the exact distance that he walked on the gravel, you assume that he covered the mean distance of 20 ft. At 4 ft/sec, this took him 5 sec. For the remaining 15.2 sec he walked on pavement, covering $5\frac{\text{ft}}{\text{sec}} \times 15.2 \text{ sec} = 76.0$ ft. Allowing for the assumed distance of 20 ft on the gravel, you know that you are located at some point on a circle of radius 96.0 ft, centered at the starting location of the messenger.

A second messenger leaves the road at a point 135° from north at 12:01 pm and walks to your position. On his arrival, your watch shows that it is 29.5 sec after he started. Assuming that he took 5 sec to walk 20 ft on the gravel, he walked 5 ft/sec 24.5 sec = 122.5 ft on the pavement. Hence, you are on a circle of radius 142.5 ft, centered at this messenger's point of departure.

The coordinates of the departure points for the two messengers are $P_1 = (100 \cdot \sin 45°, 100 \cdot \cos 45°)$ and $P_2 = (100 \cdot \sin 135°, 100 \cdot \cos 135°)$, respectively. Using our precision of one tenth of a foot, these are rounded to (70.7 70.7) and (70.7, − 70.7). Thus, the coordinates (x_0, y_0), of your position satisfy

$$\left.\begin{aligned}(x_0 - 70.7)^2 + (y_0 - 70.7)^2 &= 96.0^2\\ (x_0 - 70.7)^2 + (y_0 + 70.7)^2 &= 142.5^2\end{aligned}\right\}.$$

The system has two solutions, (−20.0, 39.2) and (161.4, 39.2), rounded to tenths. Since the latter point is outside of the lot, you can conclude that you are located 20.0 ft west and 39.2 ft north of the center of the lot. The situation is shown in FIGURE 3.

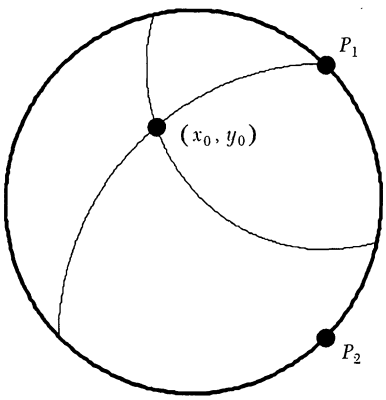

FIGURE 3
Two Messengers.

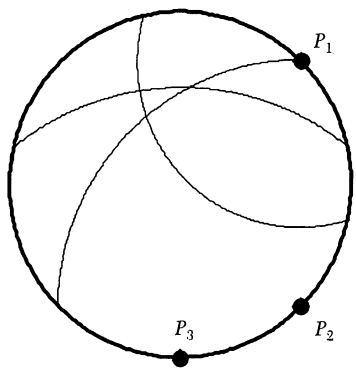

FIGURE 4
Three Messengers.

So far so good. Suppose that, just to be careful, you decide to check your position by having a third messenger leave the road at a point 180° from north and walk to your location. He leaves at 12:02 pm and, according to your watch, arrives 32.2 sec later. As before, you compute your distance from this departure point P_3. FIGURE 4 shows the result of adding information from the third messenger to your picture.

What has happened? *The most likely problem is that your watch does not agree with the times used at the departure points on the road.* Suppose that your watch runs steadily but has a fixed error of ε seconds, where a positive ε means that your watch is ahead of the road times and a negative ε means that your watch is behind the road times. If we let Δt be the time difference between departure and arrival, as shown on your watch, then the estimate for the distance traveled is

$$d(\Delta t, \varepsilon) = 20 \text{ ft} + (\Delta t \text{ sec} - \varepsilon \text{ sec} - 5 \text{ sec}) 5 \frac{\text{ft}}{\text{sec}}.$$

Thus, *the radius of each circle is in error by the same amount, $-5\ \varepsilon$ ft, and there must be a value of ε for which the three circles have a common point.* FIGURE 5 shows the effect of various watch errors.

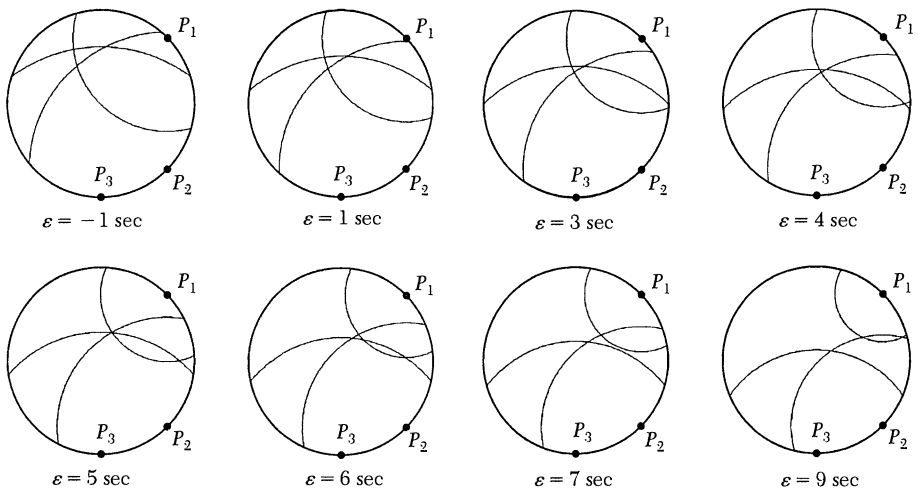

FIGURE 5
Effect of Watch Error.

It appears that your watch has an error of approximately 5 sec. The error and the coordinates of your position are a solution for the following system of equations:

$$\left\{\begin{array}{l}(x_0 - 70.7)^2 + (y_0 - 70.7)^2 = d(20.2, \varepsilon)^2 \\ (x_0 - 70.7)^2 + (y_0 + 70.7)^2 = d(29.5, \varepsilon)^2 \\ (x_0 - 0.0)^2 + (y_0 + 100.0)^2 = d(32.2, \varepsilon)^2\end{array}\right\}.$$

The system can be solved numerically, starting with seed values of 0 for ε and estimated coordinates of your position for x_0 and y_0. There is only one solution giving a location inside of our lot. Rounding this to our level of precision yields $(x_0, y_0, \varepsilon) = (10.9, 31.2, 4.9)$. You conclude that you are 10.9 ft east and 31.2 ft north of the center of the lot, and that your watch is 4.9 sec fast. You note the coordinates of your position, and discard the watch error, which is of no further interest to you.

As this example of our GPS model shows, you can use time difference information from three messengers to determine your position, relative to a coordinate system in the lot. *The only tools needed for this effort are a steady, but not necessarily accurate, watch and the ability to approximate the solution of a system of three equations in three unknowns.*

Back to the Satellites

Our "lot" is now the region inside of the satellite orbits (including the Earth), "cars on the road" are satellites, "messengers" are radio waves, and "gravel" is the Earth's atmosphere. We take the center of the Earth as the origin in our coordinate system. Working in three dimensions, we need information from four satellites. Call these S_1, S_2, S_3, and S_4; and suppose that S_i is located at (X_i, Y_i, Z_i) when it transmits a signal at time T_i. If the signals are received at times T_i', according to the clock in our receiver, we let $\Delta t_i = T_i' - T_i$, and let ε represent any error in our clock's time. The receiver allows for the mean effects of passage through the Earth's atmosphere and

computes distances $d(\Delta t_i, \varepsilon)$ that indicate how far we are from each of the satellites. Our position (x_0, y_0, z_0) is located on each of four huge spheres. In most situations, there will be only one sensible value of ε that allows the spheres to have a point in common. Our location is determined by solving a system equations.

$$\left\{\begin{array}{l}(x_0 - X_1)^2 + (y_0 - Y_1)^2 + (z_0 - Z_1)^2 = d(\Delta t_1, \varepsilon)^2 \\ (x_0 - X_2)^2 + (y_0 - Y_2)^2 + (z_0 - Z_2)^2 = d(\Delta t_2, \varepsilon)^2 \\ (x_0 - X_3)^2 + (y_0 - Y_3)^2 + (z_0 - Z_3)^2 = d(\Delta t_3, \varepsilon)^2 \\ (x_0 - X_4)^2 + (y_0 - Y_4)^2 + (z_0 - Z_4)^2 = d(\Delta t_4, \varepsilon)^2\end{array}\right\}$$

When a numerical solution is found, the rectangular coordinates (x_0, y_0, z_0) are converted into the essentially spherical coordinates of latitude, longitude, and altitude above sea level.

As a practical matter, there are times and locations when a GPS receiver can receive usable data from only three satellites. In such cases, a position at sea level can still be found. The receiver simply substitutes the surface of the Earth for the missing fourth sphere.

To summarize our results so far, the receiver is expected to (i) receive time and position information from the satellites, (ii) maintain a steady (but not necessarily accurate clock), (iii) select four satellites with a good range of positions, (iv) find an approximate numerical solution for a system of four equations, and (v) make a transformation of coordinates. Given the current state of electronics, these are easy tasks for a small hand-held instrument.

Variability of Positions

Our second question about GPS positioning causes a great deal of discussion and confusion among those who use the system. *If a person stands in one fixed location and determines repeated positions with a receiver, the coordinates of these positions will vary over time.* Since the observer's location has not changed, the changing positions are often attributed to alteration of the satellite signals by the Department of Defense. The Department does, at times, degrade the satellite data and cause a loss of GPS accuracy. This *Selective Availability* (SA) will be phased out within the next few years. (It is stated that SA is used for reasons of national security.) However, manipulation of the signals explains very little of the variation in positioning. The variation is primarily caused by random errors in measurement, the selection of different satellites, and by the effects of the atmosphere. We will illustrate these problems by returning to our simple 2-dimensional model.

In our example, you determined that the coordinates of your position were (10.9, 31.2) and that your watch was 4.9 seconds fast. *Suppose that these values are exactly correct.* After a couple of minutes you again use three messengers to determine your location. This time the first messenger leaves from the road at a point that is 47.2° from north. Rounding to your level of precision, you record the departure point as $P_1 = (73.4, 67.9)$. In this case we will assume that your information on the location of the departure point is not quite correct, and that the messenger actually left from $Q_1 = (74.1340, 67.3568)$. This is only a 1.0% error in the first coordinate and a 0.8% error in the second coordinate. Suppose also that the messenger actually encountered 25.9 ft of gravel on his way to your position.

Keeping track of 6 places, the distance from Q_1 to your location is 72.841286 ft. Covering the 25.9 ft of gravel at 4 ft/sec took the messenger 6.475000 sec, and covering the 46.941286 ft of pavement at 5 ft/sec took 9.388257 sec. The actual walking time was 15.863287 sec, which with your watch error of 4.9 sec, is 20.763257 sec. Using the allowed one place of precision, you would note $\Delta t = 20.8$ sec. Recall that, as you stand in the lot, you have no way of knowing the amount of gravel over which a messenger has walked. Hence, you always assume the mean distance of 20 ft. Under this assumption, the messenger would take 5 sec to cover the gravel, leaving 15.8 sec to walk on the pavement. At 5 ft/sec he would cover 79.0 ft. You conclude that the messenger has traveled 99.0 ft, and that you are at that distance from P_1.

To find your position, messengers leave from the road at points 138.5° and 8.1° from north. You record these departure points as $P_2 = (66.3, -74.9)$ and $P_3 = (14.1, 99.0)$. Now suppose that your information is slightly incorrect, and that the departure points are actually $Q_2 = (66.8404, -75.6490)$ and $Q_3 = (13{,}9731, 98.0100)$. In addition, assume that the second messenger walked over 22.1 ft of gravel and that the third messenger walked over 12.0 ft of gravel. Working in the same way as you did for the first messenger, you record time differences of 30.1 sec and 18.9 sec for the second and third messengers, and solve the following system of equations.

$$\left\{\begin{array}{l}(x_0 - 73.4)^2 + (y_0 - 67.9)^2 = d(20.8, \varepsilon)^2 \\ (x_0 - 66.3)^2 + (y_0 + 74.9)^2 = d(30.1, \varepsilon)^2 \\ (x_0 - 14.1)^2 + (y_0 - 99.0)^2 = d(18.9, \varepsilon)^2\end{array}\right\}$$

The solution, when rounded, gives your location as $(x_0, y_0) = (5.4, 32.3)$ and your watch error as 4.4 sec. Small errors in the location of the departure points, variation in the amount of gravel covered, and the rounding of numbers to one-place have produced a "position" that is 5.61 ft from your actual location of (10.9, 31.2).

We can let a computer simulate what happens if you stay in your fixed location and make repeated computations of your position. Each determination of a position is made with the following assumptions. (i) Three points of departure for messengers are picked at random, assuming that the angle between any two points of departure is at least 30°, but not more than 150°. (ii) The distance over which a messenger must walk on gravel is a normal random variable with a mean of 20 ft and a standard deviation of 5 ft. (iii) The relative error in each coordinate of the point of departure is a normal random variable, with a mean of 0 and a standard deviation of 0.3%.

It is common to discuss accuracy of positioning in terms of *circular errors of probability* (c.e.p.). The $n\%$ c.e.p. is the distance, d_n, such that the probability of an error that is less than or equal to d_n is $n\%$. A set of 1,000 simulated positions allowed us to estimate c.e.p.'s for our model. We found $d_{50} = 2.11$ ft and $d_{95} = 7.69$ ft. (It is interesting to note that one simulated position was 16.9 ft from the correct location.) The positions computed in a run of 50 simulations are plotted on the left side of FIGURE 6, along with circles of radii d_{50} and d_{95}. *Our probabilistic model yields results that agree quite well with plots of successive positions found with an actual GPS receiver from a fixed location.*

Commercially available GPS units operate under what is called the *Standard Positioning Service* (SPS), measuring distances using satellites' 1575.42 mHz frequency. Under the best circumstances, the 50% c.e.p. for the SPS is 40 meters. As we mentioned, selective availability adds a small amount of random error into the SPS. At almost all times the 50% c.e.p. is no more than 100 meters, with a common value being around 50 meters. Under these conditions, the 95% c.e.p. for SPS is

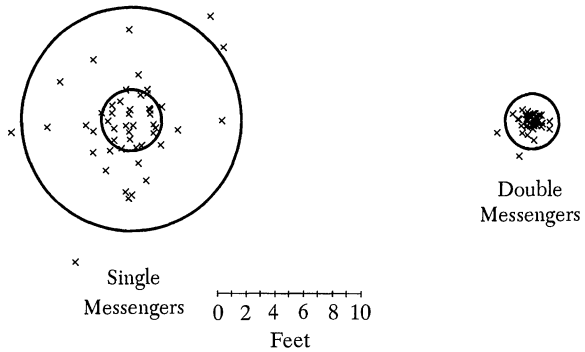

FIGURE 6
Simulations.

approximately 100 meters. As in our model, almost all of the variability in SPS positions comes from random errors that are inherent in the components of the system.

PPS and Differential GPS

What is done to remove some of the random errors from GPS positions? At the present time, there are two common methods of improving GPS accuracy. One of these is the *Precise Positioning Service* (PPS), which is available for governmental use only. This uses signals transmitted on both of the GPS frequencies to eliminate much of the variability caused by the Earth's atmosphere. Just as with various colors of light in the visible spectrum, the reduction in the speed of a radio wave as it passes through the atmosphere depends upon its frequency. Hence, measurements of the arrival times of two signals of different frequencies can be used to greatly improve the accuracy of our distance estimates.

As before, the situation is most easily understood in terms of our simple two-dimensional model. To model the PPS we will suppose that each messenger is accompanied by an assistant, who also walks at 5 ft/sec over pavement. However, while the messenger walks at 4 ft/sec over gravel, the assistant is slowed to 3 ft/sec when walking on gravel. We will return to our first example of the variability of positions and see what improvement in accuracy results from knowledge gained with assistant messengers.

Recall that your location in the lot has coordinates (10.9, 31.2), and that your watch error is 4.9 sec. The first messenger departed from $Q_1 = (74.1340, 67.3568)$ and walked over 25.9 ft of gravel while covering the 72.841286 ft to your position. With your watch error, you recorded a time difference of $\Delta t = 20.8$ sec.

The assistant messenger will require 8.633333 sec to cover the 25.9 ft of gravel at 3 ft/sec and 9.388257 sec to cover the paved part of the route at 5 ft/sec. Hence, his total walking time will be 18.021591 sec. Due to the error in your watch and the allowed level of precision, you record an elapsed time of $\Delta s = 22.9$ sec for the assistant messenger. The time differences for the messenger and the assistant messenger give you enough information to estimate the amount of gravel that lies between you and the point of departure on the road, and to estimate the total distance from your location to the point of departure. If we let G be the number of feet of gravel

and let D be the total distance, in feet, then we have the following system of linear equations:

$$\left\{\begin{array}{l} 20.8 = \dfrac{D-G}{5} + \dfrac{G}{4} \\ 22.9 = \dfrac{D-G}{5} + \dfrac{G}{3} \end{array}\right\}.$$

Solving the system at your level of precision, you conclude that the messenger and his assistant crossed 25.2 ft of gravel, and came 97.7 ft from their point of departure. Thus, as best you can tell, you are at some point on a circle of radius 97.7 ft, centered at the nominal point of departure $P_1 = (73.4, 67.9)$.

Similarly, suppose the second and third messengers also have assistants. Computations similar to those above show that the second messenger traveled 144.8 ft, including 22.8 ft over gravel, and that the third messenger traveled 91.5 ft, including 12.0 ft over gravel. (These values include any possible watch error.) Your estimate for the actual distance that a messenger has traveled is now a function of the distance, G, of gravel covered; the time difference, Δt; and your watch error, ε.

$$d(G, \Delta t, \varepsilon) = G \text{ ft} + \left(\Delta t \text{ sec} - \varepsilon \text{ sec} - \frac{G \text{ ft}}{4\dfrac{\text{ft}}{\text{sec}}}\right) 5\frac{\text{ft}}{\text{sec}}.$$

This distance formula and the three points of departure lead to a system of equations whose solution (x_0, y_0, ε) gives an estimate of the coordinates for your position and for the error of your watch.

$$\left\{\begin{array}{l} (x_0 - 73.4)^2 + (y_0 - 67.9)^2 = d(25.2, 20.8, \varepsilon)^2 \\ (x_0 - 66.3)^2 + (y_0 + 74.9)^2 = d(22.8, 30.1, \varepsilon)^2 \\ (x_0 - 14.1)^2 + (y_0 - 99.0)^2 = d(12.0, 18.9, \varepsilon)^2 \end{array}\right\}.$$

Solving this system, at your level of precision, yields a position of $(x_0, y_0) = (9.2, 31.6)$ and a watch error of 4.8 sec. Your current estimate is only 1.75 ft from your correct location of (10.9, 31.2). This compares with an error of 5.61 ft found by using single messengers.

A computer-generated set of 1,000 simulations for positions computed with messengers and assistants gave estimates of 0.50 ft and 1.90 ft for the c.e.p.'s d_{50} and d_{95}, respectively. The maximum distance of a computed position from the actual location was 3.41 ft. These simulations were based upon the same conditions that we used for our model of the SPS. The positions computed in a run of 50 simulations for our model of PPS are plotted on the right side of FIGURE 6, along with circles of radii d_{50} and d_{95}. Comparison of the two sides of FIGURE 6 shows that there is a considerable gain in accuracy when most of the variation due to distance walked over gravel is eliminated.

In the real world of satellites and positions on the Earth, the use of two radio frequencies in the PPS produces considerably more accuracy than can be obtained with the single-frequency SPS. It is believed that the PPS has a 50% c.e.p. of approximately 16 meters.

A second method for improving the accuracy of the usual SPS locations is coming into use at airports and major harbors. This is called the *Differential Global Positioning System* (DGPS). Most of the error in a GPS position is due to random variables in

the atmosphere and the satellite system. Hence, within a small geographical area, the error at any instant tends to be independent of the exact location of the receiver. DGPS exploits this situation by establishing a fixed base station, whose exact location is already known. Equipment at the base station computes its current "GPS position," compares this with its known location, and continuously broadcasts a correction term. A DGPS receiver in the area receives its own satellite information and computes its position. Simultaneously it receives the current correction from its base station, and applies this to its computed position. The result is a very accurate determination of the receiver's position; 50% c.e.p.'s for GDPS run close to 9 meters.

Conclusions

The very ingenious idea of leaving clock error as a variable allows a GPS receiver to display our position on the Earth at any location and at any time, using nothing more than simple algebra. The variations in computed positions are almost entirely due to inherent limitations on precision within the system. A second clever plan allows the use of two radio frequencies to eliminate much of the variability caused by the passage of signals through the Earth's atmosphere.

REFERENCES

1. Nathaniel Bowditch, American Practical Navigator, Defense Mapping Agency Hydrographic/Topographic Center, 1984.
2. GPS Global Positioning System, a supplemental program produced by the United States Power Squadrons, 1995.
3. Product information, West Marine, Inc., 1997.
4. United States Coast Guard navigation web site, `http://www.navcen.uscg.mil/`

A Convergence of Limits

RICHARD J. BAGBY
New Mexico State University
Las Cruces, NM 88003-8001

Introduction

When in doubt, generalize. That's often good advice for mathematicians, and we follow it here to great advantage. Intrigued by a striking similarity between recursive algorithms for approximating the arctangent and the natural logarithm, we look for a simple theory that includes both. There are certainly enough connections between the two functions to make a common source likely, even though the algorithms seem to have disparate geometrical origins. Instead of focusing on these special cases, we broaden our search, and examine a general method for producing convergent sequences in recursive form. As we study it, a simple pattern emerges, answering the original questions and leading to some unexpected additional results.

We find a simple relation between a type of recursion formula and the limit of the sequence it generates. We discover a single formula unifying our algorithms for the arctangent and the natural logarithm, and that's what produced the similarity. We find other interesting examples; one unifies recursive algorithms for computing the arcsine and the inverse hyperbolic sine. Along the way, we'll see some interesting examples of how mathematics develops. More importantly, we'll leave an idea that undergraduates can use for independent investigations, with a real opportunity to make new discoveries.

A deeper analysis of a family of recursive algorithms for approximating a number of transcendental functions appears in the 1971 article by B. C. Carlson [**1**]. For each choice of f_i and f_j from the list

$$f_1(x, y) = \tfrac{1}{2}(x + y), \qquad f_2(x, y) = \sqrt{xy}$$
$$f_3(x, y) = \sqrt{xf_1(x, y)}, \quad f_4(x, y) = \sqrt{yf_1(x, y)},$$

and for each $x_0, y_0 > 0$, he showed that both the sequences $\{x_n\}$ and $\{y_n\}$ defined recursively by

$$x_{n+1} = f_i(x_n, y_n), \quad y_{n+1} = f_j(x_n, y_n)$$

converge to an integral determined by i and j and involving x_0 and y_0 as parameters. The use of such recursive sequences to compute transcendental functions has a long history, going all the way back to Gauss; Carlson gives a lengthy bibliography. Clearly our results are related to his, but the exact relationship is far from clear; the methods employed are certainly different.

The Arctangent and the Natural Logarithm

Connections between the arctangent and the natural logarithm are known to every student of calculus, since both arise as integrals of rational functions. The connections become much stronger when the functions are extended to complex arguments; Euler's formula for $e^{i\theta}$ is probably the most concise expression of the relationship

between circular and exponential functions. Euler's formula has its origins in the relationship

$$\arctan z = \frac{1}{2i}\log\left(\frac{1+iz}{1-iz}\right),$$

discovered in differential form by John Bernoulli in 1702. Not many years later, R. Cotes found a logarithmic version of Euler's formula; he published it under the title *Harmonia Mensurarum* since it brought together measurements for the circle and the hyperbola. The history of this formula is outlined by J. Stillwell in Chapter 15 of [4].

A simple recursive algorithm for computing arctangents may have been known by Archimedes, even if the modern vocabulary wasn't. The key ideas are all present in his approximation of π by perimeters of circumscribed regular polygons; the change that results from doubling the number of sides is not too hard to analyze. Since the arctangent measures directed arc length on the unit circle, we can approximate it in much the same way as we find the arc length of the whole circle. We form a sequence of circumscribed polygonal paths, all tangent to the arc at its endpoints; the first has two segments and one corner. We form the next by cropping the corner symmetrically. Instead of thinking of the second path as having one long and two short segments, we think of it as four equal segments, each extending from a corner to a point of tangency. At each stage, the next path will be formed by cropping all the corners in the same way, so the nth polygonal path in the sequence is made up of 2^n equal segments and has 2^{n-1} corners.

The details are simple to work out if we introduce Cartesian coordinates, so that arctan x corresponds to the arc of the unit circle between the y-axis and the ray from the origin through $(x, 1)$. FIGURE 1 shows the important relationships. The figure on the left shows how the first path is formed; the one on the right shows how the second path is formed from the first. Referring to the sketch on the left, our first approximation to arctan x is $2s$, and it's easy to calculate s. Since radii and tangents meet orthogonally, the triangle with vertices $(s, 1)$, $(x, 1)$, and $\left(x/\sqrt{x^2+1},\ 1/\sqrt{x^2+1}\right)$ is similar to the one with vertices $(0, 0)$, $(x, 1)$, and $(0, 1)$. Their corresponding sides are proportional, so

$$\frac{x-s}{\sqrt{x^2+1}} = \frac{s}{1}.$$

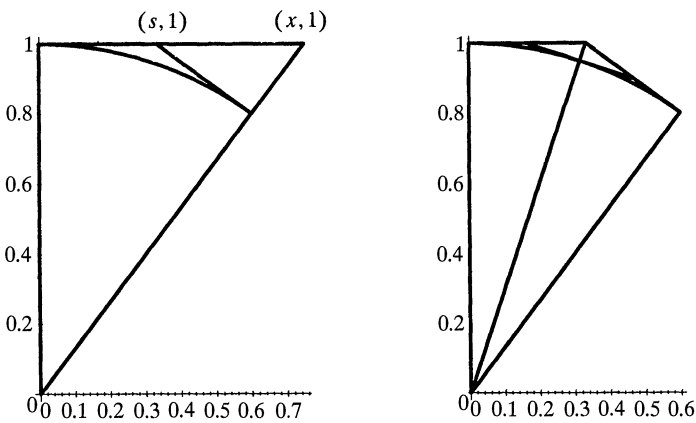

FIGURE 1
Forming circumscribed paths.

Solving for s yields

$$s = \frac{x}{1 + \sqrt{x^2 + 1}}.$$

The same formula can be used when $x < 0$, since the sign of s agrees with the sign of x. More importantly, we can use it to find the length of each of our approximating paths.

Since the nth path is formed by 2^n equal segments, our nth approximation to arctan x is $A_n(x) = 2^n s_n(x)$, with $s_{n+1}(x)$ calculated from $s_n(x)$ exactly as $s_1(x) = s$ was calculated from x:

$$s_{n+1}(x) = \frac{s_n(x)}{1 + \sqrt{s_n(x)^2 + 1}}.$$

Rewriting this in terms of $\{A_n(x)\}$, we obtain the recursive formula

$$A_{n+1}(x) = \frac{2A_n(x)}{1 + \sqrt{2^{-2n}A_n(x)^2 + 1}} \quad \text{for } n \geq 0;$$

starting with $A_0(x) = x$ gives arctan x as the limit of this sequence.

Our recursive algorithm for the natural logarithm is almost as elementary. It's based on the formula

$$\ln x = \lim_{m \to \infty} m\left(\sqrt[m]{x} - 1\right).$$

This arises in many ways; the most elementary is an explicit calculation of $\int_1^x t^{-1}\,dt$ as a limit of Riemann sums. Instead of making Δt_k constant, we partition the interval of integration into subintervals with endpoints at $x^{k/m}$ for $k = 0, 1, 2, \ldots, m$, making $t_k^{-1}\Delta t_k$ constant instead. Fermat used a similar partition to show $\int_0^x t^n\,dt = x^{n+1}/(n+1)$. (For details, see Appendix A.4 of Simmons [3].) The quantity $m(\sqrt[m]{x} - 1)$ is an upper sum for $\int_1^x t^{-1}\,dt$ when $x > 1$, and for $0 < x < 1$ it's an upper sum for $\int_x^1 t^{-1}\,dt$. FIGURE 2 shows the approximation for $x = 3$ and $m = 4$.

Instead of using the whole sequence $\{m(\sqrt[m]{x} - 1)\}$, we restrict our attention to $m = 2^n$. That accelerates the convergence, and the resulting subsequence is simpler to compute. All the roots we need are successive square roots, so we can calculate them recursively. To make the term with $n = 0$ be x instead of $x - 1$, we shift the

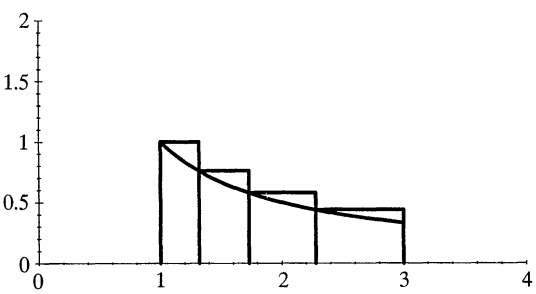

FIGURE 2
Approximating the natural logarithm.

argument and approximate $\ln(x+1)$ instead of $\ln x$. Defining

$$L_n(x) = 2^n\left(\sqrt[2^n]{x+1} - 1\right),$$

we see that $L_0(x) = x$ and

$$L_{n+1}(x) = 2^{n+1}\left(\sqrt{2^{-n}L_n(x)+1} - 1\right) = \frac{2L_n(x)}{1+\sqrt{2^{-n}L_n(x)+1}}.$$

We rewrote our recursion formula as a fraction for two reasons. The last version is computationally superior; loss of significant digits in the square root as $2^{-n}L_n(x) \to 0$ is no longer a problem. Just as importantly, it brings out the similarity between our two recursive algorithms. The similarity increases when we write the limits of the two sequences as integrals:

$$\lim_{n\to\infty} A_n(x) = \arctan x = \int_0^x \frac{dt}{t^2+1}, \quad -\infty < x < \infty,$$

and

$$\lim_{n\to\infty} L_n(x) = \ln(x+1) = \int_0^x \frac{dt}{t+1}, \quad x > -1.$$

Something seems to be happening here. To explain it, we need a general theory that includes both examples.

Generating Recursive Algorithms

An abstract method for deriving similar algorithms is suggested by examining closed-form expressions for both our sequences:

$$A_n(x) = 2^n\tan\left(2^{-n}\arctan x\right),$$

$$L_n(x) = 2^n\left(\sqrt[2^n]{x+1} - 1\right) = 2^n\left[\exp\{2^{-n}\ln(x+1)\} - 1\right].$$

Both have the form $G_n(x) = 2^nF(2^{-n}G(x))$, where F is the inverse of G. In both cases $F(0) = 0$, and that makes

$$\lim_{n\to\infty} G_n(x) = \lim_{t\to 0} \frac{F(tG(x)) - F(0)}{t} = F'(0)G(x).$$

Both have $F'(0) = 1$, and so $G_n(x) \to G(x)$. There's also a common reason why we can write the sequences recursively: in both cases we know how to write $F(\frac{1}{2}y)$ in terms of $F(y)$.

In general, that last condition is the hard one to carry out, even though it's easy in theory. Knowing F and G, we can define a halving function H by the formula $H(x) = F(\frac{1}{2}G(x))$; then for $x = F(y)$ we obtain $F(\frac{1}{2}y) = H \circ F(y)$. Then

$$G_{n+1}(x) = 2^{n+1}F\left(2^{-n-1}G(x)\right) = 2^{n+1}H \circ F\left(2^{-n}G(x)\right) = 2^{n+1}H\left(2^{-n}G_n(x)\right)$$

gives us a recursion rule for a sequence starting with $G_0(x) = F(G(x)) = x$ and converging to $G(x)$.

In practice, finding an explicit formula for H can be impossible, because we may lack a useful formula for F or G. Since H gives us an algorithm for computing G, it's

especially useful to be able to find it in these cases. Fortunately, there's a reasonable way to recognize the halving function when we see it, and it explains the relationship between H and the derivative of G. We state it formally; the proof is quite simple.

THEOREM. *Let I be an interval containing the origin in its interior, and let g be a positive, continuous function on I, with $g(0) = 1$. Let $H: I \to I$ be a solution of the initial value problem*

$$\frac{dH}{dx} = \frac{g(x)}{2g(H)}, \quad H(0) = 0.$$

Then the sequence $\{G_n(x)\}_{n=0}^{\infty}$, defined recursively by

$$G_0(x) = x, \quad G_{n+1}(x) = 2^{n+1} H(2^{-n} G_n(x)),$$

satisfies

$$\lim_{n\to\infty} G_n(x) = \int_0^x g(t)\,dt, \quad \text{all } x \in I.$$

Proof. If we define G on I by the formula $G(x) = \int_0^x g(t)\,dt$, then G is continuous and strictly increasing on I with $G(0) = 0$; it is also differentiable, with $G'(x) = g(x)$. The range of G is therefore an interval J with 0 in its interior, so the inverse F of G is a differentiable function mapping J onto I and satisfying $F'(0) = 1/g(0) = 1$. Thus, for each $x \in I$, $2^{-n} G(x) \in J$ for each nonnegative integer n, and $2^n F(2^{-n} G(x)) \to G(x)$. To complete the proof, we need only show that H is the appropriate halving function.

Define a function Φ on I by the formula

$$\Phi(x) = 2G(H(x)) - G(x), \quad x \in I.$$

Since $H(0) = G(0) = 0$ we have $\Phi(0) = 0$, and

$$\Phi'(x) = 2g(H(x))H'(x) - g(x) = 0, \quad \text{all } x \in I.$$

Hence $\Phi = 0$ on I, and so

$$G \circ H(x) = \frac{1}{2} G(x), \quad \text{all } x \in I.$$

Applying F to both sides yields

$$F\left(\frac{1}{2} G(x)\right) = F(G \circ H(x)) = H(x),$$

and the proof is complete.

In principle, one can find H by solving the initial value problem stated in the theorem. The differential equation can be solved by separation of variables, yielding

$$\int_0^H g(t)\,dt = \frac{1}{2}\int_0^x g(t)\,dt,$$

but that may be a long way from finding an explicit formula for $H(x)$. A much easier task is verifying that a given function is a solution of the differential equation, and sometimes it isn't too hard to guess a solution.

Examples

Our first example includes our recursive algorithms for the arctangent and the natural logarithm. Let a and b be arbitrary real numbers, and let I be the interval containing 0 on which $ax^2 + bx + 1$ is positive. Define g and H on I by the formulas

$$g(x) = \frac{1}{ax^2 + bx + 1}, \quad H(x) = \frac{x}{1 + \sqrt{ax^2 + bx + 1}}.$$

Simple algebraic calculations show

$$\frac{1}{g(H(x))} = aH(x)^2 + bH(x) + 1 = \frac{2(ax^2 + bx + 1) + (bx + 2)\sqrt{ax^2 + bx + 1}}{\left(1 + \sqrt{ax^2 + bx + 1}\right)^2},$$

and so

$$\frac{g(x)}{2g(H(x))} = \frac{2\sqrt{ax^2 + bx + 1} + bx + 2}{2\sqrt{ax^2 + bx + 1}\left(1 + \sqrt{ax^2 + bx + 1}\right)^2}.$$

It's easy to show that this agrees with $H'(x)$, so our theorem says the recursively generated sequence

$$G_0(x) = x, \quad G_{n+1}(x) = \frac{2G_n(x)}{1 + \sqrt{a[2^{-n}G_n(x)]^2 + b[2^{-n}G_n(x)] + 1}}$$

satisfies

$$\lim_{n\to\infty} G_n(x) = \int_0^x \frac{dt}{at^2 + bt + 1}$$

for all finite x such that the interval of integration contains no singularities.

Our next example comes from the arcsine function; the half-angle formula for the sine tells us what the halving function should be. We can include a parameter in g and H:

$$g(x) = \frac{1}{\sqrt{ax^2 + 1}}, \quad H(x) = \frac{x}{\sqrt{2 + 2\sqrt{ax^2 + 1}}}.$$

Differentiating $H(x)^2$ and simplifying the result leads to the identity

$$\frac{1}{2}xg(x) = 2H(x)H'(x),$$

and simplifying $aH(x)^2 + 1$ leads to

$$xg(H(x)) = 2H(x).$$

Division then shows

$$\frac{g(x)}{2g(H(x))} = H'(x).$$

The case $a = -1$ corresponds to an algorithm for the arcsine, while $a = 1$ gives the inverse hyperbolic sine.

Our final example involves a pair of lesser-known transcendental functions we found in Carlson [1]. They are the inverse lemniscatic sine

$$\operatorname{arcsl} x = \int_0^x \frac{dt}{\sqrt{1-t^4}}$$

and its hyperbolic twin

$$\operatorname{arcslh} x = \int_0^x \frac{dt}{\sqrt{1+t^4}}.$$

Historically, these integrals are quite important; an identity for the first, discovered by G. C. Fagnano in 1718, spurred Gauss's study of elliptic functions. Stillwell gives an account of these developments in [4].

The inverse lemniscatic sine has a simple geometric interpretation in terms of the curve defined parametrically by

$$x = \frac{1}{\sqrt{2}} t\sqrt{1+t^2}, \quad y = \frac{1}{\sqrt{2}} t\sqrt{1-t^2}, \quad -1 \le t \le 1.$$

It's plotted in FIGURE 3, along with the chord subtended by the image of $[0, 0.9]$. The parameter t is a geometric one, since $x^2 + y^2 = t^2$. The curve is easily recognized as following a lemniscate, since

$$x^2 - y^2 = t^4 = \left(x^2 + y^2\right)^2;$$

the polar form of this equation is $r^2 = \cos 2\theta$. We've parametrized the portion in the first and third quadrants. An elementary calculation shows

$$\left(\frac{dx}{dt}\right)^2 + \left(\frac{dy}{dt}\right)^2 = \frac{1}{1-t^4}.$$

Thus the integral defining arcsl x represents directed arc length along the curve, with the argument x corresponding to directed chordal length. The inverse lemniscatic hyperbolic sine derives its name from the analogy with the integrals defining the arcsine and the inverse hyperbolic sine, rather than from a geometric interpretation of the integral.

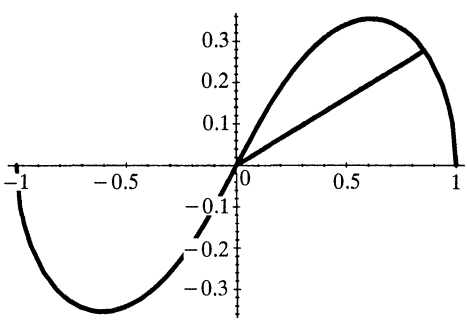

FIGURE 3
The curve defining arcsl x.

Fagnano found the duplication formula

$$\operatorname{arcsl} x = 2\operatorname{arcsl} z, \quad \text{where} \quad x = \frac{2z\sqrt{1-z^4}}{1+z^4} \quad \text{and } z^2 \le \sqrt{2}-1;$$

we solved for z to obtain a halving function. Once again we can insert a parameter to treat both arcsl x and arcslh x with a single formula. Defining

$$g(x) = \frac{1}{\sqrt{1+ax^4}} \quad \text{and} \quad H(x) = \frac{x}{\left(\sqrt{2+2\sqrt{1+ax^4}}+1+\sqrt{1+ax^4}\right)^{1/2}}$$

yields $2H'(x) = g(x)/g(H)$. The calculation justifying this equation is lengthy; we omit it.

Analyzing the Convergence

It's easy to use the closed-form expression

$$G_n(x) = 2^n F(2^{-n} G(x))$$

to establish the rate of convergence of $\{G_n(x)\}$; just use a Taylor expansion of F. For example, our sequence $\{L_n(x)\}$ converging to $\ln(1+x)$ satisfies

$$\begin{aligned} L_n(x) &= 2^n\left[\exp\left(2^{-n}\ln(1+x)\right)-1\right] \\ &= \ln(1+x) + \frac{[\ln(1+x)]^2}{2!2^n} + \frac{[\ln(1+x)]^3}{3!2^{2n}} + \cdots. \end{aligned}$$

Unless $|\ln(1+x)|$ is quite large, thirty to forty iterations of the formula will achieve the same level of accuracy available on most hand-held calculators. Comparable accuracy can be obtained more quickly by using Richardson extrapolation, a technique described in most introductory numerical analysis texts (see, e.g., **[2]**). In particular, using $2L_{n+1}(x) - L_n(x)$ leaves an error on the order of 2^{-2n} instead of 2^{-n}.

It would be interesting to find additional examples where H and G or g are both known explicitly; we certainly haven't exhausted all the possibilities. There's lots of room for experimentation here, and very little knowledge is needed to do it. In addition to starting with g and trying to find H, it's also possible to start with H and use the recursive sequence to define G. But then it's a real challenge to identify G in terms of familiar functions.

Acknowledgment. I thank the referees for a number of helpful suggestions.

REFERENCES

1. B. C. Carlson, Algorithms involving arithmetic and geometric means, *Amer. Math. Monthly* 78 (1971), 496–505.
2. D. R. Kincaid and E. W. Cheney, *Numerical Analysis*, Brooks/Cole, Pacific Grove, CA, 1991.
3. G. F. Simmons, *Calculus with Analytic Geometry*, McGraw-Hill, New York, NY, 1985.
4. J. Stillwell, *Mathematics and Its History*, Springer-Verlag, New York, NY, 1989.

NOTES

Squares Inscribed in Angles and Triangles

HERBERT BAILEY
Rose-Hulman Institute of Technology
Terre Haute, IN 47803

DUANE DETEMPLE
Washington State University
Pullman, WA 99164-3113

Introduction For a square to be inscribed in a triangle, one side of the square must rest on one side of the triangle and the other two vertices of the square must lie on the other two sides of the triangle. We define a square to be inscribed in an *angle* if one side of the square rests on one side of the angle, a third vertex is on the other side of the angle, and the fourth vertex is in the interior of the angle. These definitions include obtuse angles if the square is permitted to rest on an extended side of the triangle (or angle). With this extended definition of inscribed, the results of this paper are also valid for obtuse angles and obtuse triangles. Examples are shown in FIGURE 1.

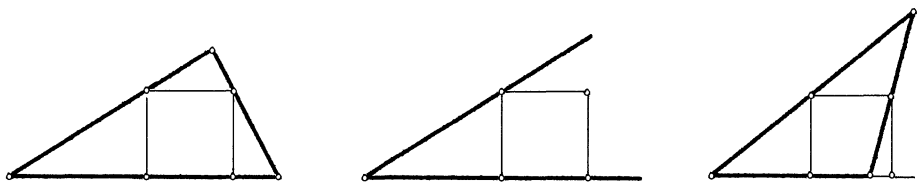

FIGURE 1
Examples of inscribed squares.

For right triangles there are only two squares that can be inscribed, and an interesting classic problem is to determine which square is the smaller. This problem was posed in a recent Rose-Hulman alumni magazine. We received about thirty solutions, with at least six essentially different methods. A dissection solution of this problem for an isosceles right triangle is given in [1]. It turns out that, for any right triangle, the inscribed square with its side along the hypotenuse is always smaller. What can be said about squares inscribed in non-right triangles?

If the triangle is not a right triangle then there will be three inscribed squares, each with one side resting along a triangle side. In this case it can be shown that *the longer the common triangle side, the smaller the corresponding inscribed square*. We will call this *the ordering property*. Martin Gardner [2] has written an enjoyable article concerning inscribing and circumscribing using rectangles, squares, and triangles. He describes a method for constructing a square inscribed in a triangle and also references a construction given by Pólya [3]. A short proof of the ordering property for acute triangles is given in [4] using some trigonometry. This proof can be easily extended to include obtuse triangles.

In this paper, we give two different proofs of the ordering property. The first is based on some results about squares inscribed in angles. For the second proof, we consider triangles of fixed area and determine how the length of the side of an inscribed square varies with the length of the triangle side on which it rests. Both of these proofs are geometric and both lead to some interesting related results.

Congruent squares inscribed in angles Consider triangle ABC and the congruent squares $PQRS$ and $P'Q'R'S'$ inscribed in angle CAB, with QR resting on side AB and $Q'R'$ resting on side AC (FIGURE 2). Let M be the intersection of QP and $Q'P'$ and let N be the intersection of RS and $R'S'$. The right triangles $AQP$and $AQ'P'$ are

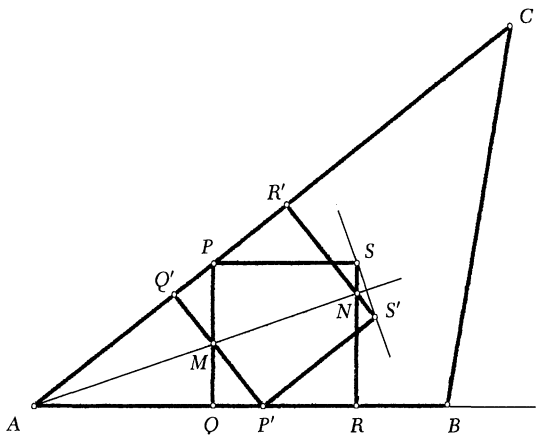

FIGURE 2
Congruent squares inscribed in angle CAB.

congruent and thus the right triangles AQM and $AQ'M$ are congruent. Hence angles QAM and $Q'A'M$ are congruent and line AM bisects angle CAB.

Also $AR = AR'$ and thus the right triangles ARN and $AR'N$ are congruent. Hence the line AN also bisects angle CAB and the points A, M, and N are collinear. The corresponding vertices of the squares are symmetrical with respect to this bisector and thus the line through S and S' is perpendicular to the bisector.

If side AC is longer than side AB and if the squares both grow larger while remaining congruent, the vertex corresponding to S' will reach side BC before the vertex corresponding to S reaches this side. The square corresponding to $P'Q'R'S'$ will then be inscribed in *triangle* CAB. The square corresponding to $PQRS$ continues to grow until it is inscribed in the triangle as the vertex corresponding to S reaches side BC. Hence the inscribed square, whose side is along the shorter triangle side AB, is larger than the inscribed square along the longer side AC. This proves the ordering property. Note that if the triangle were isosceles ($BA = CA$), then S and S' meet BC simultaneously since SS' is parallel to BC. In this case these two squares inscribed in the triangle are congruent.

A collinearity for pairs of inscribed squares For two congruent squares, $PQRS$ and $P'Q'R'S'$, inscribed on opposite sides of an angle at A, we have shown that the points A, M, and N are collinear. Surprisingly, these points are also collinear even for a noncongruent pair of squares. Consider the inscribed squares shown in FIGURE 3,

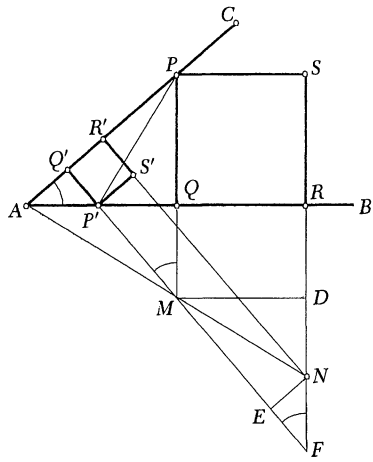

FIGURE 3
Line of intersection for squares inscribed in an angle.

where QR and $Q'R'$ lie on AB and AC respectively. Let M be the intersection of the lines through QP and $Q'P'$ and N be the intersection of the lines through RS and $R'S'$. Let F be the intersection of the lines through $Q'P'$ and SR. Let MD and NE be the line segments perpendicular to the line segments SF and $Q'F$ respectively.

The following sequence of congruences ($\cong$), similarities ($\sim$), and equalities demonstrate the result:

$$\triangle MDF \cong \triangle PQA, \qquad NE \cong P'Q', \qquad \triangle MNF \cong \triangle PP'A,$$

$$\triangle MDN \cong \triangle P'QP, \qquad \triangle AQP \sim \triangle MQP', \qquad \frac{MQ}{QA} = \frac{P'Q}{QP},$$

$$\frac{P'Q}{QP} = \frac{ND}{DM}, \qquad \triangle MQA \sim \triangle NDM, \qquad \angle QAM \cong \angle DMN.$$

Hence A, M, and N are collinear. We will call this line the *line of intersections* of the two inscribed squares.

FIGURE 4 shows a triangle, its three inscribed squares, and the three lines of intersection. It would be nice if the lines were concurrent, but this is not the case in general.

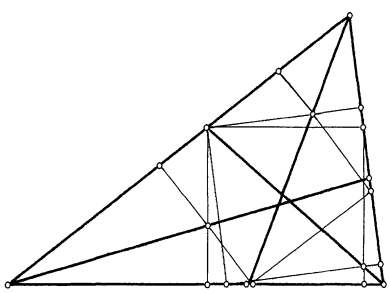

FIGURE 4
Lines of intersection for the three angles of a triangle.

Length of the side of a square inscribed in a triangle of fixed area Consider a triangle of area A with an inscribed square resting on a side of length x (FIGURE 5). Let h be the altitude of the triangle and s the length of the sides of the square.

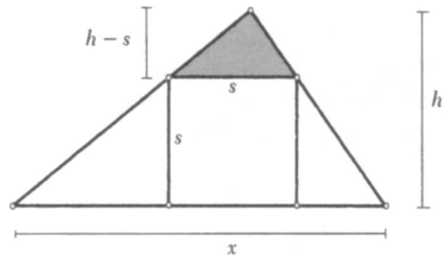

FIGURE 5
A square inscribed in a triangle of area A.

The given triangle and the shaded triangle are similar, and thus

$$\frac{h-s}{s} = \frac{h}{x} \qquad \text{hence} \qquad s = \frac{xh}{x+h} = \frac{2Ax}{x^2+2A},$$

where $h = 2A/x$ since $A = hx/2$. This formula is also given in references [2], [4], and [5]. FIGURE 6 is a graph of the above equation showing how s varies with x for fixed A.

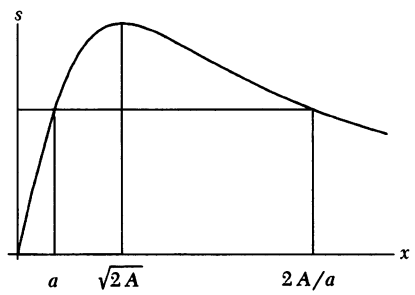

FIGURE 6
Length of the side of an inscribed square as a function of the length of the triangle side on which it rests.

The maximum point on this curve can be found by calculus or by the following variation of completing the square. Let $f(x) = 1/s$; then

$$f(x) = \frac{x^2+2A}{2Ax} = \frac{x}{2A} + \frac{1}{x} = \frac{1}{\sqrt{2A}}\left[x/\sqrt{2A} + \sqrt{2A}/x\right]$$

$$= \frac{1}{\sqrt{2A}}\left[\left(\sqrt{x/\sqrt{2A}} - \sqrt{\sqrt{2A}/x}\right)^2 + 2\right].$$

When the squared term above is zero, f assumes a minimum. Thus s assumes a maximum value at $x = \sqrt{2A}$. Note that at the maximum, the area of the square is $s^2 = A/2$ (half the area of the triangle). Indeed, at this maximum, $h = x = \sqrt{2A}$. Also note that $f(2A/a) = f(a)$ (FIGURE 6). If $x \geq \sqrt{2A}$ then the expression inside the parentheses is negative and $f(x)$ is monotone increasing, and thus $s(x)$ is monotone decreasing. Similarly if $0 < x \leq \sqrt{2A}$, then the expression inside the parentheses is positive and $s(x)$ is monotone increasing.

Now let a and b be the lengths of two sides of a triangle of area A, and s_a and s_b be the lengths of the sides of the corresponding inscribed squares. To prove the ordering property we must show that $b > a$ implies $s_b < s_a$. This follows from the monotonicity of s when $a \geq \sqrt{2A}$.

When $a < \sqrt{2A}$, we no longer have monotonicity but we can show that b is large enough to ensure $s_b < s_a$. In this case $2A/a > \sqrt{2A}$ and we have shown that $s(2A/a) = s(a)$ (FIGURE 6). Also if h_b is the altitude of the triangle to side b (FIGURE 7) is then $A = bh_b \leq ba$ and thus $b \geq 2A/a$. Since $s(x)$ is monotone decreasing for $x > 2A/a$ then $s_b < s_a$. This completes this proof of the ordering property.

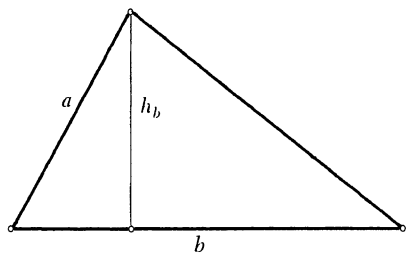

FIGURE 7
Triangle of area A and altitude h_b.

Triangles whose sides all exceed $\sqrt{2A}$ If the given triangle is equilateral with sides of length x, then $A = x^2\sqrt{3}/4$ and thus $x > \sqrt{2A}$. In this case the lengths of all three sides are greater than $\sqrt{2A}$. We will show that this is not the usual case and, in fact, "most" triangles have exactly one side with length less than $\sqrt{2A}$. First note that if c is the longest side (or one of the long sides in the isosceles case) of a triangle, and h_c the altitude to this side then $2A = ch_c \leq ca < c^2$. Thus the length of the longest side of a triangle is always greater than $\sqrt{2A}$.

The investigation of the lengths of the two shorter sides will be done numerically. To simplify the computations, we choose length units so that the longest side has length one. Let a and b be the lengths (relative to the longest side) of the two shorter sides, then the area of the triangle is given by Heron's formula $A = \sqrt{S(S-1)(S-a)(S-b)}$, where $S = (1+a+b)/2$. To see when side a is less than $\sqrt{2A}$, we plot in FIGURE 8 the pairs of points (a, b) satisfying the equation

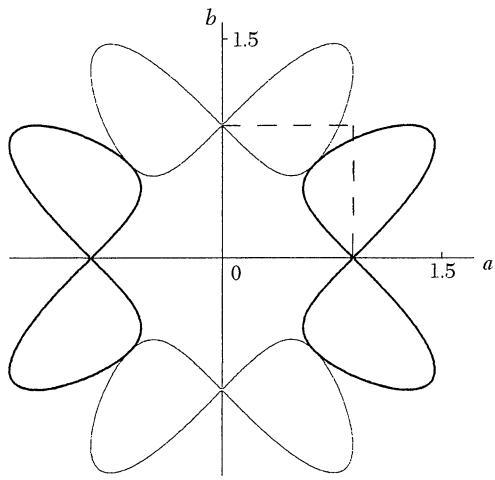

FIGURE 8
$a^4 = 4A^2$ for (a, b) on the light curves and $b^4 = 4A^2$ on the heavy curves.

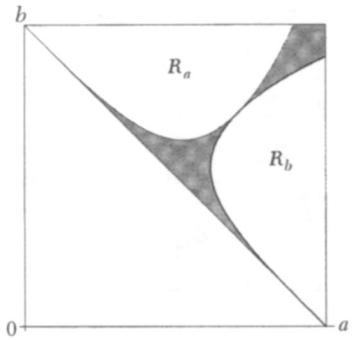

FIGURE 9
Triangles with (a, b) in the shaded region have all sides exceeding $\sqrt{2A}$.

$a^4 = 4A^2$ (light lines). The region inside these two "bow ties" corresponds to $a^4 < 4A^2$. And similarly, the heavy lines correspond to $b^4 = 4A^2$ and $b^4 < 4A^2$ in their interior.

FIGURE 9 is that part of FIGURE 8 with the restrictions $0 < a < 1$ and $0 < b < 1$. The (a, b) domain is also restricted by the triangle inequality $a + b > 1$. Since $a > 0$ and $A > 0$ then the inequality $a^4 < 4A^2$ is equivalent to $a < \sqrt{2A}$ and likewise for the corresponding b inequality. Let R_a be the region in FIGURE 9 such that $a < \sqrt{2A}$ and R_b the region with $b < \sqrt{2A}$. Thus $a < \sqrt{2A}$ if and only if (a, b) is in R_a, and $b < \sqrt{2A}$ if and only if (a, b) is in R_b. In the shaded region, both a and b are greater than $\sqrt{2A}$. The point $(1, 1)$ corresponds to equilateral triangles. The point $(\sqrt{2}/2, \sqrt{2}/2)$, where the two curves are tangent to each other, corresponds to isosceles right triangles with $a = b = \sqrt{2A}$.

Determining the areas of these regions by numerical integration shows that the probability that all three sides of a triangle have lengths exceeding $\sqrt{2A}$ is 0.134.

We now give a second method for calculating the probability that all the sides of a triangle exceed $\sqrt{2A}$. We first prove the following preliminary result. *Consider a circle* (FIGURE 10) *with center at K and radius r. Let PS be a chord of length u and PQ a line segment of length v tangent to the circle at P. Then the area of the shaded triangle PQS is* $vu^2/4r$.

To prove this, we let L be the midpoint of the chord and M be the point on PQ such that SM is perpendicular to PQ. Then the right triangles KLP and PMS are similar since angle PSM is congruent to angle KPL. Thus $\frac{u/2}{r} = \frac{h}{u}$, where h is the length of the altitude SM. Hence the area A of triangle PQS is given by

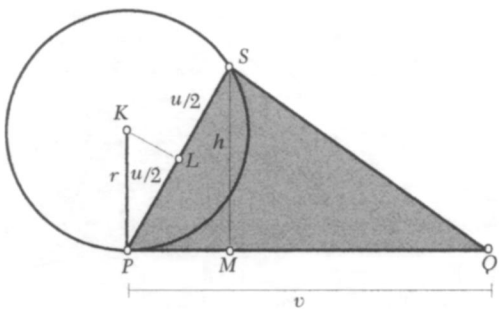

FIGURE 10
Triangle PQS with two vertices on the endpoints of a chord PS of length u, the third vertex on a tangent line through P.

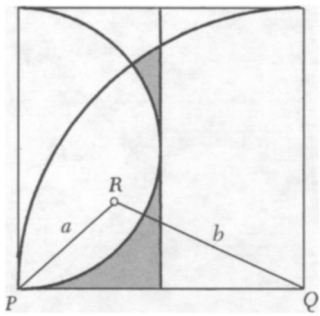

FIGURE 11
Triangle PQR with $a < b < 1$ has all sides exceeding $\sqrt{2A}$ when R is in the shaded region.

$A = vh/2 = vu^2/4r$. If $r = 1/2$ and $v = 1$, then $A = u^2/2$.

We now consider a triangle PQR with longest side PQ of length one, PR of length a, and QR of length b with $a < b$ (FIGURE 11). R must lie in the left half of the unit square with base PQ since $a < b$. Also R must lie inside the unit circle with center Q since $b < 1$. The area of the region with these boundaries is $\pi/6 - \sqrt{3}/8 \cong 0.307$. If $a > \sqrt{2A}$ then from the above preliminary result, R must lie outside the circle with center at the midpoint of the left side of the unit square and with radius $= 1/2$. This region is shaded in FIGURE 11; its area is

$$\left(12 - 3\sqrt{3} - 5\pi + 12\arcsin\tfrac{3}{5} + 3\arcsin\tfrac{4}{5}\right)/24 \cong .0667.$$

Thus the probability that the lengths of all three sides of a triangle exceed $\sqrt{2A}$ is $.0667/.307 \cong 0.217$.

It was surprising that the probabilities were different for the two methods, so we checked the results by using Monte Carlo simulation and found good agreement with the analytical results in both cases. The explanation is that, in the first calculation, we chose the lengths of the two shorter sides at random; in the second calculation, we chose the coordinates of the third vertex at random. A third method of calculation is to choose, at random, the two angles adjacent to the longest side; in this case the probability turns out to be 0.115.

This unexpected behavior of probability results based on continuous densities was first observed by Joseph Bertrand in 1889 and is known as Bertrand's paradox [e.g., **6**]. His problem was to determine the probability that the length of a random chord of a unit circle will exceed $\sqrt{3}$. He found three different answers depending on what coordinate system is chosen for the uniform continuous sample space. A brief description of this problem with some animation can be found on the Internet [**7**].

Acknowledgment Our thanks to George Berzsenyi for his help and encouragement.

REFERENCES

1. D. DeTemple and S. Harold, A round-up of square problems, this MAGAZINE 69 (1996), 21–27.
2. Martin Gardner, Some surprising theorems about rectangles in squares, *Math Horizons* (September 1997), 18–22.
3. G. Pólya, *How to Solve It*, Part I, problem 18, Princeton University Press, Princeton, NJ, 1945.
4. Eugene Sard, *Quickie* #854, this MAGAZINE 69 (1996), 305, 310.
5. Leon Bankoff, Letter in *Mathematics Teacher* 79 (May 1986), 322.
6. J. Laurie Snell, *Introduction to Probability*, Random House, New York, NY, 1988.
7. A. Bogomolny, Bertrand's paradox page, `http://mirrors.org.sg/mathi/bertrand.html`

An Unexpected Maximum in a Family of Rectangles

LEON M. HALL
ROBERT P. ROE
University of Missouri-Rolla
Rolla, MO 65409-0249

Introduction The genesis for this paper was Problem 749 from the Macalester College problem-of-the-week series:

MACALESTER PROBLEM 749. *Given a square $A_1A_2A_3A_4$ and a point P inside the square. The lengths of PA_1, PA_2, and PA_3 are 4, 3, and $\sqrt{10}$, respectively. What is the length of PA_4?*

The reader is encouraged to try to solve the problem now, before proceeding. In our solution to this problem we realized that $A_1A_2A_3A_4$ need not be a square. This observation led to the study of families of rectangles that satisfy hypotheses like those of Problem 749, and ultimately to this paper.

A quick solution to Problem 749 is provided by Theorem 1, which is a special case of Feuerbach's Relation (see [4] or [6]).

THEOREM 1. *If P is any point in the plane of rectangle $A_1A_2A_3A_4$, and if a_i is the distance from P to A_i, then $\sum_{i=1}^{4}(-1)^i a_i^2 = 0$.*

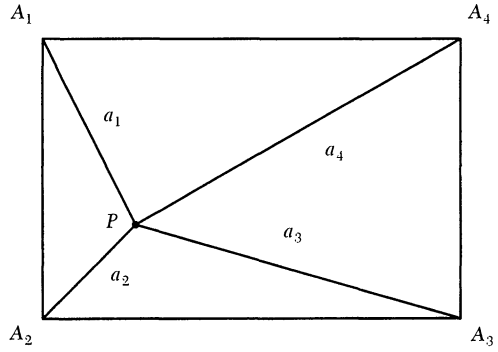

FIGURE 1
$a_1^2 + a_3^2 = a_2^2 + a_4^2$.

Thus, an ordered triple of distances from a point P to three consecutive vertices of a rectangle uniquely determines the *distance* from P to the fourth vertex, but does not uniquely determine the *rectangle*. For instance, let a_1, a_2, a_3, and a_4 be given with $\sum_{i=1}^{4}(-1)^i a_i^2 = 0$. If vertex A_2 of the rectangle is fixed at the origin and P is on the circle Γ with center A_2 and radius a_2, then vertices A_3 and A_1 will be on the x- and y-axes, respectively, and vertex A_4 will be determined by the positions of A_3 and A_1. As P moves around Γ, the rectangle changes. See FIGURE 2.

We used *The Geometer's Sketchpad* to explore various properties of the rectangles. The software allowed us to keep a_1, a_2, a_3, and a_4 fixed while moving the point P around the circle Γ, thus showing how the rectangles change. A natural question arises: *When is the area of the rectangle an extremum*? Although the perimeter is not

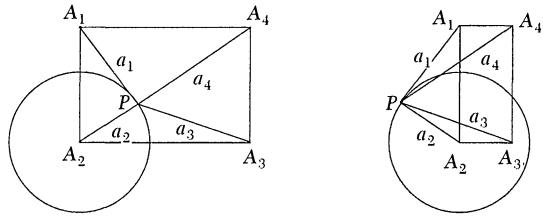

FIGURE 2
Two rectangles with the same a_i's.

constant, a reasonable-sounding guess was that the extrema occur when the rectangle is a square. Alas, experiments using the area computation feature of *The Geometer's Sketchpad* indicated that this guess was incorrect. We solve the area-optimization problem in the last section.

Another natural question is to describe the locus of A_4 under the construction given above. The "trace locus" feature of *The Geometer's Sketchpad* shows, when a_2 is the smallest distance, that this locus is a closed curve that resembles a guitar pick. See FIGURE 3. If a_2 is not less than both a_3 and a_1, then the rectangle does not exist for P on certain arcs of the circle Γ, and the locus of A_4 will be a disconnected curve. In the next section we discuss the equations for the locus of A_4.

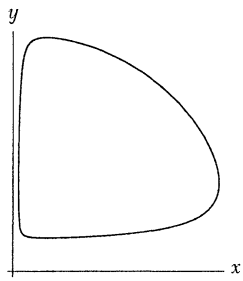

FIGURE 3
A 'guitar pick' traced by vertex A_4.

In our search of the literature we discovered that problems related to Problem 749 have a long history. For example, an old problem in geometry is to construct a specified kind of triangle when the distances from a point in the plane of the triangle to its vertices are given. Geometry problem 151 in the June-July 1901 *American Mathematical Monthly* **[3]** gave the distances from a point to three corners of a square, which is equivalent to specifying a right isosceles triangle. Baker **[1]** says the problem in **[3]** is a variation of Rutherford's problem, in which the triangle is equilateral. When the triangle is equilateral and the distances are 3, 4, and 5, Rabinowitz **[5]** and Gregorac **[2]** call the problem the 3-4-5 puzzle. Many other references may be found in **[5]**. Walter **[7]** considers distances of 3, 4, and 5 to three consecutive vertices of a rectangle. Several generalizations have been studied, such as letting the distances be a, b, and c (**[3]**, **[5]**, **[7]**), allowing the point from which the distances are measured to be above (or below) the plane of the triangle (**[7]**), replacing the triangle by a polygon (**[5]**), and replacing the triangle by a simplex in $\mathbb{R}^n$ with $n + 1$ vertices (**[2]**).

The locus of A_4 Let a_1, a_2, a_3, and a_4 be fixed, with $\sum_{i=1}^{4}(-1)^i a_i^2 = 0$. Relabel the points and distances, if necessary, so that a_2 is the minimum of the distances with A_2 fixed at the origin. Let the coordinates of A_3 be $(x, 0)$, and the coordinates of A_1 be $(0, y)$. Since P is on the circle Γ, which has radius a_2, the coordinates of P are

$(a_2\cos\theta,\ a_2\sin\theta)$, where θ is the angle measured from the positive x-axis to A_2P. Since A_3 is on the circle with center P and radius a_3,

$$(x - a_2\cos\theta)^2 + (a_2\sin\theta)^2 = a_3^2.$$

One solution to this quadratic in x is

$$x = x(\theta) = a_2\cos\theta + \sqrt{a_3^2 - a_2^2\sin^2\theta}. \tag{1}$$

Similarly, since A_1 is on the circle with center P and radius a_1, we get

$$y = y(\theta) = a_2\sin\theta + \sqrt{a_1^2 - a_2^2\cos^2\theta}. \tag{2}$$

These are parametric equations for the locus of A_4, with parameter θ in $[0, 2\pi)$. Taking the positive sign in front of the radicals guarantees that the rectangle will be in the first quadrant.

However, equations (1) and (2) are only one of four pairs of parametric equations for the locus of A_4. The other three are determined by using the negative square root in one or both equations. The four curves are given by

$$C_{mn}: \begin{cases} x = a_2\cos(\theta) + (-1)^{m+n}\sqrt{a_3^2 - a_2^2\sin^2(\theta)} \\ y = a_2\sin(\theta) + (-1)^{n+1}\sqrt{a_1^2 - a_2^2\cos^2(\theta)} \end{cases} \qquad m,n = 1,2.$$

More possibilities arise if we do not require a_2 to be the minimum distance. Again, there are four cases: (a) $a_2 < a_1$ and $a_2 < a_3$, (b) $a_2 < a_1$ and $a_2 > a_3$, (c) $a_2 > a_1$ and $a_2 < a_3$, (d) $a_2 > a_1$ and $a_2 > a_3$. In cases (b), (c), and (d), each of the curves C_{mn} is disconnected. For example, in case (b) the curve C_{11} is given by equations (1) and (2). The quantity under the radical in (1) is negative for two θ-intervals, $\theta_1 < \theta < \theta_2$, and $\theta_3 < \theta < \theta_4$. Further, $x(\theta_2) = -x(\theta_1)$ and $x(\theta_4) = -x(\theta_3)$. Thus the curve "jumps" to the second quadrant when $\theta = \theta_2$ and "jumps back" to the first quadrant when $\theta = \theta_4$. Similar behavior occurs in case (c) with (2), and in case (d) with both (1) and (2). FIGURE 4 shows all sixteen possible curves C_{mn} for cases (a)–(d), with the plot styles for the curves as shown in FIGURE 4a.

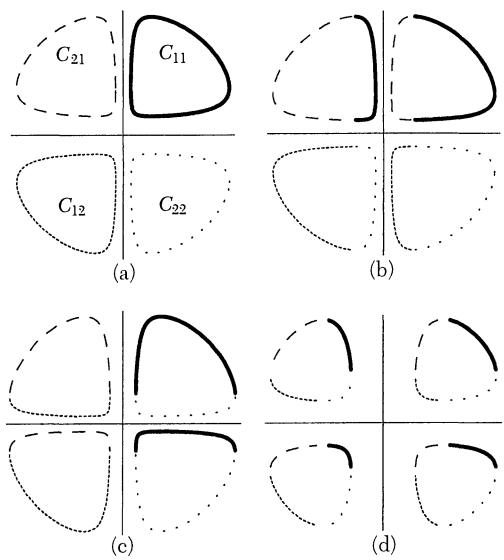

FIGURE 4

$a_i \in \{1.3, 1.5, 1.8\}$.

(a) $a_2 < a_3$ and $a_2 < a_1$ (b) $a_2 > a_3$ and $a_2 < a_1$

(c) $a_2 < a_3$ and $a_2 > a_1$ (d) $a_2 > a_3$ and $a_2 > a_1$

Optimizing the area The area of the rectangle can be expressed in terms of θ. Let

$$a(\theta) = \left(a_2\cos\theta + \sqrt{a_3^2 - a_2^2\sin^2\theta}\right)\cdot\left(a_2\sin\theta + \sqrt{a_1^2 - a_2^2\cos^2\theta}\right).$$

From (1) and (2) it follows that the area of the rectangle is $A(\theta) = |a(\theta)|$ whenever $a(\theta)$ is real-valued. Note that we are not assuming that a_2 is the least of the distances and that, because of the symmetry of the four curves in each part of FIGURE 4, we can restrict ourselves to C_{11}.

Insight into where $A(\theta)$ is optimal may be obtained by using *Mathematica* or another computer algebra system to plot $A(\theta)$, $x(\theta)$, and $y(\theta)$ on the same axes for $0 \le \theta \le 2\pi$. These graphs show that $A(\theta)$ is not necessarily largest when the rectangle is a square, as our earlier experiments with *The Geometer's Sketchpad* indicated. In FIGURE 5a (in which $a_1 = 7$, $a_2 = 3$, and $a_3 = 5$) the extrema for the area

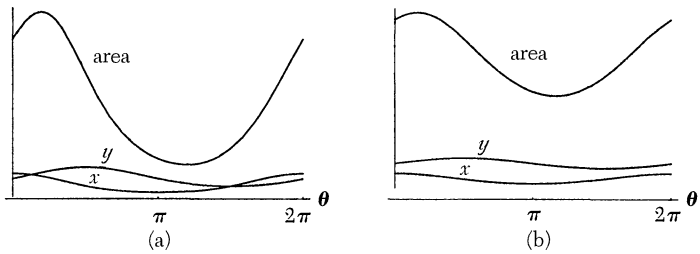

FIGURE 5
Extrema need not correspond to squares, which may not exist.

curve do not correspond to intersections of the x and y curves. In fact, the rectangle may *never* become a square, as shown in FIGURE 5b (in which $a_1 = 7$, $a_2 = 1$, and $a_3 = 4$), where the graphs of x and y do not intersect.

To optimize $A(\theta)$, we first find and simplify $a'(\theta)$.

$$a'(\theta) = \left(\frac{a_2}{\sqrt{a_1^2 - a_2^2\cos^2\theta}\,\sqrt{a_3^2 - a_2^2\sin^2\theta}}\right)\cdot \left(\cos\theta\sqrt{a_3^2 - a_2^2\sin^2\theta} - \sin\theta\sqrt{a_1^2 - a_2^2\cos^2\theta}\right)\cdot a(\theta).$$

The chain rule then gives

$$A'(\theta) = \left(\frac{a_2\cdot\left(\cos\theta\sqrt{a_3^2 - a_2^2\sin^2\theta} - \sin\theta\sqrt{a_1^2 - a_2^2\cos^2\theta}\right)}{\sqrt{a_1^2 - a_2^2\cos^2\theta}\,\sqrt{a_3^2 - a_2^2\sin^2\theta}}\right)\cdot|a(\theta)|.$$

If a_2 exceeds either a_1 or a_3 there will be intervals in which $A(\theta)$ and $A'(\theta)$ are not real valued. This is illustrated in FIGURE 6 (in which $a_1 = 5.5$, $a_2 = 6$, and $a_3 = 5$). However, the values of $A(\theta)$ and the values of the one-sided derivatives $A'_{\pm}(\theta)$ at the endpoints of each of these intervals agree. Hence, $A(\theta)$ may be viewed as being a differentiable function on the interval $[0, 2\pi]$ minus the intervals where $A(\theta)$ is not real valued. Thus, the only critical points occur when $\cos\theta\sqrt{a_3^2 - a_2^2\sin^2\theta} = \sin\theta\sqrt{a_1^2 - a_2^2\cos^2\theta}$. This condition simplifies to $\tan\theta = \pm a_3/a_1$. The negative is an extraneous solution, so the only critical points of interest occur for θ such that

$$\tan\theta = a_3/a_1. \tag{3}$$

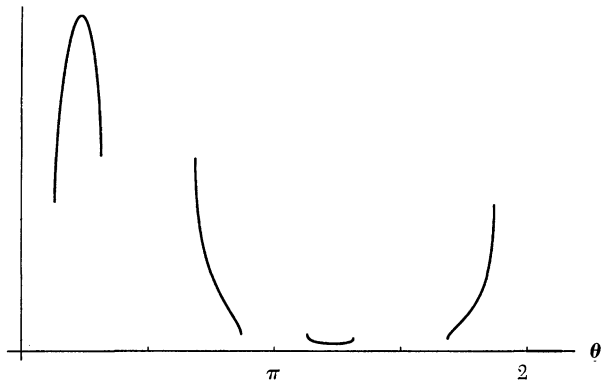

FIGURE 6
Graph of $A(\theta)$ is discontinuous if a_2 is greater than a_1 or a_3.

If $0 < \theta < \arctan(a_3/a_1)$ then $a_3/\sqrt{a_1^2 + a_3^2} < \sin\theta$ and $\cos\theta < a_1/\sqrt{a_1^2 + a_3^3}$. This observation implies that $A'(\theta) > 0$ for θ in $(0, \arctan(a_3/a_1))$. Similar reasoning shows that if $\arctan(a_3/a_1) < \theta < \pi/2$ then $A'(\theta)$ is negative. Hence, if θ satisfies (3) and lies in the first quadrant, then the corresponding rectangle has maximum area. Analogous arguments show that if θ satisfies (3) and lies in the third quadrant, the corresponding rectangle has minimum area.

To gain geometric insight into why the extrema occur when $\tan\theta = a_3/a_1$, construct the auxiliary rectangle $B_1A_2B_3B_4$ with B_3 on the x-axis, B_1 on the y-axis, $A_2B_3 = a_1$, and $A_2B_1 = a_3$. See FIGURE 7. Then the angle between the positive x-axis and A_2B_4 is the same as the angle for which the area is maximum. Further, rectangle $B_1A_2B_3B_4$ can be used to determine where P must be on Γ for a rectangle to exist for a given set of distances a_i. In the first quadrant, P must lie on the arc of Γ which is inside $B_1A_2B_3B_4$. Outside the auxiliary rectangle, either $PA_3 > a_3$ or $PA_1 > a_1$. Symmetric conditions hold in the other quadrants. The condition $\tan\theta = a_3/a_1$ for maximum area can also be thought of as describing the angle for the limiting position of P as $a_2 \to \sqrt{a_3^2 + a_1^2}$ with $a_3^2 + a_1^2$ fixed. In the special case of $a_4 = 0$, the family of rectangles has exactly four congruent members, corresponding to $\tan\theta = \pm a_3/a_1$.

The above discussion is summarized in the following theorem.

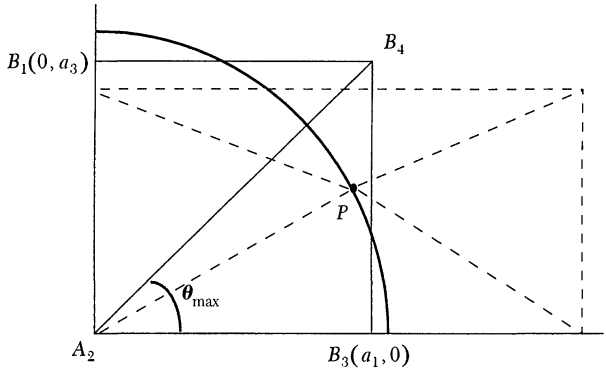

FIGURE 7
P must be on the arc inside $B_1A_2B_3B_4$.

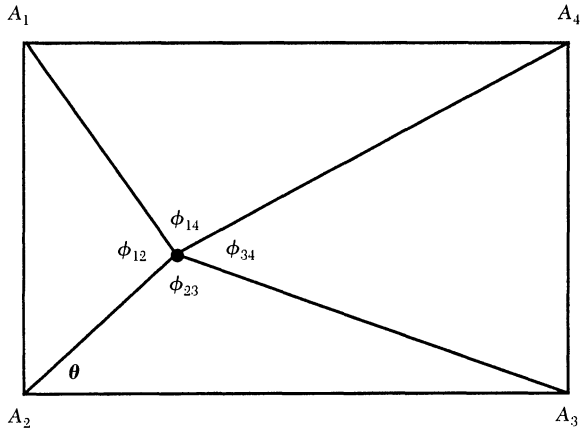

FIGURE 8
The angles around P.

THEOREM 2. *If the distances* a_1, a_2, a_3, *and* a_4 *satisfy* $\Sigma_{i=1}^{4}(-1)^i a_i^2 = 0$ *and determine a family of rectangles as described above, then the rectangle with maximum area occurs when the angle* θ *is in the first quadrant and* $\tan\theta = a_3/a_1$. *The rectangle with minimum area occurs when the angle* θ *is in the third quadrant and* $\tan\theta = a_3/a_1$.

Additional results are given as corollaries; proofs are left to the reader. Denote the angles subtended from P by the sides of the rectangle by $\phi_{ij} = \angle A_i P A_j$. See FIGURE 8.

COROLLARY 2.1. *When the area of the rectangle is maximum,* $\phi_{12} + \phi_{34} = \phi_{23} + \phi_{14} = \pi$.

Question: What is the relationship among the ϕ_{ij} when the area is minimum?

COROLLARY 2.2. *The maximum area is given by* $a_1a_3 + a_2a_4$, *and the minimum area is given by* $|a_1a_3 - a_2a_4|$. *Thus, any set* $\{a_1, a_2, a_3, a_4\}$ *of distances from* P *to consecutive vertices of a family of rectangles may be permuted, subject to* $\Sigma_{i=1}^{4}(-1)^i a_i^2 = 0$, *without changing the maximum and minimum areas.*

A second approach to finding these extrema is to use Lagrange multipliers. The vectors $\overrightarrow{A_2P}$, $\overrightarrow{PA_3}$, and $\overrightarrow{PA_1}$ can be combined to give

$$\overrightarrow{A_2A_3} = \overrightarrow{A_2P} + \overrightarrow{PA_3}; \qquad \overrightarrow{A_2A_1} = \overrightarrow{A_2P} + \overrightarrow{PA_1}.$$

Note that the (signed) area of the rectangle is the product of the first component of $\overrightarrow{A_2A_3}$ with the second component of $\overrightarrow{A_2A_1}$, and that both the second component of $\overrightarrow{A_2A_3}$ and the first component of $\overrightarrow{A_2A_1}$ must be 0 since A_3 and A_1 are on the coordinate axes. The problem becomes: Minimize

$$a(\theta, \phi_{23}, \phi_{12}) = (a_2\cos\theta - a_3\cos(\theta + \phi_{23}))(a_2\sin\theta + a_1\sin(\phi_{12} - \theta)),$$

subject to the constraints

$$a_2\sin\theta = a_3\sin(\theta + \phi_{23}) \quad \text{and} \quad a_2\cos\theta = a_1\cos(\phi_{12} - \theta).$$

Details are left to the readers (or their calculus classes).

REFERENCES

1. Marcus Baker, Solution to Geometry Problem 151, *Amer. Math. Monthly* 8 (1901), pp. 197–198.
2. R.J. Gregorac, A general 3-4-5 puzzle, *European J. Combinatorics* 17 (1996), p. 533.
3. Frank A. Griffin (proposer), G.B.M. Zerr *et al.* (solvers), Geometry Problem 151, *Amer. Math. Monthly* 8 (1901), p. 144.
4. Richard E. Pfiefer and Cathleen Van Hook, Circles, vectors and linear algebra, this MAGAZINE 66 (1993), pp. 75–86.
5. Stanley Rabinowitz, *Ptolemy's Legacy* (preliminary draft), MathPro Press, Westford, MA, 1994.
6. George Salmon, *A Treatise on Conic Sections*, Longmans, Green, and Co., London, UK, 1879.
7. Marion Walter, Exploring a rectangle problem, this MAGAZINE 54 (1981), pp. 131–134.

Counting Integer Triangles

NICHOLAS KRIER
BENNET MANVEL
Colorado State University
Ft. Collins, CO 80523-1874

Introduction How many triangles with integer sides have a given perimeter? This elementary counting problem came up in a geometry class. As we soon found out, the answer has been known for a long time. In rederiving that answer for ourselves we found the Internet and *Maple* to be valuable tools. This note describes our experiences in finding the number t_n of congruence classes of triangles with integer sides summing to n, which we will just call *integer triangles*.

Data stage Although we guessed that the answer to such a classical problem would be known, we did not have a good idea where to look for it. So we began our attack on the problem in the most primitive possible way, constructing small triangles. Obviously 1, 1, 1 is the smallest integer triple for sides of a triangle, followed by 2, 2, 1, then 2, 2, 2 and two triangles of perimeter 7: 3, 2, 2 and 3, 3, 1. Continuing in this way, we found one integer triangle of perimeter 8, three of perimeter 9, two of perimeter 10, and four of perimeter 11.

These data suggested to us two possible integer sequences. One would list perimeters of all integer triangles, and begin 3, 5, 6, 7, 7, 8, 9, 9, 9, 10, 10, 11, 11, 11, 11. The other would list the number of integer triangles of each perimeter, and so would begin 1, 0, 1, 1, 2, 1, 3, 2, 4. With these sequences in hand, we turned immediately to our battered copy of N.J.A. Sloane's classic *Handbook of Integer Sequences*. Unfortunately, we came up empty. (We would not have come up empty if we had owned the new *Encyclopedia of Integer Sequences* by N.J.A. Sloane and S. Plouffe.) So we turned to our computer, submitting the sequence to Sloane (at AT&T Research) by e-mail (address: `sequences@research.att.com`; subject: none; message: `lookup 1 0 1 1 2 1 3 2 4`). We were quickly informed that the second of our sequences was in fact *Alcuin's sequence*, the coefficients in the power series expansion of

$$\frac{x^3}{(1-x^2)(1-x^3)(1-x^4)}. \tag{1}$$

REFERENCES

1. Marcus Baker, Solution to Geometry Problem 151, *Amer. Math. Monthly* 8 (1901), pp. 197–198.
2. R.J. Gregorac, A general 3-4-5 puzzle, *European J. Combinatorics* 17 (1996), p. 533.
3. Frank A. Griffin (proposer), G.B.M. Zerr *et al.* (solvers), Geometry Problem 151, *Amer. Math. Monthly* 8 (1901), p. 144.
4. Richard E. Pfiefer and Cathleen Van Hook, Circles, vectors and linear algebra, this MAGAZINE 66 (1993), pp. 75–86.
5. Stanley Rabinowitz, *Ptolemy's Legacy* (preliminary draft), MathPro Press, Westford, MA, 1994.
6. George Salmon, *A Treatise on Conic Sections*, Longmans, Green, and Co., London, UK, 1879.
7. Marion Walter, Exploring a rectangle problem, this MAGAZINE 54 (1981), pp. 131–134.

Counting Integer Triangles

NICHOLAS KRIER
BENNET MANVEL
Colorado State University
Ft. Collins, CO 80523-1874

Introduction How many triangles with integer sides have a given perimeter? This elementary counting problem came up in a geometry class. As we soon found out, the answer has been known for a long time. In rederiving that answer for ourselves we found the Internet and *Maple* to be valuable tools. This note describes our experiences in finding the number t_n of congruence classes of triangles with integer sides summing to n, which we will just call *integer triangles*.

Data stage Although we guessed that the answer to such a classical problem would be known, we did not have a good idea where to look for it. So we began our attack on the problem in the most primitive possible way, constructing small triangles. Obviously 1, 1, 1 is the smallest integer triple for sides of a triangle, followed by 2, 2, 1, then 2, 2, 2 and two triangles of perimeter 7: 3, 2, 2 and 3, 3, 1. Continuing in this way, we found one integer triangle of perimeter 8, three of perimeter 9, two of perimeter 10, and four of perimeter 11.

These data suggested to us two possible integer sequences. One would list perimeters of all integer triangles, and begin 3, 5, 6, 7, 7, 8, 9, 9, 9, 10, 10, 11, 11, 11, 11. The other would list the number of integer triangles of each perimeter, and so would begin 1, 0, 1, 1, 2, 1, 3, 2, 4. With these sequences in hand, we turned immediately to our battered copy of N.J.A. Sloane's classic *Handbook of Integer Sequences*. Unfortunately, we came up empty. (We would not have come up empty if we had owned the new *Encyclopedia of Integer Sequences* by N.J.A. Sloane and S. Plouffe.) So we turned to our computer, submitting the sequence to Sloane (at AT&T Research) by e-mail (address: `sequences@research.att.com`; subject: none; message: `lookup 1 0 1 1 2 1 3 2 4`). We were quickly informed that the second of our sequences was in fact *Alcuin's sequence*, the coefficients in the power series expansion of

$$\frac{x^3}{(1-x^2)(1-x^3)(1-x^4)}. \tag{1}$$

In some sense, this solved our problem. We now guessed that the number of integer triangles with perimeter n was the coefficient of x^n in the expansion of expression (1). But we did not know why that was the case. And we did not know actual numerical values, beyond those given by the automated reply from Sloane's data base.

The reply from the sequence data base also included three references; two of them ([1] and [3]) were to articles that explained how the numbers t_n can be computed. We found the explanations in those articles more complex than the elegant expression (1) warranted, so we looked for a more direct approach. We discovered two rather simple explanations for why expression (1) works; these are presented in the next two sections.

We also realized that an actual formula for the number of triangles with a given integer perimeter could be obtained by finding the partial fraction expansion of expression (1). *Maple* made this rather daunting task far more fun than it would otherwise have been. We describe in the final section of this note the process we followed to find the following formula for the number t_n of integer triangles:

$$t_n = \frac{6n^2 + 18n - 1}{288} + (-1)^{n+1}\frac{2n+3}{32} + \frac{c}{72} \tag{2}$$

where $c = 7, -17, 1$, or 25, as n is congruent modulo 12 to (0 or 9), to (1, 4, 5, or 8), to (2, 7, 10, or 11), or to (3 or 6).

Reference [1] shows that, in fact, the greatest integer function $\lfloor x \rfloor$ and the nearest integer function $\{x\}$ can be used to write the numbers t_n in the following way:

$$t_n = \left\{\frac{n^2}{12}\right\} - \left\lfloor \frac{n}{4} \right\rfloor \left\lfloor \frac{n+2}{4} \right\rfloor. \tag{2'}$$

Reference [2] establishes an even more user-friendly formula for t_n, namely

$$t_n = \begin{cases} \left\{\dfrac{n^2}{48}\right\} & \text{if } n \text{ is even;} \\ \left\{\dfrac{(n+3)^2}{48}\right\} & \text{if } n \text{ is odd.} \end{cases} \tag{2''}$$

Counting by threes For the rest of this note we denote the integer sides of our triangle of perimeter n by a, b, and c, with $a \geq b \geq c$. Our first derivation of the generating function (1) for the numbers t_n begins with the following observation.

LEMMA. *For n even, $t_n = t_{n-3}$. For n odd, $t_n = t_{n-3} + \dfrac{n}{4} + \dfrac{(-1)^{(n+1)/2}}{4}$.*

Proof. We note first that subtracting one from the length of each side of an a, b, c triangle with perimeter n will usually result in an $a-1, b-1, c-1$ triangle with perimeter $n-3$. The triangle inequality requires that $b + c > a$, so shrinking works if $(b-1)+(c-1) > (a-1)$ (or $b + c > a + 1$) also holds. Thus shrinking will work unless the triangle we start with has sides satisfying the equation $b + c = a + 1$. In that case, however, the original perimeter is $2a + 1$. So if the original perimeter is even, $t_n = t_{n-3}$. If n is odd, then shrinking works for all a, b, c summing to n except in the case that $b + c = a + 1$. With $a + b + c = n$, this reduces to $a = (n-1)/2$ and $b + c = (n+1)/2$. Thus t_n is equal to t_{n-3} plus one for each solution to $b + c = (n+1)/2$ with b and c positive integers, $b \geq c$. Two examples will illustrate the general case. If $n = 9$ then $b + c = 5$ so c could be 1 or 2. If $n = 11$ then $b + c = 6$ so

c could be 1 or 2 or 3. More generally, if $n \equiv 1 \pmod 4$ then b, c can be chosen in $(n-1)/4$ ways, and if $n \equiv 3 \pmod 4$, then b, c can be chosen in $(n+1)/4$ ways. This completes the proof.

Now suppose that $t(x)$ is the generating function for the number of integer triangles with perimeter n, so that

$$t(x) = t_0 + t_1 x + t_2 x^2 + \cdots.$$

Then

$$x^3 t(x) = t_0 x^3 + t_1 x^4 + t_2 x^5 + \cdots.$$

After subtracting, we find

$$(1-x^3)t(x) = t_0 + t_1 x + t_2 x^2 + (t_3 - t_0)x^3 + (t_4 - t_1)x^4 + (t_5 - t_2)x^5 + \cdots.$$

Since $t_0 = t_1 = t_2 = 0$, the lemma above reduces the preceding equation to

$$\begin{aligned}(1-x^3)t(x) &= x^3 + x^5 + 2x^7 + 2x^9 + 3x^{11} + 3x^{13} + \cdots \\ &= x^3(1+x^2)(1+2x^4+3x^8+\cdots) = x^3(1+x^2)\frac{1}{(1-x^4)^2};\end{aligned}$$

therefore,

$$t(x) = \frac{x^3(1+x^2)}{(1-x^3)(1-x^4)(1-x^2)(1+x^2)} = \frac{x^3}{(1-x^2)(1-x^3)(1-x^4)}$$

Counting by constructing Expression (1) can be expressed rather less tidily as

$$x^3(1+x^2+x^4+x^6+\cdots)(1+x^3+x^6+x^9+\cdots)(1+x^4+x^8+x^{12}+\cdots). \quad (3)$$

The coefficient t_n of x^n in this expression is obtained by combining terms from the four factors in every way that gives a total power of n. The x^3 factor encouraged us to think of constructing triangles beginning with the 1, 1, 1 triangle and adding various amounts to the sides. We introduce the method we found for adding total lengths in multiples of 2, 3, and 4 to arrive at all the different triangles by first describing it in terms of taking lengths away.

The three complicated factors in the product correspond to three kinds of operations used to reduce a triangle. We reduce a given triangle with sides a, b, and c (with $a \geq b \geq c$) to the 1, 1, 1 triangle by repeating the following steps (we name each side according to its original length):

1. Subtract one from each of the sides a and b.
2. Subtract one from each of the sides a, b, and c.
3. Subtract two from side a and one from each of sides b and c.

In expression (3), the x^3 term corresponds to our objective, the 1, 1, 1 triangle. Our choice of terms from the second, third, and fourth factors determines how many times the steps 1, 2, and 3 above are applied to reduce a, b, c to 1, 1, 1. The remarkable fact is that each integer triangle can be reduced using a uniquely calculable number of each of these operations.

Example. We reduce a 14, 12, 7 triangle to the 1, 1, 1 triangle. First note that the longest side is 2 larger than the second longest side. Thus we will need two uses of

step 3, the only step that reduces the difference between the two longest sides. We subtract 2, 1, 1 twice from 14, 12, 7 to produce a 10, 10, 5 triangle. The two (now equal) longest sides are now 5 larger than the smallest side, so we use step 1 five times to reduce to a 5, 5, 5 triangle. Finally, we use step 2 four times to reduce to the 1, 1, 1 triangle.

More generally, this sort of reduction must use step 1 exactly $b-c$ times, step 2 exactly $c-a+b-1$ times, and step 3 exactly $a-b$ times. Thus the a, b, c integer triangle, $a \geq b \geq c$, is counted in the coefficient of expression (3) that comes from the product

$$x^3 x^{2(b-c)} x^{3(c-a+b-1)} x^{4(a-b)}.$$

The triangle a, b, c can be built up by adding to the edge lengths of the starting triangle 1, 1, 1 the edge lengths of the following triangles, two of which are degenerate:

$u = b - c$ copies of the "triangle" 1, 1, 0 (perimeter 2)
$v = c - a + b - 1$ copies of the triangle 1, 1, 1 (perimeter 3)
$w = a - b$ copies of the "triangle" 2, 1, 1 (perimeter 4)

The sides are added in the order specified to the sides to be made a, b, c, respectively. Totalling the lengths placed on each side, we find the largest side has length $1 + (b-c) + (c-a+b-1) + 2(a-b) = a$. The next side has length $1 + (b-c) + (c-a+b-1) + (a-b) = b$, and the last side has length $1 + (c-a+b-1) + (a-b) = c$. Notice that any triple of numbers a, b, c with $a \geq b \geq c$ that satisfies the triangle inequality $b + c > a$ will produce a triple u, v, w of non-negative integers. Thus every integer triangle contributes 1 to the appropriate coefficient of expression (3). Conversely, any term $t^n = t^3(t^2)^u(t^3)^v(t^4)^w$ in the expansion of expression (3) determines sides

$$a = 1 + u + v + 2w, \quad b = 1 + u + v + w, \quad \text{and} \quad c = 1 + v + w$$

of an integer triangle, since a triple a, b, c determined in this way satisfies $a \geq b \geq c$ and $b + c > a$. Thus the building-up process we have described corresponds exactly to the terms of expression (3).

Example. The 14, 12, 7 triangle gives us the values $b - c = 5$, $c - a + b - 1 = 4$, $a - b = 2$. So it contributes 1 to the term $t^3(t^2)^5(t^3)^4(t^4)^2$ in the product (3), which is the term t^{33}. Notice also how this connects with the reduction performed in the example above.

The bijection between triangles with integer sides and partitions into 2's, 3's, and 4's with at least one 3, implicit in the generating function (1) and explicit in our mappings between triples a, b, c and u, v, w, has been observed before. In an exercise toward the end of **[6]** (see page 281), interested readers can discover how this bijection is related to free commutative monoids.

Final remarks Although the formula (2″) is elegant, we wanted to derive, directly from expression (1), an explicit formula for the number t_n that did not invoke the nearest integer or greatest integer functions. To find that formula, we turned to *Maple* to expand (1) into partial fractions. The command was `convert(f, parfrac, x)`, where we had earlier defined `f` to be expression (1). The result was

$$\frac{-1}{24}\frac{1}{(x-1)^3} + \frac{13}{288}\frac{1}{x-1} - \frac{1}{16}\frac{1}{(x+1)^2} - \frac{1}{32}\frac{1}{x+1} + \frac{1}{9}\frac{x+2}{x^2+x+1} - \frac{1}{8}\frac{x+1}{x^2+1}.$$

For most of these terms, the coefficient of x^n is clear from the general binomial theorem. Thus the first four terms give the following coefficient of x^n:

$$\frac{1}{24}\binom{n+2}{2} - \frac{13}{288} - \frac{1}{16}(n+1)(-1)^n - \frac{1}{32}(-1)^n.$$

The last two terms, which involve irreducible quadratics, are trickier. They may be handled by noting that the roots are complex third and fourth roots of unity, respectively (this explains the modulo 12 format of our formula (2)). But *Maple* handles them by finding Taylor expansions. For the next to last term, the command `taylor((x+2)/(x^2+x+1), x=0, 13)` yields

$$2 - x - x^2 + 2x^3 - x^4 - x^5 + 2x^6 - x^7 - x^8 + 2x^9 - x^{10} - x^{11} + 2x^{12} + O(x^{13}).$$

This shows that the coefficient of $(x+2)/(x^2+x+1)$ is 2 if n is divisible by 3 and -1 otherwise. The coefficients of $(x+1)/(x^2+1)$ can be found with *Maple*, by use of complex roots, or by shifting the expansion of $1/(x^2+1)$. They turn out to be -1 if n is 0 or 1 modulo 4, and $+1$ otherwise. Combining all of this information, we arrived at the formula for t_n given in (2), above.

For some interesting old problems on sharing full and partially full barrels, related to counting integer triangles, see pages 150 to 165 of Olivastro's book **[4]**. Singmaster's paper **[5]** is Olivastro's source; it also contains interesting connections between counting triangles and partitions of integers into three parts. For another explanation of the connection between partitions and the number of triangles, which is more in the spirit of our approach, see the nice exposition by Honsberger **[2]**, which expands on **[1]**. For related applications of generating functions, see **[7]**.

REFERENCES

1. G. E. Andrews, A note on partitions and triangles with integer sides, *Amer. Math. Monthly*, 86 (1979), 477–478.
2. R. Honsberger, *Mathematical Gems III*, Mathematical Association of America, Washington, DC, 39–47, 1985.
3. J. H. Jordan, R. Walch, and R. J. Wisner, Triangles with integer sides, *Amer. Math. Monthly*, 86 (1979), 686–689.
4. D. Olivastro, *Ancient Puzzles*, Bantam Books, New York, NY, 1993.
5. D. Singmaster, Triangles with integer sides and sharing barrels, *College Math. J.*, 21 (1990), 278–285.
6. R. Stanley, *Enumerative Combinatorics*, Wadsworth and Brooks/Cole, Monterey, CA, 1986.
7. A. Tucker, *Applied Combinatorics*, John Wiley & Sons, New York, NY, 1980.

Math Bite: On the Nowhere Differentiability of the Coordinate Functions of the Iséki Curve

Kiyoshi Iséki modified Schoenberg's space-filling curve [**1**] to obtain a continuous curve that passes through every point of the $\aleph_0$-dimensional unit cube $[0,1]\times[0,1]\times[0,1]\times\ldots$ (see [**2**] and [**3**]). The coordinate functions of Iséki's curve are defined as follows:

$$\varphi_n(t)=\frac{1}{2}\sum_{k=0}^{\infty}\frac{p\left(3^{2^{n-1}(2k+1)-1}t\right)}{2^k},\ 0\le t\le 1,\ n=1,2,3,\ldots,$$

where the 2-periodic function p is defined for $t\in[0,1]$ by

$$p(t)=\begin{cases}0 & \text{if } t\in[0,1/3),\\ 3t-1 & \text{if } t\in[1/3,2/3),\\ 1 & \text{if } t\in[2/3,1],\end{cases}$$

and elsewhere by $p(-t)=p(t)$ and $p(t+2)=p(t)$.

To show that these coordinate functions are nowhere differentiable in $(0,1)$, let $k_q=[3^{2^n q}t]$ (where $[\ ]$ denotes the greatest integer function), and consider the two sequences

$$a_q=\frac{k_q}{3^{2^n q}}\ \text{and}\ b_q=a_q+\frac{1}{3^{2^n q}}.$$

The line of reasoning employed in our proof of the nowhere differentiability of the coordinate functions of the Schoenberg curve (see [**4**]) shows that

$$\limsup\frac{\varphi_n(b_q)-\varphi_n(a_q)}{b_q-a_q}=\infty\ \text{or}\ \liminf\frac{\varphi_n(b_q)-\varphi_n(a_q)}{b_q-a_q}=-\infty,$$

whence the desired result follows. To handle the endpoints, take

$$a_q=0, b_q=\frac{1}{3^{2^n q}}\ \text{at}\ t=0;\ a_1=1-\frac{1}{3^{2^n q}}, b_1=1\ \text{at}\ t=1.$$

REFERENCES

1. I. J. Schoenberg, The Peano curve of Lebesgue, *Bull. Amer. Math. Soc.* 44 (1938), 519.
2. K. Iséki, Simple construction of generalized Peano curve, *J. Osaka Inst. Sci. Tech.* 1 (1949), 1–2.
3. H. Sagan, *Space-filling Curves*, Springer-Verlag, New York, NY, 1994.
4. H. Sagan, An elementary proof that Schoenberg's space-filling curve is nowhere differentiable, this MAGAZINE 65 (1992), 125–128.

—HANS SAGAN
5004 GLEN FOREST DRIVE
RALEIGH, NC 27612-3132

The Sufficient Condition for the Differentiability of Functions of Several Variables

XU PINGYA
Nanjing College of Electric Power
Nanjing 210013
People's Republic of China

In courses on several variable calculus, the following observations about differentiability are made. Given a function $f: \mathbb{R}^2 \to \mathbb{R}$, it is only a necessary condition for differentiability at the point P that both partial derivatives exist at P. It has been observed in **[1]**, **[2]**, and **[3]** that if both partial derivatives exist and one of them is continuous at the point P, then f is differentiable at P. An example given in **[3]** shows that the corresponding assertion is not generally true for a function of n variables when $n \geq 3$. Specifically, for $n \geq 3$, the function need not be differentiable at the point even if all n partial derivatives exist and one of them is continuous at the point.

We will prove the following theorem.

THEOREM 1. *Suppose that the function $f: \mathbb{R}^n \to \mathbb{R}$ has the property that all n partial derivatives exist at the point P in $\mathbb{R}^n$ and $n-1$ of the partial derivatives are continuous at P. Then f is differentiable at P.*

After the proof we provide an example to show that the conclusion need not hold if two or more of the partial derivatives are discontinuous at P.

Proof. Consider $P = (x_1, \ldots, x_n)$ and suppose that all the partial derivatives f_i' exist at P and that all of them are continuous at P except possibly f_n'. Then

$$\lim_{\Delta x_n \to 0} \frac{f(x_1, \ldots, x_{n-1}, x_n + \Delta x_n) - f(x_1, \ldots, x_{n-1}, x_n)}{\Delta x_n} = f_n'(P)$$

and so

$$f(x_1, \ldots, x_{n-1}, x_n + \Delta x_n) - f(x_1, \ldots, x_{n-1}, x_n) = f_n'(P)\Delta x_n + \varepsilon_n \Delta x_n,$$

where $\lim_{\Delta x_n \to 0} \varepsilon_n = 0$. By Lagrange's mean value theorem,

$$\begin{aligned} &f(x_1, \ldots, x_{i-1}, x_i + \Delta x_i, \ldots, x_n + \Delta x_n) \\ &\quad - f(x_1, \ldots, x_{i-1}, x_i, x_{i+1} + \Delta x_{i+1}, \ldots, x_n + \Delta x_n) \\ &\quad = f_i'(x_1, \ldots, x_{i-1}, \xi_i, x_{i+1} + \Delta x_{i+1}, \ldots, x_n + \Delta x_n)\Delta x_i, \end{aligned}$$

where ξ_i is between x_i and $x_i + \Delta x_i$ for $i = 1, 2, \ldots, n-1$.

Let $\rho = \sqrt{(\Delta x_1)^2 + \cdots + (\Delta x_n)^2}$. Since f_i' is continuous at P, we have

$$\lim_{\rho \to 0} f_i'(x_1, \ldots, x_{i-1}, \xi_i, x_{i+1} + \Delta x_{i+1}, \ldots, x_n + \Delta x_n) = f_i'(P),$$

so that

$$f_i'(x_1,\ldots,x_{i-1},\xi_i,x_{i+1}+\Delta x_{i+1},\ldots,x_n+\Delta x_n)=f_i'(P)+\varepsilon_i,$$

where $\lim_{\rho\to 0}\varepsilon_i=0$ for $i=1,2,\ldots,n-1$. Hence

$$\begin{aligned}&f(x_1,\ldots,x_{i-1},x_i+\Delta x_i,\ldots,x_n+\Delta x_n)\\&\quad -f(x_1,\ldots,x_{i-1},x_i,x_{i+1}+\Delta x_{i+1},\ldots,\ x_n+\Delta x_n)\\&\quad =f_i'(x_1,\ldots,x_{i-1},\xi_i,x_{i+1}+\Delta x_{i+1},\ldots,x_n+\Delta x_n)\Delta x_i\\&\quad =f_i'(P)\Delta x_i+\varepsilon_i\Delta x_i,\end{aligned}$$

and therefore

$$\begin{aligned}&f(x_1+\Delta x_1,\ldots,x_n+\Delta x_n)-f(x_1,\ldots,x_n)\\&\quad=\sum_{i=1}^{n}\big(f(x_1,\ldots,x_{i-1},x_i+\Delta x_i,\ldots,x_n+\Delta x_n)\\&\qquad -f(x_1,\ldots,x_{i-1},x_i,x_{i+1}+\Delta x_{i+1},\ldots,x_n+\Delta x_n)\big)\\&\quad=\sum_{i=1}^{n}f_i'(P)\Delta x_i+\sum_{i=1}^{n}\varepsilon_i\Delta x_i=\sum_{i=1}^{n}f_i'(P)\Delta x_i+o(\rho).\end{aligned}$$

This shows that f is differentiable at P and completes the proof of the theorem.

Now, for each $n\geq 2$, we give an example showing that the theorem no longer remains true if more than one of the partials is allowed to be discontinuous. For $n=2$, many readers will find the example familiar. Let

$$f(x_1,\ldots,x_n)=\begin{cases}\dfrac{x_1x_2}{\sqrt{x_1^2+x_2^2}}+x_3^2+\cdots+x_n^2, & \text{if } x_1^2+x_2^2\neq 0\\ 0, & \text{if } x_1^2+x_2^2=0.\end{cases}$$

At the origin, we have

$$f_1'(0,\ldots,0)=\lim_{\Delta x\to 0}\frac{f(\Delta x,0,\ldots,0)}{\Delta x}=0;$$

for $x_1^2+x_2^2\neq 0$,

$$\lim_{x_1\to 0,\ x_2=kx_1}f_1'=\lim_{x_1\to 0,\ x_2=kx_1}\frac{x_2^3}{\left(x_1^2+x_2^2\right)^{3/2}}=\frac{k^3}{(1+k^2)^{3/2}}$$

for each k. Thus f_1' is discontinuous at the origin. Similarly, f_2' is discontinuous at the origin. Straightforward calculations show that the remaining partial derivatives are continuous at the origin. When the point $(\Delta x_1,\Delta x_2,\ldots,\Delta x_n)$ tends to the origin

along the line $x_1 = x_2 = \cdots = x_n$, we see that

$$\frac{1}{\rho}\left[\frac{\Delta x_1 \Delta x_2}{\sqrt{(\Delta x_1)^2 + (\Delta x_2)^2}} + \sum_{i=3}^{n} (\Delta x_i)^2\right]$$

$$= \frac{(\Delta x_1)^2}{\sqrt{2n(\Delta x_1)^4}} + \frac{(n-2)(\Delta x_1)^2}{\sqrt{n(\Delta x_1)^2}} \to \frac{1}{\sqrt{2n}} \neq 0.$$

This shows that function f is not differentiable at the origin.

REFERENCES

1. Zhang Jingqing, Wang Bowen, Xu Zhongyi, Tang Zhengyi, Wu Lingwen, and Chen Bisheng, *Problems Analysis of Calculus* (Part B), Jiangsu Science and Technology Publishing House, Jiangsu, China, 1983.
2. J. M. Henle, Tangent planes with infinitesimals, *Amer. Math. Monthly* 91 (1984), 433–435.
3. Li Siyuan, A note on the differentiability of functions of several variables, *Higher Mathematics* 3 (1987), 21–23.

Math Bite: Equality of Limits in Ratio and Root Tests

Relations among various tests for convergence of series arose in the note **[1]** and its corrigendum. For the convergence of series $\sum_{n=0}^{\infty} a_n$ with positive terms, two well-known tests are as follows:

D'ALEMBERT'S RATIO TEST. *Suppose that* $\lim_{n\to\infty} \frac{a_{n+1}}{a_n} = L$. *Then* $\sum a_n$ *converges if* $L < 1$ *and diverges if* $L > 1$.

CAUCHY'S ROOT TEST. *Suppose that* $\lim_{n\to\infty} a_n^{1/n} = M$. *Then* $\sum a_n$ *converges if* $M < 1$ *and diverges if* $M > 1$.

We show—using the tests themselves—that if the limits L and M exist, they must be equal. To this end, suppose that $L < M$. (The argument for the case $M < L$ is similar.) Choose a real number k such that $L < k < M$.

Now consider the series $\sum b_n$, where $b_n = a_n/k^n$. Then we have

$$\lim_{n\to\infty} \frac{b_{n+1}}{b_n} = \frac{L}{k} < 1, \qquad \text{but} \qquad \lim_{n\to\infty} b_n^{1/n} = \frac{M}{k} > 1.$$

The first limit implies that $\sum b_n$ converges; the second, that $\sum b_n$ diverges. This is a contradiction.

REFERENCES

1. D. Cruz-Uribe, SFO, The relation between the root and ratio tests, this MAGAZINE 70 (1997), 214–215; corrigendum, this MAGAZINE 70 (1997), 310–311.

—PREM N. BAJAJ
WICHITA STATE UNIVERSITY
WICHITA, KS 67260-0033

along the line $x_1 = x_2 = \cdots = x_n$, we see that

$$\frac{1}{\rho}\left[\frac{\Delta x_1 \Delta x_2}{\sqrt{(\Delta x_1)^2 + (\Delta x_2)^2}} + \sum_{i=3}^{n} (\Delta x_i)^2\right]$$

$$= \frac{(\Delta x_1)^2}{\sqrt{2n(\Delta x_1)^4}} + \frac{(n-2)(\Delta x_1)^2}{\sqrt{n(\Delta x_1)^2}} \to \frac{1}{\sqrt{2n}} \neq 0.$$

This shows that function f is not differentiable at the origin.

REFERENCES

1. Zhang Jingqing, Wang Bowen, Xu Zhongyi, Tang Zhengyi, Wu Lingwen, and Chen Bisheng, *Problems Analysis of Calculus* (Part B), Jiangsu Science and Technology Publishing House, Jiangsu, China, 1983.
2. J. M. Henle, Tangent planes with infinitesimals, *Amer. Math. Monthly* 91 (1984), 433–435.
3. Li Siyuan, A note on the differentiability of functions of several variables, *Higher Mathematics* 3 (1987), 21–23.

Math Bite: Equality of Limits in Ratio and Root Tests

Relations among various tests for convergence of series arose in the note [1] and its corrigendum. For the convergence of series $\sum_{n=0}^{\infty} a_n$ with positive terms, two well-known tests are as follows:

D'ALEMBERT'S RATIO TEST. *Suppose that* $\lim_{n\to\infty} \frac{a_{n+1}}{a_n} = L$. *Then* $\sum a_n$ *converges if* $L < 1$ *and diverges if* $L > 1$.

CAUCHY'S ROOT TEST. *Suppose that* $\lim_{n\to\infty} a_n^{1/n} = M$. *Then* $\sum a_n$ *converges if* $M < 1$ *and diverges if* $M > 1$.

We show—using the tests themselves—that if the limits L and M exist, they must be equal. To this end, suppose that $L < M$. (The argument for the case $M < L$ is similar.) Choose a real number k such that $L < k < M$.

Now consider the series $\sum b_n$, where $b_n = a_n/k^n$. Then we have

$$\lim_{n\to\infty} \frac{b_{n+1}}{b_n} = \frac{L}{k} < 1, \qquad \text{but} \qquad \lim_{n\to\infty} b_n^{1/n} = \frac{M}{k} > 1.$$

The first limit implies that $\sum b_n$ converges; the second, that $\sum b_n$ diverges. This is a contradiction.

REFERENCES

1. D. Cruz-Uribe, SFO, The relation between the root and ratio tests, this MAGAZINE 70 (1997), 214–215; corrigendum, this MAGAZINE 70 (1997), 310–311.

—PREM N. BAJAJ
WICHITA STATE UNIVERSITY
WICHITA, KS 67260-0033

Turning Lights Out with Linear Algebra

MARLOW ANDERSON
Colorado College
Colorado Springs, CO 80903

TODD FEIL
Denison University
Granville, OH 43023

The game *Lights Out*, commercially available from Tiger Electronics, consists of a 5×5 array of 25 lighted buttons; each light may be on or off. A *move* consists of pushing a single button. Doing so changes the on/off state of the light on the button pushed, and of all its vertical and horizontal neighbors. Given an initial configuration of lights which are turned on, the object is to turn out all the lights.

A complete strategy for the game can be obtained using linear algebra, requiring only knowledge of Gauss-Jordan elimination and some facts about the column and null spaces of a matrix. All calculations are done modulo 2.

We make some initial observations.

1. Pushing a button twice is equivalent to not pushing it at all. Hence, for any given configuration, we need consider only solutions in which each button is pushed no more than once.
2. The state of a button depends only on how often (whether even or odd) it and its neighbors have been pushed. Hence, the order in which the buttons are pushed is immaterial.

We will represent the state of each light by an element of $\mathbb{Z}_2$, the field of integers modulo 2; 1 for on, and 0 for off. We will denote the state of the light in the ith row and jth column by $b_{i,j}$, an element of $\mathbb{Z}_2$, and the entire array by a 25×1 column vector $\vec{b}$, with entries ordered as follows:

$$\vec{b} = (b_{1,1}, b_{1,2}, \cdots, b_{1,5}, b_{2,1}, \cdots b_{5,5})^T$$

(T stands for transpose). We will call such a vector a *configuration* of the array.

Pressing a button changes the configuration vector by adding to $\vec{b}$ a vector that has 1's at the location of the button and its neighbors and 0's elsewhere. The order of pushing buttons makes no differences, so we may represent a *strategy* by another 25×1 column vector $\vec{x}$, where $x_{i,j}$ is 1 if the (i,j) button is to be pushed, and 0 otherwise.

If we start with all the lights out and configuration $\vec{b}$ is obtained by strategy $\vec{x}$, then

$$b_{1,1} = x_{1,1} + x_{1,2} + x_{2,1},$$

$$b_{1,2} = x_{1,1} + x_{1,2} + x_{1,3} + x_{2,2},$$

$$b_{1,3} = x_{1,2} + x_{1,3} + x_{1,4} + x_{2,3}.$$

More generally, it is straightforward to check that the result $\vec{b}$ of the strategy $\vec{x}$ is the matrix product $A\vec{x} = \vec{b}$, where A is the 25×25 matrix:

$$A = \begin{pmatrix} B & I & O & O & O \\ I & B & I & O & O \\ O & I & B & I & O \\ O & O & I & B & I \\ O & O & O & I & B \end{pmatrix}$$

here I is the 5×5 identity matrix, O is the 5×5 matrix of all zeros, and B is the matrix

$$B = \begin{pmatrix} 1 & 1 & 0 & 0 & 0 \\ 1 & 1 & 1 & 0 & 0 \\ 0 & 1 & 1 & 1 & 0 \\ 0 & 0 & 1 & 1 & 1 \\ 0 & 0 & 0 & 1 & 1 \end{pmatrix}$$

Note that B is a symmetric matrix, and so A is symmetric too.

Given an arbitrary configuration $\vec{b}$, we will say that $\vec{b}$ is *winnable* if there exists a strategy $\vec{x}$ to turn out all the lights in $\vec{b}$. The key observation is as follows:

> *If a set of buttons is pushed to create a configuration, then starting with that configuration and pressing the same set of buttons will turn the lights out.*

That is, to find a strategy to turn out all the lights in $\vec{b}$, we need to solve $\vec{b} = A\vec{x}$. Thus, a configuration $\vec{b}$ is winnable if and only if it belongs to the column space of the matrix A; we denote the latter by $\mathrm{Col}(A)$.

To analyze $\mathrm{Col}(A)$, we perform Gauss-Jordan elimination on A. This would be tedious to perform by hand, but is easier using any computer algebra system capable of handling matrices with entries from $\mathbb{Z}_2$; *Maple* or *Mathematica* will do the job. Gauss-Jordan will yield $RA = E$, where E is the Gauss-Jordan echelon form, and R is the product of the elementary matrices which perform the reducing row operations. The matrices R and E are rather formidable, and not particularly illuminating. We will not display them here but invite the reader to calculate them using a favorite computer algebra system.

Having done this calculation, we see that the matrix E is of rank 23, with two free variables $x_{5,4}$ and $x_{5,5}$ in the last two columns. Indeed, the last two columns of E are

$$(0,1,1,1,0,1,0,1,0,1,1,1,0,1,1,1,0,1,0,1,0,1,1,0,0)^T$$

and

$$(1,0,1,0,1,1,0,1,0,1,0,0,0,0,0,1,0,1,0,1,1,0,1,0,0)^T.$$

Now A is a symmetric matrix, and so $\mathrm{Col}(A)$ equals the row space of A, denoted $\mathrm{Row}(A)$. But $\mathrm{Row}(A)$ is the orthogonal complement of the null space of A (denoted $\mathrm{Null}(A)$), which in turn equals $\mathrm{Null}(E)$. So, to describe $\mathrm{Col}(A)$, we need only determine a basis for $\mathrm{Null}(E)$.

Since E is in Gauss-Jordan echelon form, it is easy to find an orthogonal basis for $\mathrm{Null}(E)$ by examining the last two columns of E:

$$\vec{n}_1 = (0,1,1,1,0,1,0,1,0,1,1,1,0,1,1,1,0,1,0,1,0,1,1,1,0)^T$$

and

$$\vec{n}_2 = (1,0,1,0,1,1,0,1,0,1,0,0,0,0,0,1,0,1,0,1,1,0,1,0,1)^T.$$

Putting this together, we have the following:

THEOREM 1. *A configuration $\vec{b}$ is winnable if and only if $\vec{b}$ is perpendicular to the two vectors $\vec{n}_1$ and $\vec{n}_2$.*

Therefore, to see if a configuration is winnable, we simply compute the dot product of that configuration with $\vec{n}_1$ and $\vec{n}_2$. For example, consider the configurations below (which we have shaped as 5×5 arrays):

$$\vec{f} = \begin{pmatrix} 0 & 1 & 0 & 0 & 0 \\ 0 & 0 & 1 & 0 & 0 \\ 0 & 1 & 0 & 1 & 0 \\ 0 & 1 & 1 & 0 & 1 \\ 1 & 0 & 0 & 0 & 0 \end{pmatrix} \qquad \vec{g} = \begin{pmatrix} 1 & 0 & 0 & 1 & 0 \\ 0 & 0 & 1 & 0 & 0 \\ 0 & 1 & 1 & 0 & 1 \\ 0 & 1 & 0 & 0 & 0 \\ 1 & 0 & 0 & 0 & 0 \end{pmatrix}.$$

Then $\vec{f}$ is winnable, while $\vec{g}$ is not ($\vec{g}$ is not perpendicular to $\vec{n}_2$).

Since the dimension of the null space is 2, and the scalar field is $\mathbb{Z}_2$, it follows from this theorem that of the 2^{25} possible configurations, only one-fourth of them are winnable. Furthermore, if $\vec{b}$ is a winnable configuration with winning strategy $\vec{x}$, then $\vec{x} + \vec{n}_1$, $\vec{x} + \vec{n}_2$ and $\vec{x} + \vec{n}_1 + \vec{n}_2$ are also winning strategies.

Suppose now that $\vec{b}$ is a winnable configuration. We would like to find one of the four strategies $\vec{x}$ for which $A\vec{x} = \vec{b}$. But since we need only find one solution, we may as well set the two free variables $x_{5,4}$ and $x_{5,5}$ equal to zero. In this case $\vec{x} = E\vec{x}$. So, $\vec{x} = E\vec{x} = RA\vec{x} = R\vec{b}$. Explicitly, we have a winning strategy given by $\vec{x} = R\vec{b}$. We thus have the following theorem:

THEOREM 2. *Suppose that $\vec{b}$ is a winnable configuration. Then the four winning strategies for $\vec{b}$ are*

$$R\vec{b}, \quad R\vec{b} + \vec{n}_1, \quad R\vec{b} + \vec{n}_2, \quad R\vec{b} + \vec{n}_1 + \vec{n}_2.$$

We observed above that the configuration $\vec{f}$ is winnable. To find a winning strategy, we compute $R\vec{f}$ (where we reshape $\vec{f}$ as a column vector):

$$R\vec{f} = (0,0,1,1,0,0,0,0,0,1,0,0,0,0,1,0,1,0,0,0,1,0,0,0,0)^T.$$

This theorem gives our solutions in closed, computable form. Admittedly, this computation is tedious to do by hand, preserving the game's appeal. We can do better than completing the entire computation, if we proceed algorithmically. For suppose we only compute the strategy for the first row (that is, the first five entries in the column $R\vec{b}$). We then carry out these moves; Theorem 2 says that no more moves in the first row are necessary. We then look to see if there are any lights on in the first row. The only way to turn these out, using moves in the last four rows, is to push the button immediately below each light which is on. Having now determined a strategy for the first two rows, we then move on to each successive row in the same way.

Lights Out can be generalized to an $n \times n$ array of lights. One can proceed in a manner similar to the way we solved the 5×5 case. What is interesting is the dimension of the null space of the corresponding matrices for various values of n (we call these $n^2 \times n^2$ matrices A_n); the table below summarizes the results.

Of course if the dimension of the null space is zero, every configuration is winnable and the solution unique (if no buttons are pressed more than once). We haven't spent any time trying to solve some of these larger puzzles, but they must be very difficult!

n	Dimension of Null(A_n)	n	Dimension of Null(A_n)
2	0	12	0
3	0	13	0
4	4	14	4
5	2	15	0
6	0	16	8
7	0	17	2
8	0	18	0
9	8	19	16
10	0	20	0
11	6	21	0

A further natural generalization is to consider *Lights Out* on a torus; that is, lights on the top row are considered neighbors of lights on the bottom row, and likewise for the leftmost and rightmost columns. This "wrap around" changes the matrices A_n, of course. (We leave this as an exercise for the reader.) Here are some corresponding results for the game on tori of various sizes:

n	Dimension of Null(A_n)	n	Dimension of Null(A_n)
2	0	12	16
3	4	13	0
4	0	14	0
5	8	15	12
6	8	16	0
7	0	17	16
8	0	18	8
9	4	19	0
10	16	20	32
11	0	21	4

Acknowledgment Our thanks to our colleague John Watkins for his suggestions on writing this paper.

Digitally Determined Periodic Points

DAVID SPROWS
Villanova University
Villanova, PA 19085-1699

Introduction One of the most remarkable and surprising results in iteration theory is the fact that a continuous function from a closed interval to itself that has a point of period three must have points of period n for all natural numbers n. An excellent description and proof of this result is given in [**2**]. The presentation in [**2**] is especially suitable for students since it requires nothing more advanced than the intermediate value theorem, and uses as its main illustrative example the elementary piecewise linear function given by

$$f(x) = \begin{cases} x + \frac{1}{2}, & 0 \le x < \frac{1}{2}, \\ 2 - 2x, & \frac{1}{2} \le x \le 1. \end{cases} \tag{1}$$

It is not hard to establish the fact that this function has a point of period three since $f(0) = \frac{1}{2}$, $f(\frac{1}{2}) = 1$ and $f(1) = 0$. It is less obvious that there are points of period n for all other n. Although [**2**] gives arguments to show that these points must exist, it does not give any specific examples of such points. In this brief note we will show how a reformulation of the definition of f in binary notation makes it possible to determine in a very straightforward manner periodic points of any period.

Periodic points Given x in $[0, 1]$, let $x = .a_1\, a_2\, a_3 \ldots$ be the binary representation of x (for $x = 1$, let $a_k = 1$ for all k). Note that if $0 \le x < \frac{1}{2}$, then $a_1 = 0$. This means that the first half of the definition of f can be rewritten as

$$f(.0a_2\, a_3 \ldots) = .1a_2\, a_3 \ldots .$$

If $\frac{1}{2} \le x \le 1$, then $a_1 = 1$, so the second part of the definition of f becomes $f(.1a_2\, a_3 \ldots) = 2 - 1.a_2\, a_3\, a_4 \ldots = 1 - .a_2\, a_3\, a_4 \ldots = .a_2'\, a_3'\, a_4' \ldots$, where $a_k' = 1 - a_k$ for all k.

Thus in binary notation, (1) can be expressed as follows:

$$f(.a_1\, a_2\, a_3 \ldots) = \begin{cases} .1a_2\, a_3 \ldots & \text{if } a_1 = 0, \\ .a_2'\, a_3'\, a_4' \ldots & \text{if } a_1 = 1. \end{cases}$$

Note that, in general, $(a_k')' = a_k$. This means that a number with binary representation $.10a_3a_4 \ldots$ will have the property that

$$f^2(.10a_3\, a_4 \ldots) = .a_3\, a_4 \ldots . \tag{2}$$

This fact will prove useful in the following.

Our goal is to determine for each natural number n an example of a point x that satisfies the condition $f^n(x) = x$ and $f^k(x) \ne x$ for $k < n$.

A consequence of (2) is that the point $x = .101010 \cdots = .\overline{10}$ satisfies $f^2(x) = x$, but a check shows that, in fact, this point has period 1, not period 2. To get a point of

period 2 we can start with $a_1 = 0$ and note that

$$f^2(.0a_2\,a_3\ldots) = .a'_2\,a'_3\,a'_4\ldots. \tag{3}$$

Thus $f^2(x) = x$ provided $a'_2 = 0$, $a'_3 = a_2$, $a'_4 = a_3, \ldots$, which gives $x = .010101\cdots = .\overline{01}$ as a point of period 2.

Combining (2) and (3) it is possible to find periodic points of any even order. For example, to get a point of period 4 we set $a'_2 = 1$ and $a'_3 = 0$ in (3). This gives $f^4(.001a_4\,a_5\ldots) = f^2(.10a'_4\,a'_5\ldots) = .a'_4\,a'_5\ldots$. Thus $x = .001a_4\,a_5\ldots$ satisfies $f^4(x) = x$ provided $a'_4 = 0$, $a'_5 = 0$, $a'_6 = 1, \ldots$. This yields $x = .\overline{001110}$, which a quick check shows does not satisfy $f^k(x) = x$ for $k < 4$, so x does have period 4.

Continuing, we can start with $x = .001a_4\,a_5\ldots$ and set $a'_4 = 1$ and $a'_5 = 0$. Solving $f^6(x) = x$ we get $x = .\overline{0010111010}$ as a point of period 6.

In general, this technique yields a point of period $2 + 2k$ of the form $x = .\overline{0a_1\ldots a_{2k}1a'_1\ldots a'_{2k}}$, where $a_j = 0$ if j is odd and $a_j = 1$ if j is even, $1 \le j \le 2k$.

The above approach can be adapted to find points of odd period. For example, if we set $a_2 = 0$ in (3) we get

$$f^3(.00a_3\,a_4\ldots) = f(.1a'_3\,a'_4\ldots) = .a_3\,a_4\ldots. \tag{4}$$

Note that an immediate consequence of (4) is that zero is a point of period 3. To get a point of period 5, we set $a_3 = 1$ and $a_4 = 0$ and use (2) to obtain $f^5(.0010a_5\,a_6\ldots) = .a_5\,a_6\ldots$. Thus $x = .0010a_5\,a_6\ldots$ satisfies $f^5(x) = x$ provided $a_5 = 0$, $a_6 = 0$, $a_7 = 1, \ldots$. This gives $x = .\overline{0010}$.

In general, this procedure yields a point of period $3 + 2k$ of the form $x = .\overline{00a_1\ldots a_{2k}}$ where $a_j = 1$ if j is odd and $a_j = 0$ if j is even, $1 \le j \le 2k$.

This approach of using binary digits to determine periodic points can also be used for the "tent" function, i.e., the function from [0, 1] to itself given by

$$f(x) = \begin{cases} 2x, & 0 \le x < \frac{1}{2} \\ 2 - 2x, & \frac{1}{2} \le x \le 1. \end{cases}$$

For this function, the n^{th} iterate of f can be expressed in binary notation by

$$f^n(.a_1\,a_2\ldots) = \begin{cases} .a_{n+1}\,a_{n+2}\ldots, & \text{if } a_n = 0, \\ .a'_{n+1}\,a'_{n+2}\ldots, & \text{if } a_n = 1. \end{cases}$$

Thus any number that can be represented in base two in the form $.\overline{a_1\ldots a_n}$, where $a_n = 0$, is periodic. (The period may be less than n; e.g., $.\overline{10}$ has period 1.)

In addition to exhibiting periodic points, these binary representations can be used to illustrate such properties as sensitivity to initial conditions. One of the main advantages of this digital approach is that it is suitable not only as the basis for a more extensive discussion of iteration theory, but also as a stand-alone glimpse of some of the rich dynamics exhibited by some very elementary functions.

REFERENCES

1. Denny Gulick, *Encounters with Chaos*, McGraw-Hill, New York, NY, 1992.
2. Xun-Cheng Huang, From intermediate value theorem to chaos, this MAGAZINE 62 (1992), 91–103.

When is a Limit Function Continuous?

RUSSELL A. GORDON
Whitman College
Walla Walla, WA 99362

Introduction Let $\{f_k\}$ be a sequence of functions that converges pointwise on an interval I to a function f and suppose that each of the functions f_k is continuous at a point $c \in I$. Must the limit function f be continuous at c? It is not difficult to find examples to show that the answer is no. Something more than pointwise convergence is required to guarantee that the limit function inherits the property of continuity. The simplest sufficient condition is uniform convergence, but this requirement is actually much stronger than necessary. The purpose of this note is to find the minimum requirement to add to pointwise convergence that will guarantee continuity of the limit function.

Examples To say that $\{f_k\}$ *converges pointwise* to f on I means that the sequence $\{f_k(x)\}$ converges to $f(x)$ for each $x \in I$. Consider the following explicit examples, all on the interval $[0, 1]$:

1. $f_k(x) = x/k; \quad f(x) = 0.$
2. $f_k(x) = \sin(k\pi x)/k; \quad f(x) = 0.$
3. $f_k(x) = \begin{cases} k^2 x & \text{if } 0 \le x < 1/k, \\ 1/x & \text{if } 1/k \le x \le 1; \end{cases} \qquad f(x) = \begin{cases} 0 & \text{if } x = 0, \\ 1/x & \text{if } 0 < x \le 1. \end{cases}$
4. $f_k(x) = x^k; \qquad f(x) = \begin{cases} 0 & \text{if } 0 \le x < 1, \\ 1 & \text{if } x = 1. \end{cases}$
5. $f_k(x) = \begin{cases} kx & \text{if } 0 \le x \le 1/k, \\ 2 - kx & \text{if } 1/k < x \le 2/k, \\ 0 & \text{if } 2/k < x \le 2; \end{cases} \quad f(x) = 0.$

We leave it to the reader to verify that each sequence $\{f_k\}$ converges pointwise on $[0, 1]$ to the corresponding f. (Sketching a few graphs of the f_k's gives a graphical sense of the convergence in each case.) All of the functions f_k are continuous on $[0, 1]$, but the limit function in Example 3 is not continuous at 0, and the limit function in Example 4 is not continuous at 1.

In Example 4, the limit function f is continuous at each point of $[0, 1)$; it fails to be continuous only at a single point. However, once it is known that "bad" behavior appears at one point, it is possible to extend the effect. Consider, for instance, the sequence $f_k(x) = \cos^{2k}(4\pi x)$ on the interval $[0, 1]$. Basic properties of the cosine function imply that the limit function f is identically zero on $[0, 1]$ except on the set $\{0, 1/4, 1/2, 3/4, 1\}$, where $f(x) = 1$. Thus the pointwise limit function has five points of discontinuity, even though each f_k is continuous on $[0, 1]$. Similarly, if $f_k(x) = \cos^{2k}(1000!\pi x)$, then the limit function will have discontinuities at each point $x \in [0, 1]$ with the property that $1000!x$ is an integer—and there are quite a few such points. In fact, the situation can be made even worse. The limit function in the last example has many—but only finitely many—points of discontinuity. Using techniques beyond the scope of this note (some ideas from measure theory), one can show that the pointwise limit of a sequence of continuous functions can have infinitely many,

even uncountably many, discontinuities. On the other hand, it is known that the pointwise limit of a sequence of continuous functions (such a function is said to be of *Baire class one*) must have *some* points of continuity. For an elementary discussion of this result, see [1].

Uniform convergence Suppose that $\{f_k\}$ converges pointwise to f on I. For $x \in I$ and $\epsilon > 0$, there exists a positive integer $K(\epsilon, x)$ such that $|f_k(x) - f(x)| < \epsilon$ for all $k \geq K(\epsilon, x)$. For a fixed but arbitrary $\epsilon > 0$, the integer $K(\epsilon, x)$ will, in general, depend on x. If, for each fixed $\epsilon > 0$, the integer $K(\epsilon, x)$ can be chosen independently of x on an interval I, then the convergence is uniform. More precisely, the sequence $\{f_k\}$ *converges uniformly* to f on I if for each $\epsilon > 0$ there exists a positive integer K such that $|f_k(x) - f(x)| < \epsilon$ for all $x \in I$ and for all $k \geq K$.

The sequences in Examples 1 and 2 converge uniformly on [0, 1]; those in Examples 3, 4, and 5 do not. (Proving these statements is good practice with the definition.) The following theorem and proof are well known; we include them for comparison to Theorem 2.

THEOREM 1. *Suppose that $\{f_k\}$ converges pointwise to a function f on an interval I, let $c \in I$, and assume that each f_k is continuous at c. If $\{f_k\}$ converges uniformly to f on I, then f is continuous at c.*

Proof. Let $\epsilon > 0$. Since $\{f_k\}$ converges uniformly to f on I, there exists a positive integer p such that $|f_p(x) - f(x)| < \epsilon/3$ for all $x \in I$. Since f_p is continuous at c, there exists $\delta > 0$ such that $|f_p(x) - f_p(c)| < \epsilon/3$ for all $x \in I$ that satisfy $|x - c| < \delta$. For these same values of x,

$$\begin{aligned} |f(x) - f(c)| &\leq |f(x) - f_p(x)| + |f_p(x) - f_p(c)| + |f_p(c) - f(c)| \\ &< \epsilon/3 + \epsilon/3 + \epsilon/3 = \epsilon. \end{aligned}$$

Hence, the function f is continuous at c.

Quasi-uniform convergence Example 5 illustrates that the limit function may be continuous even when the convergence is not uniform. It is easy to verify that this sequence converges uniformly on the interval $[a, 1]$ for each $a > 0$; the difficulty lies at 0. Although 0 is the only "problem point," this non-uniform effect can be extended to an infinite number of points as mentioned earlier. In other words, the limit function can be continuous even when the convergence is far from uniform. Even without an example, we can see from the preceding proof that the assumption of uniform convergence is overkill by looking closely at the key inequality

$$|f(x) - f(c)| \leq |f(x) - f_p(x)| + |f_p(x) - f_p(c)| + |f_p(c) - f(c)|.$$

The last term can be made small by the pointwise convergence at c. The middle term can be made small for x near c by the continuity of f_p at c. The first term also needs to be small for all x near c—here is where something stronger than pointwise convergence is required. However, we do not need $|f(x) - f_k(x)| < \epsilon$ for all $k \geq K$ and for all $x \in I$. We need only that $|f(x) - f_k(x)| < \epsilon$ when $k = p$ and for all $x \in I$ that are near c. These considerations lead to the following definition:

DEFINITION. *Let $\{f_k\}$ be a sequence of functions defined on an interval I, such that $\{f_k\}$ converges pointwise to a function f defined on I. The sequence $\{f_k\}$ converges quasi-uniformly to f at the point $c \in I$ if for each $\epsilon > 0$ and positive integer K there exist $\delta > 0$ and a positive integer $m \geq K$ such that $|f_m(x) - f(x)| < \epsilon$ for all $x \in I$ that satisfy $|x - c| < \delta$.*

It is not difficult to show that the sequence in Example 5 converges quasi-uniformly at 0. The foregoing discussion shows that quasi-uniform convergence is sufficient to guarantee that the limit function is continuous; in fact, quasi-uniform convergence is necessary as well.

THEOREM 2. *Suppose that $\{f_k\}$ converges pointwise to a function f on an interval I, let $c \in I$, and assume that each f_k is continuous at c. Then $\{f_k\}$ converges quasi-uniformly to f at c if and only if f is continuous at c.*

Proof. Suppose first that $\{f_k\}$ converges quasi-uniformly to f at c and let $\epsilon > 0$. Choose a positive integer K such that $|f_k(c) - f(c)| < \epsilon/3$ for all $k \geq K$. Since $\{f_k\}$ converges quasi-uniformly to f at c, there exist $\delta > 0$ and a positive integer $m \geq K$ such that $|f_m(x) - f(x)| < \epsilon/3$ for all $x \in I$ that satisfy $|x - c| < \delta$. Since f_m is continuous at c, there exists a positive number $\delta_1 < \delta$ such that $|f_m(x) - f_m(c)| < \epsilon/3$ for all $x \in I$ that satisfy $|x - c| < \delta_1$. For these same values of x,

$$\begin{aligned} |f(x) - f(c)| &\leq |f(x) - f_m(x)| + |f_m(x) - f_m(c)| + |f_m(c) - f(c)| \\ &< \epsilon/3 + \epsilon/3 + \epsilon/3 = \epsilon. \end{aligned}$$

Hence, the function f is continuous at c.

Now suppose that f is continuous at c. Let $\epsilon > 0$ and let K be a positive integer. Since $\{f_k(c)\}$ converges to $f(c)$, there exists an integer $m \geq K$ such that $|f_m(c) - f(c)| < \epsilon/3$. Since both f_m and f are continuous at c, there exists $\delta > 0$ such that for all $x \in I$ that satisfy $|x - c| < \delta$,

$$|f_m(x) - f(c)| < \epsilon/3 \qquad \text{and} \qquad |f(x) - f(c)| < \epsilon/3.$$

It follows that

$$\begin{aligned} |f_m(x) - f(x)| &\leq |f_m(x) - f_m(c)| + |f_m(c) - f(c)| + |f(c) - f(x)| \\ &< \epsilon/3 + \epsilon/3 + \epsilon/3 = \epsilon \end{aligned}$$

for all $x \in I$ that satisfy $|x - c| < \delta$. Hence, the sequence $\{f_k\}$ converges quasi-uniformly to f at c.

Note An interesting discussion of the history of this idea can be found in **[2]**. Chapter 2 of **[3]** also considers several ideas related to the convergence properties of sequences of continuous functions.

REFERENCES

1. R. A. Gordon, *Real Analysis, A First Course*, Addison-Wesley, Reading, MA, 1997.
2. G. H. Hardy, Sir George Stokes and the concept of uniform convergence, *Proc. Camb. Phil. Soc.* 19 (1918), 148–156.
3. E. W. Hobson, *The Theory of Functions of a Real Variable*, Vol. 2, Cambridge University Press, Cambridge, UK, 1926.

Cusps on Wheels on Wheels on Wheels

PETER GIBLIN
University of Liverpool
Liverpool L69 3BX
England

MATTHEW TROUT
Cross Hall High School
Ormskirk, Lancashire
England

We were intrigued by the article by Frank Farris [1] in this MAGAZINE, showing how to connect curves produced by a trio of rotating wheels with Fourier series. We drew some of Farris's curves and observed that some had cusps, and in this note we investigate the conditions that make this happen.

Consider the family of curves

$$f(t) = e^{it} + \frac{1}{d_1}e^{qit} + \frac{i}{d_2}e^{-rit}, \tag{1}$$

where d_1, d_2 are real, and q, r are positive integers—this makes the curve close up at $t = 2\pi$. We ask: For which q, r, d_1, d_2, does the curve given by (1) have cusps and, when it does, how many are there? We begin by changing variables and turning the question into one about intersecting circles in the plane.

Differentiating (1) with respect to t and equating this to zero gives the condition for the curve parametrized by f to have singularities, which will usually be cusps. After cancelling through by e^{it}, we arrive at an equation of the form

$$1 + ae^{imt} = be^{i(\frac{\pi}{2} - nt)}, \tag{2}$$

where new variables a, m, b, n are related to those above by

$$d_1 = \frac{m+1}{a}, \quad q = m+1, \quad d_2 = \frac{n-1}{b}, \quad r = n\ -1,$$

so that m is an integer ≥ 0 and n is an integer ≥ 2. We shall now concentrate on (2), in which we take a, b real and > 0.

Of course (2) just expresses the fact that two circles, one radius b centered at the origin and the other radius a centered at the complex point 1, intersect, as in FIGURE 1(i). Note that, since a, b determine this figure, it is clear that the marked angles may not have the form mt and $\frac{\pi}{2} - nt$ for the same t and *integers* m and n. So we need to ask for values of a, b which *do* allow integer values to be chosen for m and n, and, for such a, b we want to find the number of possible t, each giving a cusp on the curve parametrized by f. It is also possible that for the same t *both* intersections of the circles allow integral values of m and n, in which case we can expect the cusps arising from each of the intersection points to combine on the same curve.

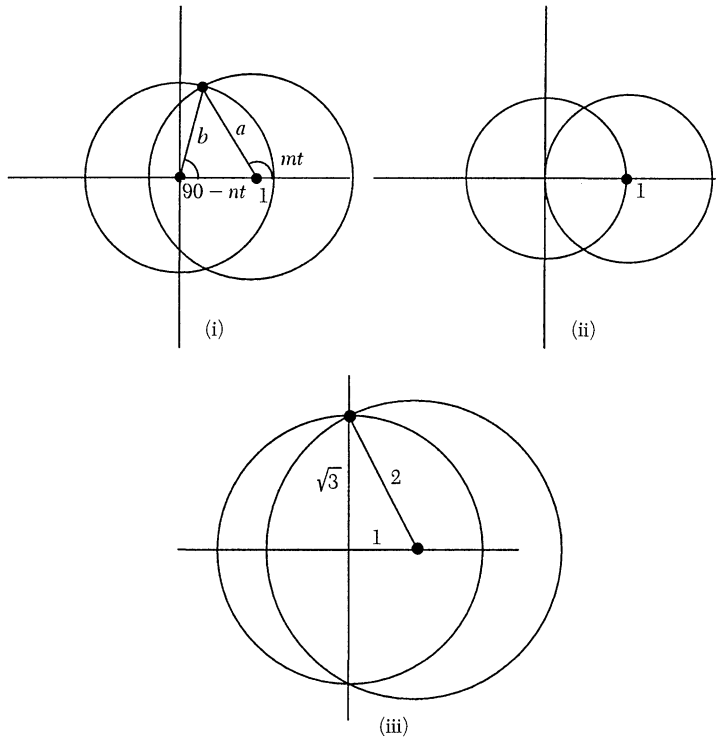

FIGURE 1
(i) The general setup for finding cusps from intersections of two circles;
(ii) and (iii) two special cases where m, n can be chosen integral.

Here is an example where m and n can be chosen to be integral. In FIGURE 1(ii) the circles are of unit radius ($a = b = 1$) and they intersect at the points $\left(\frac{1}{2}, \pm\frac{\sqrt{3}}{2}\right)$, so that, for integers k, l, k', l', we have, for the upper and lower intersection respectively,

$$mt = \frac{2\pi}{3} + 2k\pi, \quad nt = \frac{\pi}{6} + 2l\pi, \quad \text{resp. } mt = \frac{4\pi}{3} + 2k'\pi, \quad nt = \frac{5\pi}{6} + 2l'\pi. \quad (3)$$

Hence

$$\frac{m}{n} = \frac{4 + 12k}{1 + 12l}; \qquad \text{or} \qquad \frac{8 + 12k'}{5 + 12l'}. \quad (4)$$

Suppose we select any integers k,l and then choose integers m, n with m/n given by the first of the above ratios. The curve (1) given by these m, n and $a = 1$, $b = 1$ will then have cusps corresponding to the upper intersection of the two circles. How many cusps? To answer this we want to know, for these fixed values of m and n, how many values of t between 0 and 2π satisfy the first two equations of (3) for *some* k,l. This number is easily checked to be the greatest common divisor (m, n).

We can also select any integers k', l' and then choose m and n with m/n equal to the second of the ratios in (4). The resulting curve (1), with $a = b = 1$, will have (m, n) cusps corresponding to the lower of the two intersections of the circles. In this example, it happens that choosing k,l is actually *the same* as choosing k',l': in fact taking $k' = -3 - 7k$, $l' = -1 - 7l$ takes the second fraction to the first, showing that any m, n which create cusps from the upper intersection automatically create cusps

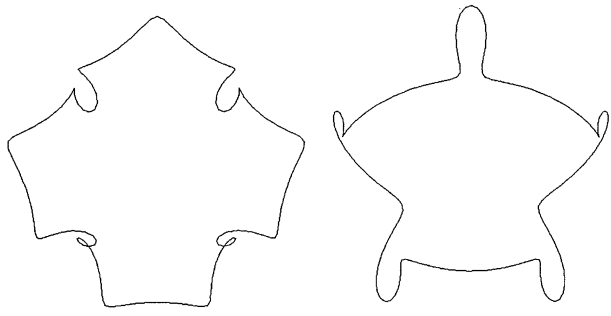

$a = 1, b = 1, m = 4, n = 13$ $a = 1, b = 1, m = 8, n = 5$

FIGURE 2
Two examples with $a = b = 1$.

from the lower intersection. The result is always a bilaterally symmetric curve with $2(m, n)$ cusps. For example, taking $m = 4$, $n = 13$ or $m = 8, n = 5$ gives the curves in FIGURE 2.

Incidentally, it is easy to check that, if m is even and n is odd, then $f(\pi - t) = -\overline{f(t)}$, resulting in bilateral symmetry about the y-axis. Similarly, if m and n are both even, then $f(\pi + t) = -f(t)$, resulting in rotational symmetry with angle π about the origin.

Here is an example where m, n can be chosen integral, but the two intersection points of the circles do not necessarily correspond to the same choice of m and n. Consider FIGURE 1(iii), where we have $a = 2, b = \sqrt{3}$ and

$$mt = \frac{2\pi}{3} + 2k\pi, \quad nt = 2l\pi$$

for the upper intersection, and

$$mt = \frac{4\pi}{3} + 2k'\pi, \quad nt = \pi + 2l'\pi$$

for the lower intersection. As before, k,l,k',l' are integers. Then

$$\frac{m}{n} = \frac{1 + 3k}{3l} \quad \text{or} \quad \frac{4 + 6k'}{3 + 6l'}.$$

In this case it is not true that the m,n arising from a choice of k, l always match those arising from a choice of k', l'. In fact starting with k, l we can find k', l' giving the same ratio m/n if and only if the following holds. We must have k odd; let $s = \frac{1}{2}(1 + 3k)$. Then the largest power of 2 in s must be no less than the largest power of 2 in l. For example, if $k = 5$ then $s = 8$ so the power of 2 in l must not exceed 3. So taking $k = 5, l = 8$, $\frac{m}{n} = \frac{16}{24} = \frac{2}{3}$ will give a bilaterally symmetrical curve with $2(m, n)$ cusps. See FIGURE 3(left) for the case $m = 2, n = 3$. On the other hand taking $k = 5, l = 16$, $\frac{m}{n} = \frac{16}{48} = \frac{1}{3}$ we get a curve with rotational symmetry and (m, n) cusps. See FIGURE 3(right) for the case $m = 2, n = 6$.

Question What exactly distinguishes the two cases just considered? How can we predict whether both intersection points of the circle will be "used," thereby creating $2(m, n)$ cusps?

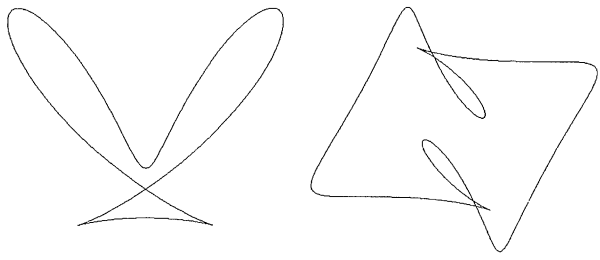

$a = 2, b = 1.732, m = 2, n = 3$ $a = 2, b = 1.732, m = 2, n = 6$

FIGURE 3
Two examples with $a = 2$, $b = \sqrt{3}$.

Another approach is to choose integers m and n in advance and find all compatible values of a and b. We simply equate coordinates at an intersection of the circles, and solve for a, b. Writing $u = mt, v = nt$ we obtain

$$a = -\frac{\cos v}{\cos(u+v)}, \qquad b = -\frac{\sin u}{\cos(u+v)}.$$

Thus given m, n, we obtain all possible values of a, b giving cusps by choosing u, v with $u/v = m/n$ and finding a, b from the formulae.

For example, let us choose $m = 2$, $n = 4$, so that $v = 2u$, and we get

$$a = -\frac{\cos 2u}{\cos 3u}; \qquad b = -\frac{\sin u}{\cos 3u}.$$

Suppose for example that $a = 3$. We can find all possible u using a numerical equation solver and substitute to find the corresponding b. In fact the latter come to approximately

$$\pm 2.15, \ \pm 3.06, \ \pm 3.88.$$

Note that one value is very close to $b = 3$; however it is not hard to show that when $m = 2$, $n = 4$ we cannot have $a = b$ and still have cusps.

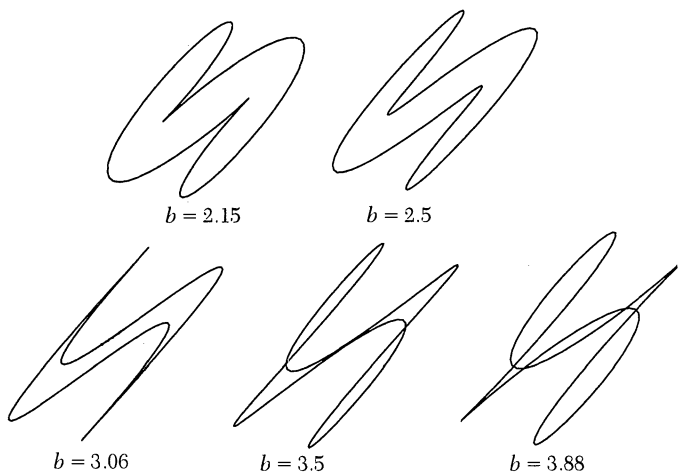

$b = 2.15$ $b = 2.5$

$b = 3.06$ $b = 3.5$ $b = 3.88$

FIGURE 4
Various curves with $a = 3$, $m = 2$, $n = 4$; the first, third and fifth have two cusps.

FIGURE 4 shows the curves corresponding to various values of b which include the three positive ones giving cusps. Thus we can see how the cusps evolve from smooth curves in the family.

REFERENCES

1. F. A. Farris, Wheels on wheels on wheels—surprising symmetry, this MAGAZINE 69 (1996), 185–189.

The Telescoping Series in Perspective

MARC FRANTZ
Indiana University – Purdue University Indianapolis
Indianapolis, IN 46202-3216

The telescoping series

$$\sum_{k=1}^{\infty} \frac{1}{k(k+1)}$$

gets its name because the sum of the first n terms collapses:

$$\sum_{k=1}^{n} \frac{1}{k(k+1)} = \sum_{k=1}^{n} \left(\frac{1}{k} - \frac{1}{k+1} \right) = 1 - \frac{1}{n+1}.$$

We conclude, letting $n \to \infty$, that the series converges to 1. The telescoping series is more than just an algebraic curiosity! In fact, we see examples of it almost every day. One is shown in FIGURE 1.

FIGURE 1 shows that the apparent horizontal separations a_n of the telephone poles satisfy (assuming infinitely many poles) $\sum_{n=1}^{\infty} a_n = S$. This series turns out, in fact, to

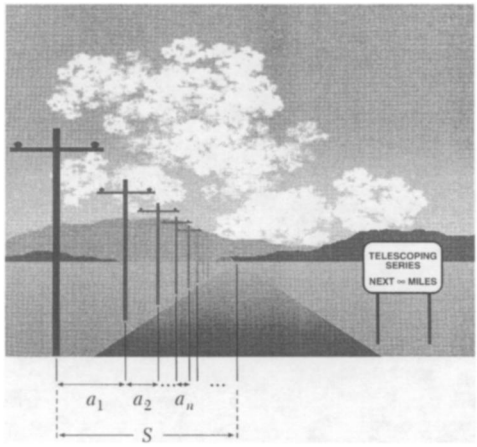

FIGURE 1

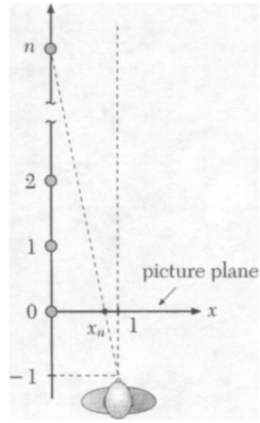

FIGURE 2

FIGURE 4 shows the curves corresponding to various values of b which include the three positive ones giving cusps. Thus we can see how the cusps evolve from smooth curves in the family.

REFERENCES

1. F. A. Farris, Wheels on wheels on wheels—surprising symmetry, this MAGAZINE 69 (1996), 185–189.

The Telescoping Series in Perspective

MARC FRANTZ
Indiana University – Purdue University Indianapolis
Indianapolis, IN 46202-3216

The telescoping series

$$\sum_{k=1}^{\infty} \frac{1}{k(k+1)}$$

gets its name because the sum of the first n terms collapses:

$$\sum_{k=1}^{n} \frac{1}{k(k+1)} = \sum_{k=1}^{n} \left(\frac{1}{k} - \frac{1}{k+1} \right) = 1 - \frac{1}{n+1}.$$

We conclude, letting $n \to \infty$, that the series converges to 1. The telescoping series is more than just an algebraic curiosity! In fact, we see examples of it almost every day. One is shown in FIGURE 1.

FIGURE 1 shows that the apparent horizontal separations a_n of the telephone poles satisfy (assuming infinitely many poles) $\sum_{n=1}^{\infty} a_n = S$. This series turns out, in fact, to

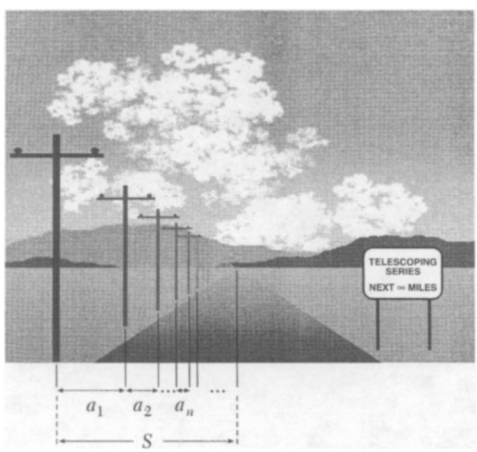

FIGURE 1

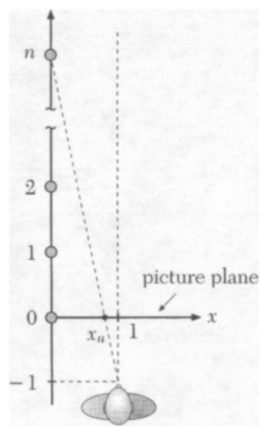

FIGURE 2

be a version of the telescoping series. For simplicity, we'll consider the special case shown in FIGURE 2. The idea behind a perspective drawing (FIGURE 2) is that a viewer, seen from above, stands in front of a "picture plane" that in this case is perpendicular to the ground and contains the x-axis. The viewer uses only one eye, and thus is idealized as a single point. As light rays travel in straight lines from objects in the real world to the viewer's eye, they pierce the picture plane, leaving behind appropriately colored dots that, taken together, depict the scene.

For convenience, we take as our unit of measure the (uniform) separation between the telephone poles, and we locate the picture plane and the viewer as shown in FIGURE 2. For $n \geq 1$, the use of similar triangles shows that the x-coordinate x_n of the image of the nth pole satisfies

$$\frac{x_n}{n} = \frac{1 - x_n}{1} \Rightarrow x_n = \frac{n}{n+1}.$$

Thus, for $n \geq 1$, the nth gap between x_{n-1} and x_n has width a_n, where

$$a_n = x_n - x_{n-1} = \frac{1}{n(n+1)}.$$

Moreover, comparing FIGURE 2 to FIGURE 1 shows that $S = 1$: the row of telephone poles appears to vanish precisely when the viewer looks straight ahead.

Proof Without Words: The Area of a Right Triangle

The area of a right triangle is $\frac{1}{8}$(hypotenuse)^2 if and only if one acute angle is $\frac{\pi}{12}$.

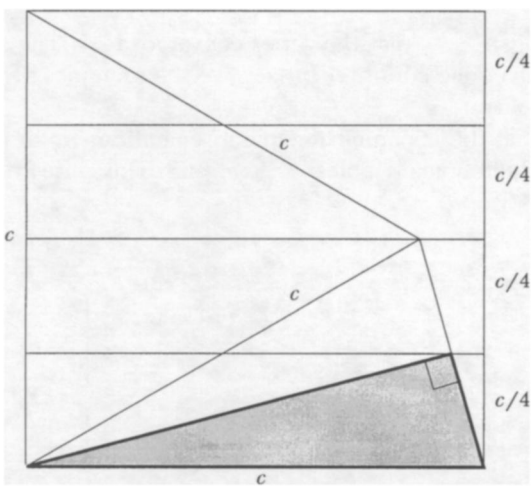

—KLARA PINTER
H – 6729 SZEGED
SZIGONY U. 41
HUNGARY

---

be a version of the telescoping series. For simplicity, we'll consider the special case shown in FIGURE 2. The idea behind a perspective drawing (FIGURE 2) is that a viewer, seen from above, stands in front of a "picture plane" that in this case is perpendicular to the ground and contains the x-axis. The viewer uses only one eye, and thus is idealized as a single point. As light rays travel in straight lines from objects in the real world to the viewer's eye, they pierce the picture plane, leaving behind appropriately colored dots that, taken together, depict the scene.

For convenience, we take as our unit of measure the (uniform) separation between the telephone poles, and we locate the picture plane and the viewer as shown in FIGURE 2. For $n \geq 1$, the use of similar triangles shows that the x-coordinate x_n of the image of the nth pole satisfies

$$\frac{x_n}{n} = \frac{1 - x_n}{1} \Rightarrow x_n = \frac{n}{n+1}.$$

Thus, for $n \geq 1$, the nth gap between x_{n-1} and x_n has width a_n, where

$$a_n = x_n - x_{n-1} = \frac{1}{n(n+1)}.$$

Moreover, comparing FIGURE 2 to FIGURE 1 shows that $S = 1$: the row of telephone poles appears to vanish precisely when the viewer looks straight ahead.

Proof Without Words: The Area of a Right Triangle

The area of a right triangle is $\frac{1}{8}$(hypotenuse)^2 if and only if one acute angle is $\frac{\pi}{12}$.

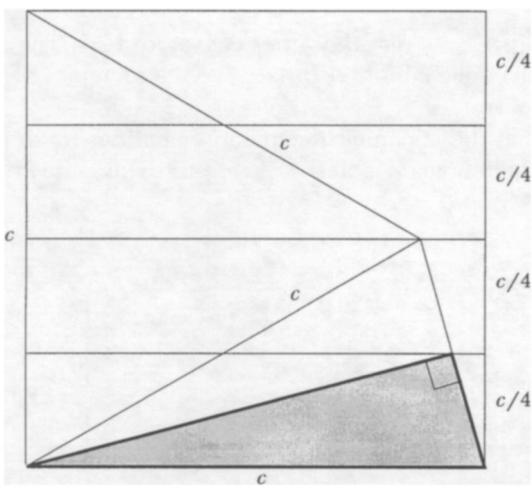

—KLARA PINTER
H – 6729 SZEGED
SZIGONY U. 41
HUNGARY

PROBLEMS

GEORGE T. GILBERT, *Editor*
Texas Christian University

ZE-LI DOU, KEN RICHARDSON, and SUSAN G. STAPLES, *Assistant Editors*
Texas Christian University

Proposals

To be considered for publication, solutions should be received by March 1, 1999.

1554. *Proposed by Howard Cary Morris, Germantown, Tennessee.*

For $0 \le r \le 1$, find the volume $V_n(r)$ of

$$\left\{(x_1, \ldots, x_n) \in [0,1]^n : \prod_{i=1}^{n} x_i \le r\right\}.$$

1555. *Proposed by Mihály Bencze, Braşov, Romania.*

Given a, b, and c_k, $k = 1,2,\ldots,n$, all greater than 1, find all real solutions x of

$$\sum_{k=1}^{n} (x+a)^{\log_a c_k} = \sum_{k=1}^{n} (x+b)^{\log_b c_k}.$$

1556. *Proposed by Gregory Galperin and Hillel Gauchman, Eastern Illinois University, Charleston, Illinois.*

Let $a_1, \ldots, a_n$ be positive numbers with $a_1 a_2 \cdots a_n = 1$. Set $x_i = \left(\sum_{k=1}^{n} a_k\right) - a_i$ for each $i = 1, \ldots, n$. Prove that

$$\sum_{i=1}^{n} \frac{1}{1+x_i} \le 1.$$

We invite readers to submit problems believed to be new and appealing to students and teachers of advanced undergraduate mathematics. Proposals must, in general, be accompanied by solutions and by any bibliographical information that will assist the editors and referees. A problem submitted as a Quickie should have an unexpected, succinct solution.

Solutions should be written in a style appropriate for this MAGAZINE. *Each solution should begin on a separate sheet containing the solver's name and full address.*

Solutions and new proposals should be mailed to George T. Gilbert, Problems Editor, Department of Mathematics, Box 298900, Texas Christian University, Fort Worth, TX 76129, or mailed electronically (ideally as a LaTeX file) to `g.gilbert@tcu.edu`. *Readers who use e-mail should also provide an e-mail address.*

1557. *Proposed by Peter Y. Woo, Biola University, La Mirada, California.*

Let PQ be a diameter of a circle, with A and B two distinct points on the circle on the same side of PQ. Let C be the intersection of the tangents to the circle at A and B. Let the tangent to the circle at Q meet PA, PB, and PC at A', B', and C', respectively. Prove that C' is the midpoint of $A'B'$.

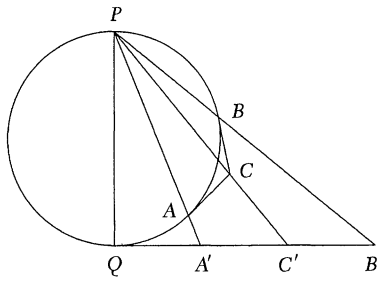

1558. *Proposed by Mansur Boase, student, St. Paul's School, London, England.*

Let the sequence $(K_n)_{k\geq 1}$ be defined by $K_1 = 2$, $K_2 = 8$, and $K_{n+2} = 3K_{n+1} - K_n + 5(-1)^n$. Prove that if K_n is prime, then n must be a power of 3.

Quickies

Answers to the Quickies are on page 322.

Q883. *Proposed by Murray S. Klamkin, University of Alberta, Edmonton, Alberta, Canada.*

Given n rays in $\mathbb{R}^n$ forming a non-degenerate n-hedral angle with vertex O and a point P in the interior of this angle, find points on the rays minimizing the volume of the simplex formed by the points and O under the restriction that P is in the hyperplane formed by the points.

(This generalizes Q847 from the April 1996 issue of this MAGAZINE.)

Q884. *Proposed by Emeric Deutsch, Polytechnic University, Brooklyn, New York.*

Find the number of ordered rooted trees with n edges that have exactly one node with more than one child.

(A tree is *rooted* if each edge is directed away from a designated node or "root." The direction is considered to be from "parent" to "child." It is *ordered* if the children of each node form a sequence rather than a set.)

Solutions

An Integral Sum of Cube Roots — October 1997

1529. *Proposed by David C. Kay, University of North Carolina at Asheville, Asheville, North Carolina.*

For what positive numbers a is

$$\sqrt[3]{2+\sqrt{a}} + \sqrt[3]{2-\sqrt{a}}$$

an integer?

Solution by Dennis Reigle, Beth Stockslager, and Karen Blount, students, Shippensburg University, Shippensburg, Pennsylvania.

The expression is an integer for $a = 100/27$ and $a = 5$.

We prove a generalization of the stated problem. For fixed $k \geq 0$ and $a \geq 0$, define

$$z = z(a) := \sqrt[3]{k+\sqrt{a}} + \sqrt[3]{k-\sqrt{a}} = \sqrt[3]{\sqrt{a}+k} - \sqrt[3]{\sqrt{a}-k}\,.$$

Observe that $a > 0$ implies that $z(a) > 0$ and $|\sqrt{a}+k| > |\sqrt{a}-k|$. Thus

$$z'(a) = \frac{1}{6\sqrt{a}\left(\sqrt{a}+k\right)^{2/3}} - \frac{1}{6\sqrt{a}\left(\sqrt{a}-k\right)^{2/3}} < 0$$

for all $a > 0$, $a \neq k^2$. Since $z(0) = 2\sqrt[3]{k}$ and $z(a)$ is continuous, it follows that the integer values of z are precisely the integers in the interval $\left(0, 2\sqrt[3]{k}\right]$. To find the value of a that produces the integer z, we solve for a in terms of z,

$$a = \frac{\left(z^3+k\right)^2\left(8k-z^3\right)}{27z^3}.$$

For $k = 2$, the only possibilities are $z = 1$ when $a = 5$ and $z = 2$ when $a = 100/27$.

Also solved by Fasakin Dlumuyiwa Adeyemi, Reza Akhlaghi, Anchorage Math Solutions Group, Michael H. Andreoli, Angelo State Problem Group, Marcia Ascher, Herb Bailey, Matt Baker (graduate student), Roy Barbara (Lebanon), Brian D. Beasley, Rebecca Berg, J. C. Binz (Switzerland), Jean Bogaert (Belgium), Stan Byrd, Maureen T. Carroll, Sabin Cautis (Canada), Robin Chapman (United Kingdom), John Christopher, Charles K. Cook, Daniel J. Curtin, Ann Davis (student), Dan Davis, Thomas Dence, Daniele Donini (Italy), Robert L. Doucette, Roger B. Eggleton, Milton P. Eisner, Russell Euler and Jawad Sadek, Habibollah Y. Far, Tim Flood, Arthur H. Foss, Matt Foss, Lorraine L. Foster, Marty Getz and Dixon Jones, John F. Goehl, Jr., Natalio H. Guersenzvaig (Argentina), Bradley Gunsalus (student) and Paul Deiermann, Lee O. Hagglund, D. Kipp Johnson, Geoffrey A. Kandall, Hans Kappus (Switzerland), James Kiefer, Kee-Wai Lau (China), Norman F. Lindquist, Nick Lord (England), George B. Marketos, Jack McCown, Edwin P. McCrary, Mark McKinzie, Ioana Mihaila, Can A. Minh (graduate student), Atar Sen Mittal, Lucas Monzon, Alan Murra (student), William A. Newcomb, Stephen Noltie, Thomas J. Osler and James Chappell (student), Yi-chuan Pan, P. J. Pedler (Australia), R. Glenn Powers, Neville Robbins, Kenneth Rogers, Daniel M. Rosenblum, Shiva K. Saksena, Zeke Sarfa, Volkhard Schindler (Germany), Harry Sedinger, Heinz-Jürgen Seiffert (Germany), Michael Semenoff, Nicholas C. Singer, Jason Skinner, W. R. Smythe, Anthony Sofo (Australia), Stephen Swiniarski, Richard L. Syverson, TAMUK Problem Solvers, R. W. W. Taylor, R. S. Tiberio, University of Central Florida Problems Group, Jack V. Wales, Jr., Charles H. Webster, Western Maryland College Problems Group, Nathan Wetzel, Joseph Wiener, Michael Woltermann, Kenneth L. Yocom, Monte J. Zerger, and the proposer. There were eleven incorrect solutions and two incomplete solutions.

Tower of Bubbles — October 1997

1530. *Proposed by Allen J. Schwenk, Western Michigan University, Kalamazoo, Michigan.*

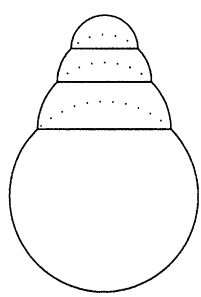

$n = 4$

A spherical bubble of radius 1 is surmounted by a smaller, hemispherical bubble, which in turn is surmounted by a still smaller hemispherical bubble, and so forth, until n chambers including the initial sphere are formed. What is the maximum height of any bubble tower with n chambers?

I. Solution by Stephen Noltie, Ohio University, Lancaster, Ohio.

The maximum height of any bubble tower with n chambers is $1+\sqrt{n}$.

We compute the maximum height assuming all bubbles, including the bottom one, are hemispherical. We can then add 1 at the end to answer the original question. More generally, let $h(r,n)$ be the maximum height of a stack of n hemispherical bubbles with bottom hemisphere of radius r. Clearly, $h(r,n)=r\cdot h(1,n)$ since r is just a "scale factor." We prove that $h(1,n)=\sqrt{n}$ by induction, beginning with the obvious $h(1,1)=1$. Now assume that $h(1,n)=\sqrt{n}$. Then the maximal height of a tower with $n+1$ chambers, whose second-from-bottom hemisphere has radius r, is $f(r)=\sqrt{1-r^2}+h(r,n)=\sqrt{1-r^2}+r\sqrt{n}$. Maximizing $f(r)$ for $0\le r\le 1$ yields a maximum value of

$$f\left(\sqrt{\frac{n}{n+1}}\right)=\sqrt{n+1}.$$

This completes the induction. Furthermore, we see that the radii of the bubbles for the maximal tower of n bubbles are 1, $\sqrt{(n-1)/n}$, $\sqrt{(n-2)/n}$, $\sqrt{(n-3)/n},\ldots,\sqrt{1/n}$.

II. Solution by Nick Lord, Tonbridge School, Kent, England.

The height of a tower with hemispherical chambers of radii $1>r_1>r_2>\cdots>r_{n-1}$ is

$$h=1+\sqrt{1-r_1^2}+\sqrt{r_1^2-r_2^2}+\cdots+\sqrt{r_{n-2}^2-r_{n-1}^2}+r_{n-1}.$$

Now apply the Cauchy-Schwarz inequality to

$$(1,1,\ldots,1) \quad \text{and} \quad \left(\sqrt{1-r_1^2},\sqrt{r_1^2-r_2^2},\ldots,\sqrt{r_{n-2}^2-r_{n-1}^2},r_{n-1}\right) \quad \text{in } \mathbb{R}^n$$

to see that $h\le 1+\sqrt{n}$ with equality if and only if

$$\sqrt{1-r_1^2}=\sqrt{r_1^2-r_2^2}=\cdots=\sqrt{r_{n-2}^2-r_{n-1}^2}=r_{n-1},$$

which gives $r_i=\sqrt{(n-i)/n}$ for $1\le i\le n-1$.

III. Solution by Michael Vowe, Therwil, Switzerland.

Denote the radii by $r_1=1,r_2,r_3,\ldots,r_n$. Then we obtain for the height of the bubble tower with n chambers

$$h=r_1+\sqrt{r_1^2-r_2^2}+\cdots+\sqrt{r_{n-1}^2-r_n^2}+r_n.$$

Then by the concavity of the square root function (Jensen's inequality),

$$h\le r_1+n\sqrt{\frac{r_1^2-r_2^2+r_2^2-r_3^2+\cdots+r_{n-1}^2-r_n^2+r_n^2}{n}}=r_1+r_1\sqrt{n}=1+\sqrt{n},$$

with equality if and only if

$$r_1^2-r_2^2=r_2^2-r_3^2=\cdots=r_{n-1}^2-r_n^2=r_n^2,$$

or $r_i=\sqrt{(n-i+1)/n}$.

Also solved by Herb Bailey, Matt Baker (graduate student), Roy Barbara (Lebanon), J. C. Binz (Switzerland), Jean Bogaert (Belgium), Gerald D. Brown, Sabin Cautis (Canada), Robin Chapman (United Kingdom), Haiwen Chu (high school student), Dan Davis, Paul Deiermann, Daniele Donini (Italy), Robert L. Doucette, John D. Eggers, Roger B. Eggleton, Russell Euler and Jawad Sadek, Tom Gettys, Marty Getz and Dixon Jones, John F. Goehl, Jr., David C. Kay, James Kiefer, Emil F. Knapp, Neela Lakshmanan, Kee-Wai Lau (China), Can A. Minh (graduate student), Thomas J. Osler, Robert Patenaude, P. J. Pedler (Australia), Gao Peng (graduate student), Volkhard Schindler (Germany), Edward Schmeichel, Harry Sedinger, Chris Sliger and Gerald Thompson, W. R. Smythe, TAMUK Problem Solvers, Andrew Wade (Canada), Jack V. Wales, Jr., Western Maryland College Problems Group, Yongzhi Yang, and the proposer. There were twelve incorrect solutions and one incomplete solution. The main error was to assume the radii form a geometric progression.

Distances Moved Under a Permutation **October 1997**

1531. *Proposed by Claus Mazanti Sorensen, student, Aarhus University, Aarhus, Denmark.*

For which positive integers n does there exist a permutation σ in the symmetric group S_n such that the map $k \mapsto |\sigma(k) - k|$, $k \in \{1, 2, \ldots, n\}$, is injective?

Solution by Gao Peng, physics graduate student, University of Oklahoma, Norman, Oklahoma.

There exists such a permutation if and only if n is of the form $4m$ or $4m + 1$ for some integer m.

First observe that, for any permutation σ,

$$\sum_{k=1}^{n} |\sigma(k) - k| \equiv \sum_{k=1}^{n} (\sigma(k) - k) = 0 \pmod 2.$$

Next observe that the required σ must be a bijection between $\{1, 2, \ldots, n\}$ and $\{0, 1, \ldots, n-1\}$. We then have

$$\sum_{k=1}^{n} |\sigma(k) - k| = \sum_{k=0}^{n-1} k = \frac{(n-1)n}{2}.$$

For n of the form $4m + 2$ or $4m + 3$, this sum is odd, so no such σ exists.

For $n = 4m$, define σ by

$$\sigma(k) = \begin{cases} 4m + 1 - k & \text{if } 1 \le k \le m \text{ or } 2m + 1 \le k \le 3m - 1, \\ 4m - k & \text{if } m + 1 \le k \le 2m - 1, \\ 4m + 2 - k & \text{if } 3m + 1 \le k \le 4m, \\ 1 & \text{if } k = 2m, \\ 3m & \text{if } k = 3m. \end{cases}$$

For $n = 4m + 1$, define σ by

$$\sigma(k) = \begin{cases} 4m + 2 - k & \text{if } 1 \le k \le m \text{ or } 2m + 2 \le k \le 3m, \\ 4m + 1 - k & \text{if } m + 1 \le k \le 2m, \\ 4m + 3 - k & \text{if } 3m + 2 \le k \le 4m + 1, \\ 1 & \text{if } k = 2m + 1, \\ 3m + 1 & \text{if } k = 3m + 1. \end{cases}$$

It is routine to verify that $\sigma \in S_n$ and that $k \mapsto |\sigma(k) - k|$ is injective in both cases. To better see what is going on, we write σ in cycle notation for $n = 12$ and $n = 13$: $(1, 12, 2, 11, 3, 10, 4, 8, 5, 7, 6)(9)$ and $(1, 13, 2, 12, 3, 11, 4, 9, 5, 8, 6, 7)(10)$.

Comment. D. J. Rogers and Robin Chapman, as well as Achilleas Sinefakopoulos, note that the problem was proposed by M. J. Pelling as E3269 in the *American Mathematical Monthly*, whose statement and solution appeared in the June-July 1988 and November 1989 issues, respectively.

Also solved by Roy Barbara (Lebanon), Jean Bogaert (Belgium), Robin Chapman (United Kingdom), Daniele Donini (Italy), Roger B. Eggleton, Marty Getz and Dixon Jones, W. R. Smythe, University of Central Florida Problems Group, Michael Woltermann, and the proposer.

Concurrency of an Altitude and Two Cevians **October 1997**

1532. *Proposed by Herbert Gülicher, Westfälische Wilhelms–Universität, Münster, Germany.*

Let $\triangle ABC$, $\triangle ACP$ and $\triangle BCQ$ be non–overlapping triangles in the plane with $\angle CAP$ and $\angle CBQ$ right angles. Let M be the foot of the perpendicular from C to AB. Prove that lines AQ, BP, and CM are concurrent if and only if $\angle BCQ = \angle ACP$.

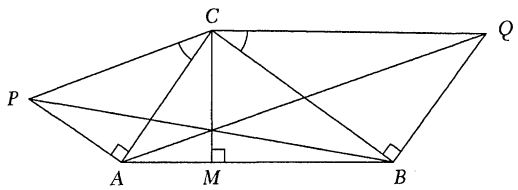

The problem statement should have included the condition that neither $\angle ABC$ nor $\angle BAC$ is a right angle.

I. Solution by Hans Kappus, Rodersdorf, Switzerland.

Orient $\triangle ABC$ in the complex plane so that $A = a$, $B = b$, and $C = ic$ with $a, b, c \in \mathbb{R}$ and $a < b$. Let $\alpha := \angle ACP$ and $\beta := \angle BCQ$. Then

$$P = a + i(ic - a)\tan\alpha = a - c\tan\alpha - ia\tan\alpha.$$

The line through B and P is given by the parametric equation

$$z = (1-\lambda)b + \lambda(a - c\tan\alpha - ia\tan\alpha), \quad \lambda \in \mathbb{R}.$$

Its point of intersection with the line CM, the imaginary axis, is found by setting $\operatorname{Re} z = 0$ and turns out to be

$$z_1 = \frac{iab\tan\alpha}{a - b - c\tan\alpha}.$$

Similarly, we see that AQ intersects CM at

$$z_2 = \frac{iab\tan\beta}{a - b - c\tan\beta}.$$

When neither $\angle ABC$ nor $\angle BAC$ is a right angle $ab \neq 0$. It now follows that $z_1 = z_2$ if and only if $\tan\alpha = \tan\beta$, or $\alpha = \beta$.

II. Solution by Achilleas Sinefakopoulos, student, University of Athens, Athens, Greece.

Because neither $\angle ABC$ nor $\angle BAC$ is a right angle, A does not lie on line BP and B does not lie on line AQ. Furthermore the perpendiculars from A to BP and from

B to AQ intersect the line CM, say at points R and S respectively. Then $\triangle ACR$ and $\triangle PAB$ are similar, since $\angle PBA = \angle ARC$ and $\angle ACR = \angle CAB + \angle CMA = \angle PAB$. Thus, $AC/AP = CR/AB$. The same reasoning yields $BC/BQ = CS/AB$.

Now notice that $\angle BCQ = \angle ACP$ if and only if $BC/BQ = AC/AP$ if and only if R and S coincide. If R and S coincide, then AQ, BP, and CM meet at the orthocenter of $\triangle ABR$. Conversely, if AQ, BP, and CM intersect at K, then K must be the orthocenter of $\triangle ABR$. Hence AK is perpendicular to BR. But AK is also perpendicular to BS. Accordingly, R and S must coincide.

Also solved by Reza Akhlaghi, Herb Bailey, Roy Barbara (Lebanon), Francisco Bellot Rosado (Spain), J. C. Binz (Switzerland), Robert X. Brennan, Gerald D. Brown, Sabin Cautis (Canada), Robin Chapman (United Kingdom), Miguel Amengual Covas (Spain), Daniele Donini (Italy), David Doster, Robert L. Doucette, Ragnar Dybvik (Norway), Milton P. Eisner, Lorraine L. Foster, Marty Getz and Dixon Jones, D. Kipp Johnson, James Kiefer, Neela Lakshmanan, Nick Lord (England), Robert Patenaude, Gao Peng (graduate student), Volkhard Schindler (Germany), Harry Sedinger, Michael Vowe (Switzerland), Michael Woltermann, Bilal Yurdakul (student, Turkey), and the proposer.

A Quadratic Recurrence Relation — October 1997

1533. *Proposed by Joaquin Gómez Rey, I. B. "Luis Buñuel," Alcorcón, Madrid, Spain.*

Solve the recurrence relation $a_{n+1} = \sum_{k=0}^{n} \binom{n}{k} a_k a_{n-k}$ in terms of a_0.

I. Solution by most solvers.

We show that $a_n = n! a_0^{n+1}$ by induction. The claim is clear for $n = 0$, so assume $a_k = k! a_0^{k+1}$ for $0 \le k \le n$. Then

$$a_{n+1} = \sum_{k=0}^{n} \binom{n}{k} k! a_0^{k+1} (n-k)! a_0^{n-k+1} = \sum_{k=0}^{n} n! a_0^{n+2} = (n+1)! a_0^{n+2},$$

completing the proof.

II. Solution by Western Maryland College Problems Group, Westminster, Maryland.

We define $b_k := a_k/k!$ and $B(t) := \sum_{k=0}^{\infty} b_k t^k$. After dividing the original recurrence by $n!$, we see that the sequence (b_n) satisfies

$$(n+1) b_{n+1} = \sum_{k=0}^{n} b_k b_{n-k}.$$

This leads to the differential equation $B'(t) = [B(t)]^2$, $B(0) = a_0$. Its unique power series solution is

$$B(t) = \frac{a_0}{1 - a_0 t} = \sum_{k=0}^{\infty} a_0^{k+1} t^k,$$

and the result follows.

Also solved by Ed Adams, Robert A. Agnew, Reza Akhlaghi, Anchorage Math Solutions Group, P. J. Anderson (Canada), Michael H. Andreoli, Angelo State Problem Group, Marcia Ascher, Matt Baker (graduate student), Roy Barbara (Lebanon), J. C. Binz (Switzerland), Jean Bogaert (Belgium), Paul Bracken (Canada), Gerald D. Brown, Dale R. Buske, Stan Byrd, Sabin Cautis (Canada), Robin Chapman (United Kingdom), John Christopher, Haiwen Chu (high school student), C. Coker, Charles K. Cook, Paul Deiermann, Emeric Deutsch, Daniele Donini (Italy), Robert L. Doucette, Ragnar Dybvik (Norway), John D. Eggers, Roger B. Eggleton, David Flannery (Ireland), Matt Foss, Lorraine L. Foster, Marty Getz and Dixon Jones, Michael Golomb, Natalio H. Guersenzvaig (Argentina), James C. Hickman, Danrun Huang, Jeffrey J. Ibbotson, Hengli Jiao, D. Kipp Johnson, Hans Kappus (Switzerland), Parviz Khalili, James

Kiefer, Tom Kilkelly, Emil Knapp and Alan Murra (student), Harris Kwong, Kee-Wai Lau (China), Carl Libis, Norman F. Lindquist, Nick Lord (England), R. F. McCoart, Jr., Jack McCown, Mark McKinzie, Janice A. Meegan, Ioana Mihaila, Lucas Monzon, Kandasamy Muthuvel, William A. Newcomb, Thomas J. Osler, P. J. Pedler (Australia), Gao Peng (graduate student), R. Glenn Powers, Robert L. Raymond, Jorge Rodriguez, Kenneth Rogers, M. A. Roondog, Daniel M. Rosenblum, Zeke Sarfa, Edward Schmeichel, Volkhard Schindler (Germany), Randy K. Schwartz, R. P. Sealy (Canada), Heinz-Jürgen Seiffert (Germany), Alexander Shaumyan, Achilleas Sinefakopoulos (student, Greece), Nicholas C. Singer, W. R. Smythe, Albert Stadler (Switzerland), David R. Stone, Richard L. Syverson, TAMUK Problem Solvers, Gerald Thompson, R. S. Tiberio, William F. Trench, Trinity University Problem Solving Group, Michael Vowe (Switzerland), Joseph Wiener, Michael Woltermann, Yongzhi Yang, Kenneth L. Yocom, Bilal Yurdakul (student, Turkey), and the proposer. There was one incomplete solution.

Answers

Solutions to the Quickies on page 316.

A883. Choosing the origin to be at O, let $\mathbf{v}_i$ denote the unique vectors from O along the ith ray such that $\mathbf{v}_1 + \cdots + \mathbf{v}_n = \mathbf{P}$. If the chosen points are $x_i\mathbf{v}_i$, then the restriction implies that $1/x_1 + \cdots + 1/x_n = 1$. The volume of the simplex is

$$x_1 \cdots x_n \det(\mathbf{v}_1 \ldots \mathbf{v}_n)/n!.$$

The arithmetic-geometric mean inequality implies the volume is minimized when

$$x_1 = \ldots = x_n = n,$$

so that P is the centroid of the $(n-1)$-simplex formed by the n chosen points.

A884 *I.* The number of ordered trees with k edges in which only the root of the tree has more than one child is $2^{k-1} - 1$, the number of ordered partitions of k into at least two parts. Then the required number is $\sum_{k=2}^{n}(2^{k-1} - 1) = 2^n - n - 1$.

II. Provided by the Editors. Suppose this one special node has k children, $2 \le k \le n$. Then we must distribute the remaining $n - k$ vertices among the ancestors of this special node and the lines of descent of its k children. In other words, we must place $n - k$ balls in $k + 1$ boxes. There are $\binom{n}{k}$ ways to do this, so the number we seek is

$$\sum_{k=2}^{n} \binom{n}{k} = 2^n - 1 - n.$$

(The numbers $2^n - 1 - n$ are sometimes called Eulerian numbers.)

Correction

1525, June 1998. Dennis P. Walsh was inadvertently omitted from the list of solvers.

Kiefer, Tom Kilkelly, Emil Knapp and Alan Murra (student), Harris Kwong, Kee-Wai Lau (China), Carl Libis, Norman F. Lindquist, Nick Lord (England), R. F. McCoart, Jr., Jack McCown, Mark McKinzie, Janice A. Meegan, Ioana Mihaila, Lucas Monzon, Kandasamy Muthuvel, William A. Newcomb, Thomas J. Osler, P. J. Pedler (Australia), Gao Peng (graduate student), R. Glenn Powers, Robert L. Raymond, Jorge Rodriguez, Kenneth Rogers, M. A. Roondog, Daniel M. Rosenblum, Zeke Sarfa, Edward Schmeichel, Volkhard Schindler (Germany), Randy K. Schwartz, R. P. Sealy (Canada), Heinz-Jürgen Seiffert (Germany), Alexander Shaumyan, Achilleas Sinefakopoulos (student, Greece), Nicholas C. Singer, W. R. Smythe, Albert Stadler (Switzerland), David R. Stone, Richard L. Syverson, TAMUK Problem Solvers, Gerald Thompson, R. S. Tiberio, William F. Trench, Trinity University Problem Solving Group, Michael Vowe (Switzerland), Joseph Wiener, Michael Woltermann, Yongzhi Yang, Kenneth L. Yocom, Bilal Yurdakul (student, Turkey), and the proposer. There was one incomplete solution.

Answers

Solutions to the Quickies on page 316.

A883. Choosing the origin to be at O, let $\mathbf{v}_i$ denote the unique vectors from O along the ith ray such that $\mathbf{v}_1 + \cdots + \mathbf{v}_n = \mathbf{P}$. If the chosen points are $x_i\mathbf{v}_i$, then the restriction implies that $1/x_1 + \cdots + 1/x_n = 1$. The volume of the simplex is

$$x_1 \cdots x_n \det(\mathbf{v}_1 \ldots \mathbf{v}_n)/n!.$$

The arithmetic-geometric mean inequality implies the volume is minimized when

$$x_1 = \ldots = x_n = n,$$

so that P is the centroid of the $(n-1)$-simplex formed by the n chosen points.

A884 *I.* The number of ordered trees with k edges in which only the root of the tree has more than one child is $2^{k-1} - 1$, the number of ordered partitions of k into at least two parts. Then the required number is $\sum_{k=2}^{n}(2^{k-1} - 1) = 2^n - n - 1$.

II. Provided by the Editors. Suppose this one special node has k children, $2 \le k \le n$. Then we must distribute the remaining $n-k$ vertices among the ancestors of this special node and the lines of descent of its k children. In other words, we must place $n-k$ balls in $k+1$ boxes. There are $\binom{n}{k}$ ways to do this, so the number we seek is

$$\sum_{k=2}^{n} \binom{n}{k} = 2^n - 1 - n.$$

(The numbers $2^n - 1 - n$ are sometimes called Eulerian numbers.)

Correction

1525, June 1998. Dennis P. Walsh was inadvertently omitted from the list of solvers.

REVIEWS

PAUL J. CAMPBELL, *editor*
Beloit College
1997–98: Universität Augsburg,
Germany

Assistant Editor: Eric S. Rosenthal, West Orange, NJ. Articles and books are selected for this section to call attention to interesting mathematical exposition that occurs outside the mainstream of mathematics literature. Readers are invited to suggest items for review to the editors.

Singh, Simon (director). *The Proof. Mathematics' Holy Grail: Proving Fermat's Last Theorem.* Film, color, 60 min., 1996; $19.95 from `http://www.pbs.org/wgbh/shop/novavideo.html` . Transcript and teacher's guide at `http://www.pbs.org/wgbh/nova/proof` .

This film conveys extremely well the tension, excitement, and emotional ups and downs of the mathematical proof that was Andrew Wiles's dream since age 10. Interviews with colleagues at Princeton, Berkeley, and Cambridge are interspersed with interviews with Wiles, including a teary-eyed scene where he notes that nothing that he will ever do again will be so important. Are viewers sober or do they laugh at Barry Mazur's remark, "You may never have heard of elliptic curves but they're extremely important"? Surely Shimura's observation "I found out that it was very difficult to make good mistakes" elicits smiles. I wish the film identified the speakers at each appearance; and some computer graphics and the lyrics "One way or another" appear too often. Viewers will enjoy the contrast between Wiles's messy and chaotic "public" desk at his office and the stern simplicity of his attic home study, the latter reflecting his singular purpose working there on FLT. Some mathematicians will cheer, and others deplore, his remark, "I never use a computer." (Thanks to Jürgen Ritter of Universität Augsburg for loaning me his copy.)

Aronofsky, Darren, π. Film, B&W, 1998. Distributed by Artisan Entertainment. A peep into the pi perplex. *New York Times* (5 July 1998) Style Section, 3. Berardinelli, James. Darren Aronofsky's piece of the π, *ReelViews* (7 July 1998) (`http://movie-reviews.colossus.net/comment/070798.html`). Holden, Stephen, "Pi": Living life by the numbers can give a guy a headache. *New York Times* (10 July 1998) E18 (`http://www.nytimes.com/library/film/071098pi-film-review.html`). O'Sullivan, Michael, Darren Aronofsky: "Pi" in the Sky, *Washington Post* (26 July 1998) G1, `http://www.washingtonpost.com/wp-srv/Wplate/1998-07/26/070I-072698-idx.html` . Blatner, David, *The Joy of Pi*, Walker & Co., 1997, $18. ISBN 0–802713327. Berggren, Lennart, Jonathan Borwein, and Peter Borwein (eds), *Pi: A Source Book*, Springer-Verlag, 1997; 736 pp, $59.95. ISBN 0–387–949240.

Pi is having its fifteen minutes of fame. Now, coming to a theater near you: π, the movie! New Yorkers have already seen the symbol π on sidewalks all over the city, done as a promotion for this thriller movie made for under $100,000. A mathematician figures out how to predict the stock market and is pursued by a brokerage house (who want to cash in) and by a rabbi (who wants him to decode the secret name of God). The film won the Directing Award at the Sundance Film Festival. The schedule of venues where the film will play is at `http://www.pithemovie.com/theat.html` . (I haven't seen the film.) Meanwhile, you can be the first in your department to wear the new fragrance Pi, due out from Parfums Givenchy this fall and billed as "a salute to the sex appeal of intelligence."

Hill, Theodore P., The first digit phenomenon, *American Scientist* 86 (4) (July-August 1998) 358–363. Browne, Malcolm W., Following Benford's law, or looking out for No. 1, *New York Times* (4 August 1998) F4. Peterson, Ivars, First digits, `http://www.maa.org/mathland/mathtrek_6_29_98.html` .

Benford's "law" is that the leading digit of elements of many data sets is d with frequency $\log_{10}(1 + 1/d)$ for $d = 1, \ldots, 9$. In particular, the frequency of a leading 1 is $\log_{10} 2 \approx .3$. Despite the name, Benford's law was known to Simon Newcomb in 1881, who observed greater wear on pages of logarithm tables for smaller leading digits. Benford's law, which is scale-invariant, is named after an engineer at General Electric who verified it empirically for many data sets. Nonconformance of data to Benford's law has been used to detect fraud in accounting and tax data, as well as errors in computer programs.

Browne, Malcolm W., Scruffy is badge of pride, but some physicists long for cool, *New York Times* (21 July 1998), `http://www.nytimes.com/library/national/science/072198sci-essay.html` .

Can you spot mathematicians, on the plane to a national convention or walking around there, from how they dress? A letter by Jeremy Levy (University of Pittsburgh) in *Physics Today* (July 1998) chides physicists for their shabby look and suggests a connection with dropping enrollments in physics. He claims that physicists can't educate a clothes-conscious public about the importance and fascination of basic research without looking "cool." Levy also deplores a shortage at physics meetings of Internet facilities, laser pointers (I find it distracting how they jiggle all over), computer projection displays, and other up-to-date accoutrements: "We look and act like losers." Of course, he's talking just about physicists, not mathematicians.

Kolata, Gina, A mystery unraveled, twice, *New York Times* (14 April 1998) F1, F8. Peterson, Ivars, Cracking a medieval code, `http://www.maa.org/mathland/mathtrek_5_4_98.html` . Reeds, James A., Solved: The ciphers in Book III of Trithemius's *Steganographica* (26 March 1998), `http://www.research.att.com/~reeds/` , to appear in *Cryptologia*. Ernst, Thomas, Schwarzweiße Magie. Der Schlüssel zum dritten Buch der Steganographia des Trithemius, *Daphnis* 25 (1996) (1); also published as a book by Editions Rodopi, ISBN 9051839855.

Johannes Trithemius (1462–1516) was a German abbot who dabbled in what was in his time considered an occult subject: cryptography. He was the author of the first several books on the subject, which were devoted mainly to steganography ("hidden writing"), the concealment of a secret message as a subsequence of letters in an innocent-appearing cover letter. (Trithemius, however, talked in terms of incantations and invoking spirits, and concealed his messages in long strings of demonic-sounding names—which led to the Roman Catholic Church placing his books on its list of forbidden books.) His incomplete third book, however, featured three-digit numbers ("astronomical data") and he did not publish a key to decrypting them. The possibility that the contents were just demonology enhanced Trithemius's reputation as a magician. In fact, however, James A. Reeds (AT&T Labs) and Thomas Ernst (La Roche College, Pittsburgh) independently discovered that the book features numerical substitution ciphers with multiple numerical equivalents for each plaintext letter. The plaintext is disappointingly banal (no secrets of the universe). In 1676, W.E. Heidel, a lawyer who worked for the Archbishop of Mainz, claimed to have deciphered the book—but wrote about his discovery in his own cryptograms, which no one could decipher. Ernst cracked Heidel's cipher too: Heidel was indeed the first to decrypt the book. (Moral: If you make a discovery that is potentially interesting to the public, don't encrypt your paper about it, and be sure that your organization distributes a press release.)

NEWS AND LETTERS

Letters to the Editor

Dear Editor:

In the charming article "Functions with compact preimages of compact sets" in the December 1997 issue of *Mathematics Magazine*, two topology students and their instructor discuss functions from the real line into itself with the property that the preimage of every compact set is compact. They show that such a "preimage-compact" function need not be continuous, but its set of discontinuities must be a closed, nowhere dense set, and they give some examples to show that this discontinuity set can be rather large.

A slight adaptation of the authors' introductory example shows that *every* closed, nowhere dense set F is the set of discontinuities of some preimage-compact function. Indeed, define a function f via $f(x) = x$ if $x \in F$ and $f(x) = x + \operatorname{dist}(x, F)^{-1}$ when $x \notin F$. Evidently f is continuous on the complement of F and unbounded in a neighborhood of every point of F. Hence F is the set of discontinuities of f. Since F is closed, the restriction of f to F is preimage-compact. On the other hand, if $x \notin F$, then $f(x)$ blows up when x approaches either F or infinity, and consequently the restriction of f to the complement of F is also preimage-compact.

Incidentally, a real-valued function that is both continuous and preimage-compact is a special case of what is called a "proper mapping" in the terminology popularized by Bourbaki's *General Topology*.

Harold Boas
Texas A&M University
College Station, Texas 77843-3368

Dear Editor:

The article "Trisection of angles, classical curves, and functional equations," in the June 1998 issue of *Mathematics Magazine*, contains a historical error on page 186: The first full paragraph states that Dinostratus lived *before* Hippias. He lived *after* Hippias. The facts are: Hippias invented the trisectrix in order to trisect any angle, probably by about 430 BC. Dinostratus some 80 years later realized that the same curve could be used to square the circle, and hence renamed it the quadratrix (cf. Boyer, *A History of Mathematics*, 1968, page 106).

Ernest Fandreyer
Fitchburg State College
Fitchburg, MA 01420-1930

Carl B. Allendoerfer Awards – 1998

The Carl B. Allendoerfer Awards, established in 1976, are made to authors of expository articles published in *Mathematics Magazine*. Carl B. Allendoerfer, a distinguished mathematician at the University of Washington, served as President of the Mathematical Association of America, 1959–60. This year's award was presented at the July 1998 Mathfest, in Toronto. The citations follow.

Dan Kalman, Robert Mena, and Shahriar Shahriari, "Variations on an Irrational Theme—Geometry, Dynamics, Algebra," Mathematics Magazine 70 (April 1997). To quote the authors of the paper, "If someone mentions irrational numbers, what do you think of?" Kalman, Mena, and Shahriari begin with the early history of irrational numbers—the Pythagoreans' discomfort with incommensurable line segments—but quickly turn to what is interesting and novel. A geometric argument for incommensurability based on infinite descent is used to motivate the use of matrix algebra to show the irrationality of the square root of two in dynamical terms. The use of dynamical systems enables the authors to present elegant proofs of some well-known results about the monic polynomials with integer coefficients (for example, the real roots are either integral or irrational) and to generalize these results to monic polynomials over an integral domain. It's all interesting, novel, beautifully written, and a pleasure to read.

Biographical Notes Dan Kalman has been a member of the mathematics faculty at American University, Washington, DC, since 1993. Before that he worked for eight years in the aerospace industry, and taught at the University of Wisconsin, Green Bay. During the 1996–97 academic year, he served as an Associate Executive Director of the Mathematical Association of America. Kalman has a B.S. from Harvey Mudd College and a Ph.D. from the University of Wisconsin, Madison.

Kalman was recognized by the MAA with a Pólya Award in 1994 and a Trevor Evans Award in 1997. He has been a frequent contributor to all of the MAA journals and is an Associate Editor for *Mathematics Magazine*. His book, *Elementary Mathematical Models*, has been published in the MAA's Classroom Resources series. One of his mathematical interests is automatic differentiation, the subject of an invited address he presented at the January 1997 joint mathematics meetings in San Diego.

Robert Mena has been at Long Beach State since 1988, after 15 years at the University of Wyoming. His favorite courses include combinatorics, number theory, statistics, and history of mathematics.

Shahriar Shahriari has been teaching mathematics at Pomona College since 1989. He received a B.A. (with high honors) from Oberlin College in 1977, and a Ph.D. from the University of Wisconsin–Madison in 1986. His thesis advisor was I. Martin Isaacs, and his area of research was representation theory of finite groups. Shahriari's current research interest is in the combinatorics of finite sets.

Among the course Shahriari teaches at Pomona is an alternative to second semester Calculus in which calculus topics are taught in the context of number theory, and the students develop all the material through solving problems. He also teaches a combinatorics class, which is "writing intensive." In addition to the usual homework assignments, the students work on "labs" in a collaborative learning environment and write two expository papers.

A Web-Searchable Database for *Mathematics Magazine*

We are happy to inform readers of the Magazine's useful new Web-searchable database of Articles, Notes, Proofs Without Words, and more. The database can be found through MAA Online, at

`http://www.maa.org`

(click on Journals and then on Mathematics Magazine), or directly from its "home" at Harvey Mudd College, at

`http://www.math.hmc.edu/MathMag/`

The database currently contains information going back to 1974. We plan in the near future to extend the database back to the *Magazine*'s inception, in 1927. The database contains the title, author, and first paragraph (and, in many cases, author's summary) of almost every Article, Note, and Proof Without Words published in the *Magazine* since 1974. An easy-to-use search engine allows users to search for specific lists of records, or to browse the full contents of any single issue.

The database and the search page were created by Harvey Mudd College mathematics students as part of Harvey Mudd's Undergraduate Math Forum, run by Professor Arthur Benjamin in the 1997–1998 academic year. (Arthur Benjamin is also an Associate Editor of the *Magazine*.)

The participating students are: Aaron Archer, Drew Bernat, Neil Burrell, Carrie Crum, Celeste Elton, Patri Forwalter-Friedman, Matthew Fluet, Ryan Gatti, Rif Hutchings, Jennifer Jack, Nathan Jakubiak, Brian Johnson, Christian Jones, Bill Kalahurka, John Larkin, Jeff Liebert, Naveen Mathew, Dominic Mazzoni, Andy Olson, Scott Robertson, David Rudel, Thara Salamone, Stacy Sanders, Itai Seggev, Marie Snipes, Jascha Swisher, Jennifer Weber, Bill Williams, and Andromeda Yelton.

Each student was assigned a volume of *Mathematics Magazine*, and gave two presentations based on his or her reading. Each student also entered the first paragraph of each note and article on a web page designed by Christian Jones. Dominic Mazzoni designed the search engine, and Matthew Fluet has helped extend and upgrade the database.

We thank all of these students for their useful efforts, and we hope that readers, prospective authors, and researchers will all find the database useful and inviting.

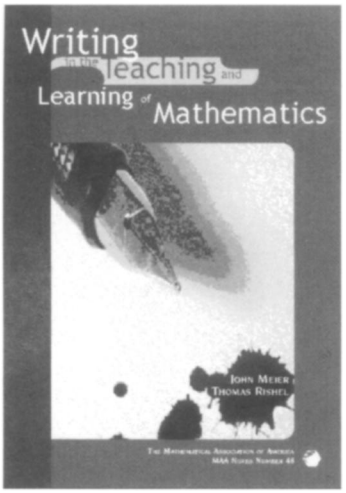

Writing in the Teaching and Learning of Mathematics

JOHN MEIER AND THOMAS RISHEL

Series: MAA Notes

Writing in the Teaching and Learning of Mathematics discusses both how to create effective writing assignments for mathematics classes and why instructors ought to consider using such assignments. The book is more than just a user's manual for what some have termed "writing to learn mathematics;" it is an argument for engaging students in a dialogue about the mathematics they are trying to learn.

The first section, "First Steps," contains chapters addressing the nuts and bolts of how to design and evaluate writing assignments. The second section, "Listening to Others," introduces ideas such as audience, narrative, prewriting and process writing, which our colleagues in writing departments have found useful. Specific examples illustrate how these are important for writing in mathematics classes. After the third section, "Major Projects," the text concludes with "Narrating Mathematics," a section making explicit what is implicit in the rest of the text: writing, speaking and thinking are all intertwined. By asking good questions and critiquing students' manuscripts in an open, yet rigorous manner, instructors can get students at any level of ability and background to a deeper awareness of the beauty and power of mathematics.

Catalog Code: NTE-48/JR
114 pp., Paperbound, 1998
ISBN 0-88385-158-X
List: $18.95 MAA Member: $14.95

CONTENTS

ARTICLES

NOTES

PROBLEMS

REVIEWS

NEWS AND LETTERS

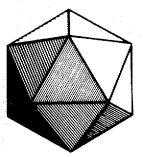

THE MATHEMATICAL ASSOCIATION OF AMERICA
1529 Eighteenth Street, NW
Washington, D.C. 20036